SPARK IGNITION, DIRECT INJECTION ENGINE R&D

2001
ANNUAL
PROGRESS
REPORT

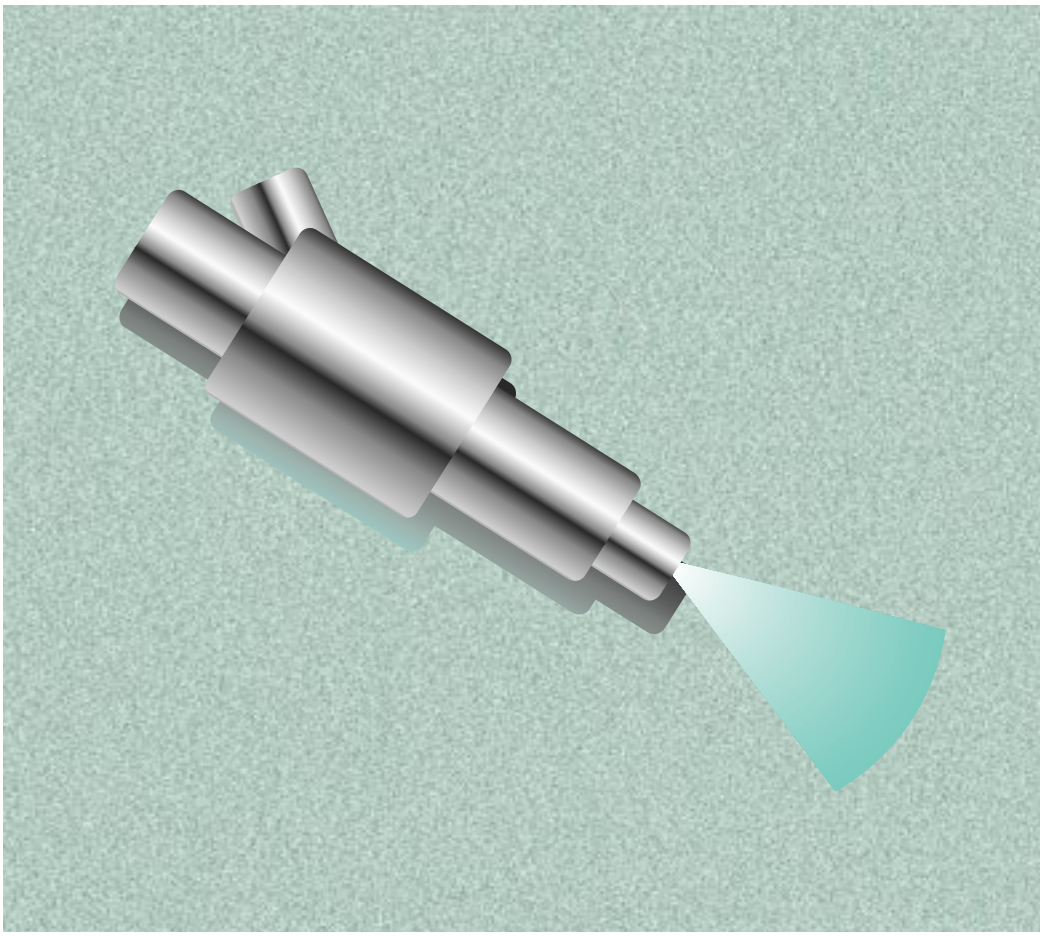

U.S. Department of Energy

Energy Efficiency and Renewable Energy

Office of Transportation Technologies

ACKNOWLEDGEMENT

We would like to express our sincere appreciation to Argonne National Laboratory and Computer Systems Management, Inc., for their artistic and technical contributions in preparing and publishing this report.

In addition, we would like to thank all our program participants for their contributions to the programs and all the authors who prepared the project abstracts that comprise this report.

U.S. Department of Energy
Office of Transportation Technologies
1000 Independence Avenue, S.W.
Washington, DC 20585-0121

FY 2001

Progress Report for the Spark Ignition Direct Injection R&D Program

Energy Efficiency and Renewable Energy
Office of Transportation Technologies

March 2002

CONTENTS

II. INTRODUCTION

Advancing Fuel Efficient Automotive Technologies Through SIDI R&D

Rogelio Sullivan, Program Manager

On behalf of the Department of Energy's Office of Transportation Technologies (OTT), I am pleased to introduce the Fiscal Year (FY) 2001 Annual Progress Report for the Spark Ignition Direct Injection Engine R&D Program. Together with DOE National Laboratories and in partnership with private industry and universities across the United States, OTT engages in R&D that provides enabling technology for fuel efficient and environment-friendly vehicles. The Program is focused on exploring the fundamental combustion characteristics of spark ignition, direct injection (SIDI) engines, development of components specific to SIDI engines such as new fuel injection systems, development of exhaust emission control devices, and development of new sensors to control fuel injection and emission control systems. This report marks the conclusion of the SIDI R&D Program within DOE, though its many developments have broad utility and will live on as part of other DOE R&D Programs.

SIDI engines use direct in-cylinder fuel injection of gasoline which results in a more efficient engine because of less need for intake air throttling and because they can be operated with lean air/fuel ratios. Under laboratory conditions simulating congested urban driving, SIDI engines have demonstrated the potential for fuel economy improvements of up to 30 percent. Under less congested driving conditions, the gains are likely to be about half this amount. SIDI engines have advantages in noise and vibration, cost, and specific power output relative to compression ignition, direct injection (CIDI) engines (an advanced version of the diesel engine) which makes them viable contenders for use in future, more fuel efficient vehicles using gasoline as fuel. SIDI engines have the potential to lower engine-out hydrocarbons because less fuel is quenched in crevices, and precise fuel metering reduces the need for cold start enrichment. They are more tolerant of exhaust gas recirculation (EGR), which can help to control NO_x.

SIDI Technology Status

In Europe and Japan, SIDI vehicles are being deployed to improve the efficiency of light-duty vehicles using gasoline. Mitsubishi, a leader in SIDI technology has four-, six-, and eight-cylinder SIDI engines in production, and all the cars it builds in Europe have SIDI engines. Mitsubishi has built SIDI engines since 1996, and has produced close to 1 million to date. Audi has just announced a four-cylinder, 2-liter SIDI engine for use in Europe, and Volkswagen has announced a similar four-cylinder, 1.6 liter SIDI engine. Nissan recently announced that they will soon have a complete line of four-, six-, and eight-cylinder SIDI engines that will be capable of meeting the 2005 Euro-IV emission standards. Saab implemented SIDI by incorporating the fuel injector with the spark plug in experimental versions of their engines that will be able to meet the California ULEV-II emission standards.

Orbital Engine Company is a leading international developer of SIDI fuel systems for all types of light-duty engines. Orbital and Siemens Automotive created a 50:50 joint venture called Synerject to manufacture air-assisted direct injection fuel systems (Synerject is located in Newport News, Virginia). In the fall of 2001, Orbital announced several new developments:

- They signed a technical transfer and license agreement giving Delphi Automotive Systems rights to manufacture and sell Orbital direct-injection technology.
- General Motors unveiled a V-8 concept engine incorporating Orbital air-assisted direct-injection fuel system.
- Four motorcycle manufacturers announced new products using Orbital direct-injection fuel injection systems.
- Orbital teamed with Johnson Matthey to develop a test vehicle with 12 percent better fuel economy while meeting Euro-IV emission standards. Besides improved fuel economy, this combination of Orbital direct-injection technology and Johnson Matthey catalyst technology does not require ultra-low sulfur gasoline. However, with ultra-low sulfur gasoline, significant further reductions in NOx emissions are possible with this system.

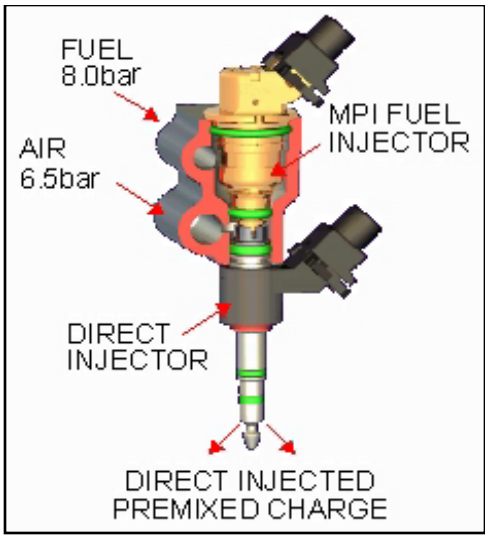

Cross-Section of the Synerject Air-Assisted Injector (Courtesy of Synerject)

SIDI development in the U.S. is likely to take a slightly different path than the SIDI engines being developed in Europe and Japan. SIDI engines have not been introduced into the U.S. because of their additional cost over conventional port injection engines, and uncertainty about their ability to meet future emissions regulations (more stringent than those of Japan and Europe). The first U.S. SIDI engines are likely to maintain a stoichiometric air/fuel ratio over most of the operating range because that will allow use of proven 3-way catalyst technology. Despite forgoing the advantages of lean-burn, these SIDI engines will likely still be more efficient than similar port fuel injected gasoline engines because of the ability to use higher compression ratios and less throttling. As lean-NO_x emission control devices improve and U.S. gasoline sulfur content is reduced, SIDI engines should be able to employ lean-burn operation, resulting in additional fuel economy improvements.

Technical Leadership

The SIDI R&D Program sharply focused on improving SIDI combustion and emission control technologies through cost-shared projects with industry partners. Substantial progress was made in the areas of new emission sensors, fundamental combustion analysis and modeling, fuel spray imaging, and low-friction coatings. These advancements have furthered progress in overcoming the critical technical barriers associated with SIDI engines, namely, higher than desired levels of NO_x and particulate matter (PM) in the exhaust, expansion of the stratified charge operating regime, and higher cost fuel systems. But just as importantly, these advancements are equally applicable to development of other advanced engine technologies with CIDI engines being the foremost example. DOE could not provide this leadership without the cooperative assistance of General Motors, DaimlerChrysler and Ford through participation in the Partnership for a New Generation Vehicle (PNGV) technical teams and the Low Emission Partnership (LEP).

The unique scientific capabilities and facilities of the national laboratories offered us the opportunity to target those technical areas of highest priority and those that require high-risk R&D that are often overlooked by industry. The National Laboratories are a much valued asset in this endeavor. We worked with industry and through the PNGV technical teams to ensure that National Laboratory R&D activities fulfilled industry's needs for basic scientific understanding and development of new research tools, materials, and processes. The R&D projects conducted were reviewed each year internally and by representatives from the auto manufacturers and emission control device manufacturers. This assures that the work completed was relevant to the ultimate users of the technologies.

ACCOMPLISHMENTS

Fundamental Combustion and Modeling Studies

The projects in the Fundamental Combustion and Modeling area are aimed at developing research tools, collecting engine data, and providing a more complete understanding of SIDI in-cylinder phenomena. To achieve high efficiency and low emissions, parameters such as air/fuel ratio and EGR will have to be pushed to the limits of stable combustion. The research in this portion of the SIDI Program identifies these limits through the development of models and analytical tools. The key processes that have been explored include: fuel injection; fuel vaporization; fuel-wall interaction; fuel-air mixing; ignition; and flame propagation and combustion. The projects have been conducted primarily at national laboratories and universities, using advanced diagnostics in optical research engines and a variety of air flow and combustion simulation capabilities. Detailed models of SIDI combustion chambers were created in KIVA and simulations of fuel sprays and combustion were performed to verify the experimental results. The tools and data developed are being shared with SIDI engine developers to assist them in devising strategies to achieve high efficiency with low emissions.

Argonne National Laboratory Advances Fuel Spray Imaging Technology

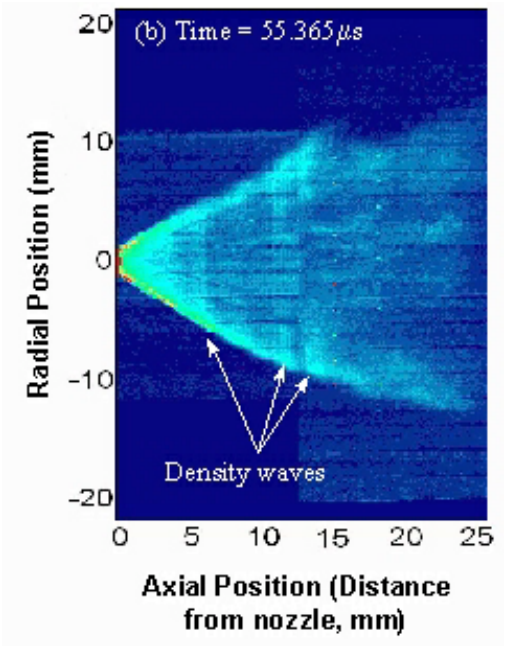

X-Ray Snapshot of Direct Injection Fuel Spray Showing Density Waves Emanating from the Injector

Argonne National Laboratory (ANL) demonstrated that the combination of high intensity x-ray beams from wide-band-pass x-ray optics and a fast 2-D x-ray detector can collect the radiographic images of gasoline injector sprays much more efficiently. The image collection time has been reduced from 1 week to a few hours per injection condition. This advancement makes this method practical as a diagnostic technique for fuel injection equipment manufacturers and the auto industry to use in designing new injectors. Using a Delphi injector, ANL has clearly shown the ability to measure the asymmetry of the spray cone and variations in the density of the spray. Spatial temporal resolution and mass distribution of the entire spray event can be captured in unprecedented detail. This measurement technique is so precise that pressure waves are detected emanating from the injector. This is the first time this phenomena has been observed, and this project was awarded ANL's Director's Award in June 2001 because of it. This work paves the way to a comprehensive understanding of the dynamic characteristics of high-pressure fuel spray in near-nozzle regions that can potentially benefit designers of fuel injectors for SIDI engines, and other applications.

Sandia National Laboratory Identifies Improved Fuel Blend for Laser-Induced Fluorescence Studies

Using evaporation experiments, Sandia National Laboratory (SNL) demonstrated that 3-pentanone is preferentially evaporated from isooctane-3-pentanone mixtures commonly used for laser-induced fluorescence (LIF) measurements of direct injection fuel spray inside the cylinder. By blending the two fluorescent fuel tracers being used in an optimized ternary fuel mixture, SNL found that a much more uniform LIF signal is obtained during the evaporation process. This results in LIF being able to accurately track fuel vapor concentration during fuel injection and evaporation in SIDI engines. These results and tests of the ternary fuel/tracer blend in a fired SIDI engine have been submitted for publication.

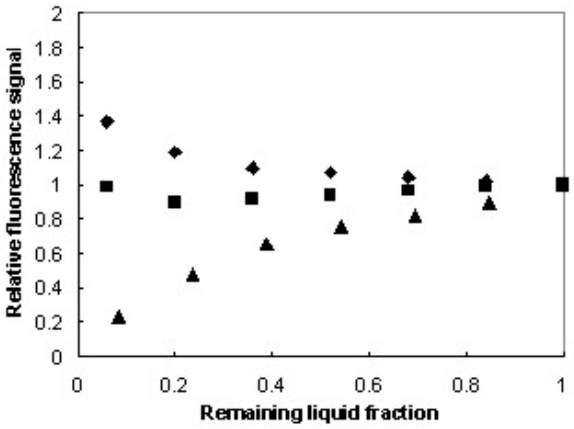

Los Alamos National Laboratory Develops Multicomponent Fuel Model for Modeling SIDI Combustion

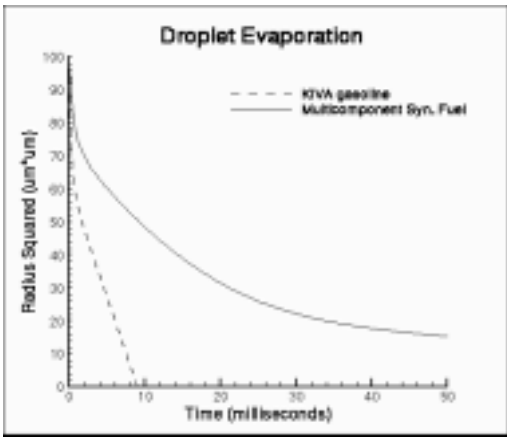

Los Alamos National Laboratory (LANL) improved the modeling capabilities of KIVA-3V by developing a multicomponent fuel model and by incorporating it into the the spray and wall film submodels of KIVA-3V. This model (unlike others), tracks temperature and mass concentration variations within the interior of the fuel droplet or wall film using an efficient computational scheme. LANL found that tracking internal variations inside the fuel is necessary in order to capture the complex spatial and temporal variations that occur during multicomponent fuel evaporation. The results of this work have been published and several presentations have been made at meetings during the past year.

University of Michigan Uses Active Flow Control to Design SIDI Combustion Systems

The cycle-to-cycle variation in turbulence and fuel-air-residual exhaust gas mixing is of primary importance to stratified charge SIDI engines. Recent research has shown a significant interaction between the mean flow and the fluctuating parts of the in-cylinder velocity. In order to design better lean burn engines, one has to have a better understanding of the flow patterns during the compression stroke and a way needs to be found to reduce cycle-to-cycle variation. If cycle-to-cycle variation is reduced, the in-cylinder flows are more predictable and thus one could employ leaner combustion without large torque variability or misfire. The objective of this study was to investigate the effects of perturbing the flow in the engine cylinder using controlled acoustic excitation. This study was conducted using a 1999 model year Ford cylinder head with 4 valves

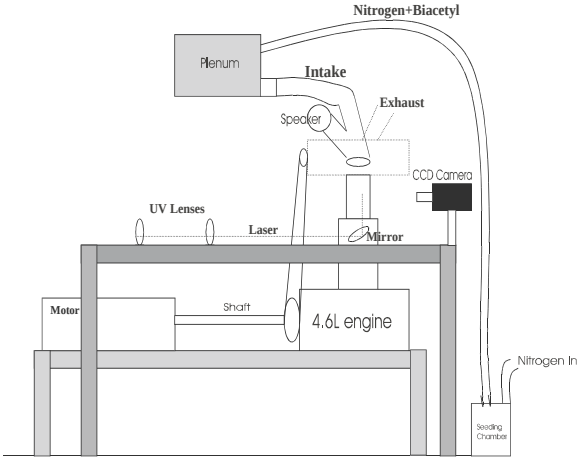

and double overhead cams. A flat-head, optical access piston was used in the experiment. Molecular Tagging Velocimetry (MTV) was used to measure the velocity profiles at a tumble plane which is located at the center of the cylinder, about 2 cm from each side of the cylinder wall. The most advantageous operation of the system showed a 25 percent reduction in the variation of in-cylinder flow velocities.

Engine and Component R&D

The objective of the projects in the Engine and Component Research portion of the SIDI Program is to address the system level barriers to commercialization of SIDI engines. These barriers include: lack of effective and durable NO_x emission control devices; excess injector and combustion chamber deposits; the cost of fuel injection system components; and quantification and control of PM emissions. The projects in this portion of the SIDI Program are being conducted by national laboratories, universities, and through cooperative agreements with industry. Each of the individual projects is focused on a research topic that has a high potential to overcome one or more of the key barriers to commercialization. Each project is closely tied to a potential customer or system developer through a cooperative agreement or similar mechanism to transfer technology to industry.

Argonne National Laboratory Demonstrates Durability of Low-Friction Injector Coatings

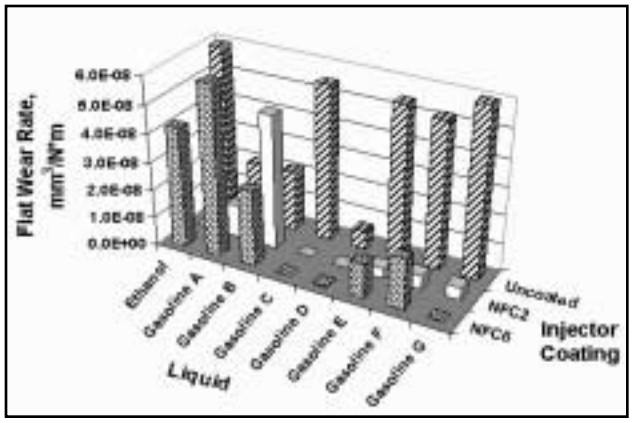

Argonne National Laboratory (ANL) has developed low-friction coatings for SIDI fuel injectors. These coatings may help offset the reduced lubricity of low-sulfur fuels. Million-cycle wear tests were conducted using two different coating formulations and seven different gasolines plus pure ethanol. The fuels represented summer and winter blends, premium and regular octane levels, and some contain additives under consideration for future blends. The low-friction coatings were found to provide clear reductions in friction over the uncoated fuel injectors. One coating showed 27% lower friction, while use of the other coating resulted in a friction reduction by nearly a factor of two. Equally important, is the reduction in wear that the coatings provide. Because of the high level of precision and tight tolerances in injector tips, any wear or erosion can be very detrimental to spray quality. The ANL coatings have been shown to dramatically reduce wear (and potentially deposit accumulation), helping to maintain injector performance over its useful life.

Delphi Advances Development of a Low-Pressure Direct Injection Fuel System

Delphi Energy & Engine Management Systems has been developing a low-pressure direct injection fuel system that would enable SIDI engines to meet their efficiency targets. Low fuel pressure is beneficial in that less energy is needed to generate good fuel spray characteristics, and only a single pump is needed, which reduces cost. However, getting sufficiently atomized fuel becomes more difficult as fuel injection pressure is reduced. A total of 42 initial injector atomizer designs were considered, and five were tested during the past year. Of these five, three underwent extensive testing and one has emerged as having the best combination of performance characteristics. For the fuel pump, an internal gear pump was found to be the best to

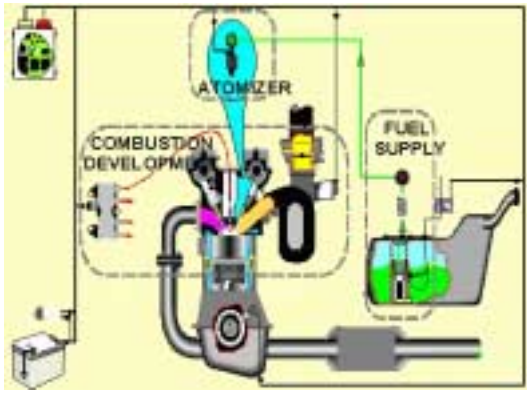

develop the required pressure. Improved performance was achieved by minimizing clearances, optimizing valve ports, and improving the design of the interface between the pump and drive mechanism. Optimization of the fuel pump durability continues through material selection, lubrication, and optimum application of pressure balancing. Additional component development will be performed and a final report will then be issued.

Emission Sensor Development

The projects in the Sensor Development portion of the SIDI Program are directed towards the development of new sensors to control SIDI engine operation, diagnostics, and emission control systems. However, practical sensors must be capable of withstanding harsh engine environments while being highly species selective, fast responding, and inexpensive. Examples of the sensors that are being developed include those that can detect hydrocarbons (HCs) and NO_x with high precision and fast response, and sensors that can measure a wide-range of oxygen in the exhaust gases. Through industry feedback and technical collaboration, the feasibility of particular sensor concepts is evaluated at the outset of each project. Prototype sensors are evaluated against performance targets using bench rigs, and those that show promise will be evaluated for robustness and durability through engine tests. All of the projects include industry partners who perform these tests.

Los Alamos National Laboratory Develops Low-Cost Solid-State Non-Methane HC Sensor

Los Alamos National Laboratory (LANL) has developed low-cost, solid-state non-methane hydrocarbon sensors that will be useful to control SIDI emission control systems. These sensors are based on thin-film transition metal oxide catalyst/noble metal composites deposited on oxygen ion conducting solid-state electrolytes. These sensors are very small and have demonstrated the ability to reproducibly measure hydrocarbon emissions under laboratory conditions for long time periods. They exhibit almost no cross sensitivity for nitric oxide, water vapor or carbon dioxide gases. They have better than 95 percent device-to-device response uniformity and the response time has been improved from a minute to less than 3 seconds. The automotive Cooperative Research and Development Agreement (CRADA) partners for this project have also extensively tested these devices under laboratory and engine exhaust conditions. A number of automotive sensor suppliers have expressed interest in the possible testing and subsequent commercialization of this sensor.

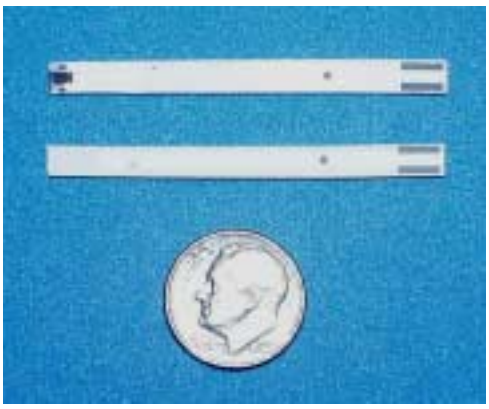

Pacific Northwest National Laboratory Advanced NO_x Sensor Development

SIDI engines will likely need to rely on sensors to control regeneration of NO_x adsorption catalysts. The signal for regeneration will be when the NO_x catalyst approaches full adsorption and NO_x escapes from the catalyst outlet. Pacific Northwest National Laboratory compared several variations of two-stage zirconia-membrane based prototype NO_x sensors and the important parameters investigated included: electrode thickness, triple phase boundary lengths, pore size/distribution, and primary grain size/distribution. They discovered that optimal design and fabrication of diffusion channels to

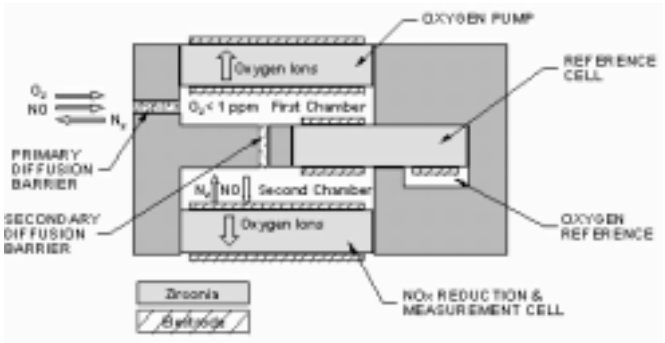

control gas flow to the oxygen pump cavity is critical for developing accurate and sensitive sensor elements, and that carefully optimized grain morphology and pore structure in the electrode is required to obtain the desired electrocatalytic reduction behavior from electrode structures. As quantification of these relationships is completed, PNNL will provide recommendations for optimal NO_x sensor designs.

Honors and Special Recognition

Jin Wang, Ramesh Poola, Chris Powell, and Yong Yue of Argonne National Laboratory were finalists in the Discover Awards, for their work on using x-rays to image and measure fuel injector spray patterns. The award is issued by Discover Magazine.

Patents

1. Matthews, R.D.,R. Stanglmaier, G.C. Davis, and W. Dai, "On-Board Gasoline Distillation for Reduced Hydrocarbon Emissions at Start-Up", U.S. Patent No. 6,119,637, issued Sept. 19, 2000.
2. "Mixed potential hydrocarbon sensor with low sensitivity to methane and carbon monoxide" R. Mukundan, E.L. Brosha, F.H. Garzon inventors. Patent pending - case #94675.
3. "Enhanced Electrodes for Solid State Gas Sensors" F.H. Garzon and E.L. Brosha inventors. U.S. Patent Granted.

Summary

The remainder of this report highlights progress achieved during FY 2001 under the Spark Ignition Direct Injection R&D Program. The following 16 abstracts of industry and national laboratory projects provide an overview of the exciting work conducted to tackle tough technical challenges associated with SIDI engines, including fuel injection, fuel/air mixing, combustion chamber design, sensor development, and catalytic exhaust treatment devices for controlling emissions. The commitment of Japanese and European manufacturers to SIDI technology and the recent interest by U.S. manufacturers and suppliers suggests a bright future for SIDI engines and more efficient vehicles because of them.

I would like to personally thank all of the researchers at the national laboratories, universities, and in industry, for all your contributions to this Program. Your hard work and ingenuity have resulted in a measurable advancement in the state of knowledge about the real potential and remaining challenges for SIDI engines.

Rogelio Sullivan, Program Manager
Office of Advanced Automotive Technologies
Office of Transportation Technologies

II. FUNDAMENTAL COMBUSTION AND MODELING STUDIES

A. Gasoline Fuel Spray Studies Using Synchrotron X-Rays

Jin Wang (Primary Contact) and Roy Cuenca
Argonne National Laboratory
9700 South Cass Avenue
Argonne, IL 60439
(630) 252-9125, fax: (630) 252-9303, e-mail: wangj@aps.anl.gov

DOE Program Manager: Rogelio Sullivan
(202) 586-8042, fax: (202) 586-1600, e-mail: Rogelio.Sullivan@ee.doe.gov

Objectives

- Characterize gasoline spark-ignited, direct-injection (SIDI) engine fuel injector hollow-cone spray structure and dynamics in the region near the nozzle.
- Develop highly efficient, highly quantitative and time-resolved radiographic methods and instrumentation to achieve the above goal.
- Obtain the axial, radial, and angular distribution of mass flux in fuel injector sprays to characterize the core and study the mechanism leading to spray breakup and atomization.

Approach

- Use the combination of high intensity x-ray beams from wide-band-pass x-ray optics and a two-dimensional (2-D) x-ray detector to collect the radiographic images of the gasoline sprays more efficiently.
- Develop data analysis methods and computational programs to process the image data for quantitative evaluation of such spray characteristics as fuel mass distribution and flux.
- Use theoretical modeling and computational approaches to improve the understanding of the hollow-cone sprays.

Accomplishments

- We have demonstrated that the combination of high intensity x-ray beams from wide-band-pass x-ray optics and a fast 2-D x-ray detector can collect the radiographic images of the gasoline sprays much more efficiently. The image collection time has been reduced from 1 week to a few hours per injection condition. Therefore, the method is practical as a diagnostic technique for injection equipment manufacturers and the auto industry.
- We have studied thoroughly the fuel sprays from a Delphi gasoline direct injection (GDI) system. Tomographic-type measurements have been performed with high image quality, revealing never-seen-before characteristics of hollow-cone gasoline sprays.
- We have developed a comprehensive analysis program to quantitatively evaluate the fuel distribution at any given time and spatial location.

Future Directions

- We plan to develop and implement a system consisting of dedicated x-ray optics and detectors suitable for 2-D data collection to further improve the efficiency of the testing.
- We will perform the spray measurement of the Delphi injector under high pressure and temperature environments to simulate actual gasoline engine cylinder conditions.
- We will develop better software so that the data analysis can be performed in a more automated mode.

Introduction

Using synchrotron X-radiography and mass deconvolution techniques, this research reveals never-before-seen structure characteristics of the direct injection (DI) gasoline hollow-cone sprays in the near-nozzle region, paving a way for a revolution in gasoline direct injection (GDI) technology. A series of experiments were conducted with the world's most brilliant monochromatic X-ray beams. Employed to measure gasoline sprays, X-radiography allows quantitative determination of the fuel distribution in this optically impenetrable region with a time resolution of better than 1 μs, revealing the most detailed near-nozzle mass distribution of a fuel spray ever detected. Based on the X-radiographs of the spray collected from four different perspectives, enhanced mathematical and numerical analysis was developed to deconvolute the mass density of the gasoline hollow-cone spray. This lead to efficient and accurate regression curve fitting of the measured experimental data to obtain essential parameters of the density distribution, which are then utilized in reconstructing the cross-sectional density distribution at various times and locations. The fuel density distribution of the near-nozzle region may greatly affect the fuel's atomization further downstream in GDI systems. The quantitative observation of the severe asymmetry associated with the sprays will allow the automobile industry to design better injection nozzles and combustion engines with a clearer understanding of the key components that affect the spray's structure in this region.

Approach/Results

In this research, a series of intensive experiments have been conducted to measure the DI gasoline sprays in the near-nozzle region at the APS and Cornell High Energy Synchrotron Source (CHESS).

Parameters	Quantity and Properties
Injection system	GDI with outwardly opening injector
No. of orifices	1
Orifice diameter, mm	1.9
Fill gas and pressure, MPa	N_2, 0.1
Fill gas temperature, °C	25 to 30
Fuel	Viscor (the calibration fluid) with Ce- additive
Specific gravity, g/mL	0.8405
Spray duration, μs	1000
Spray cone-angle	65° (nominal)

Table 1. Parameters of the GDI system and the injection conditions

A GDI injection system with an outwardly opening injector was employed. Injection was performed into a spray chamber filled with nitrogen gas at atmospheric pressure and room temperature. The spray chamber (10.16 cm in width, 12.7 cm in height, 20.32 cm in depth) is designed to hold the injector, contain the spray plume, and allow the nitrogen to scavenge the fuel vapors. The chamber has 63.5-mm-long by 63.5-mm-wide windows of Kapton film that provide line-of-sight access for the x-rays. A gentle flow of nitrogen was maintained through the chamber to scavenge the fuel spray mist. The fuel used in this study was a blend of calibration-type gasoline fuel (Viscor) and a cerium-containing additive with a final cerium concentration of 4.2% by weight. Table 1 provides a summary of the injection system, test fuel, and test conditions employed for the x-ray absorption measurements. The focused X-ray beam was collimated by a pair of X-Y slits to a size of about 13 mm (horizontal) x 2.5 mm (vertical). The collimated beam then passed into the injection chamber for probing the fuel sprays. An extremely brilliant monochromatic x-ray beam tuned to 6.0 keV was used; this x-ray photon energy is slightly above the several cerium L resonance absorption edges near

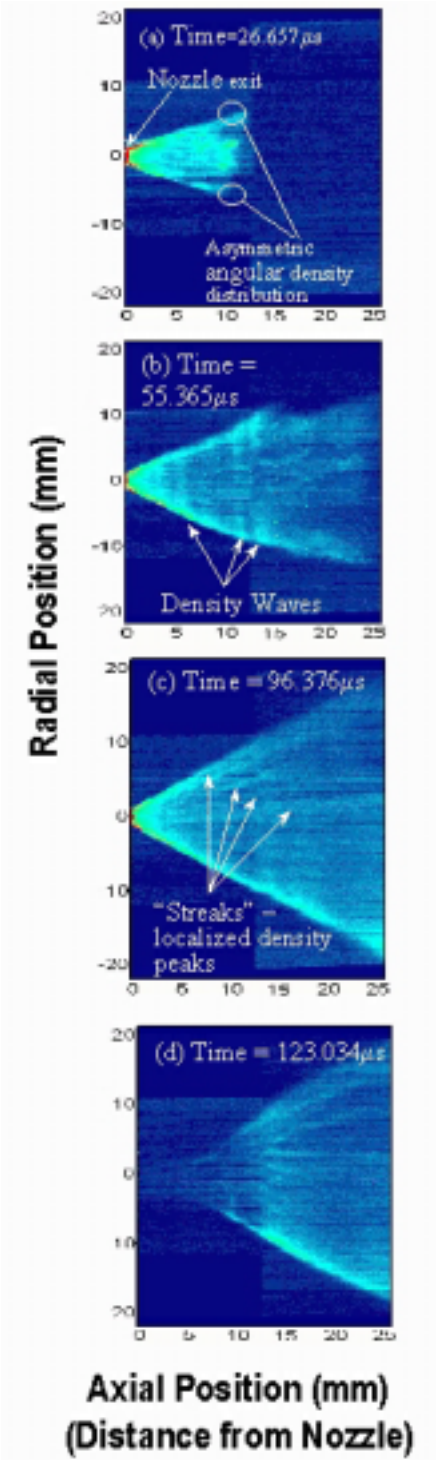

Figure 1. Transmission snapshots of x-ray measurement of fuel spray (beam rotation angle is 45°); (a) time=26.657 s, when the spray is just exiting the nozzle; (b) time=55.365 s, when the spray is forming its hollow-cone shape; (c) time=96.376 s, when the spray is extended to its full range; (d) time=123.034 s, after the nozzle is closed.

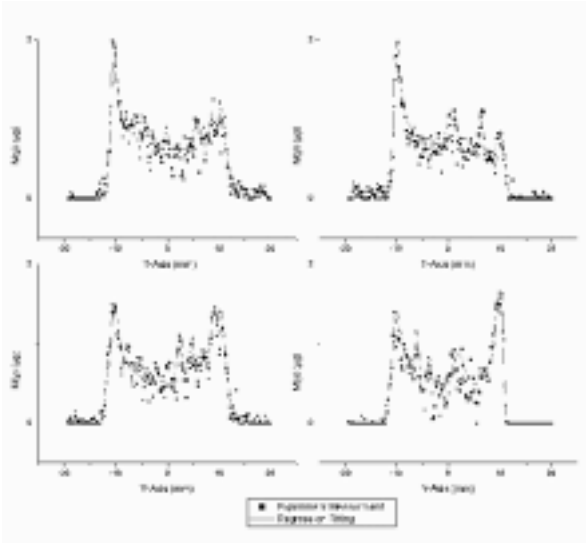

Figure 2. Diagram illustrating the reconstruction of the cross-sectional density distribution rings from mass deconvolution fitting at four directions.

5.7 keV. This maximizes absorption by the fuel jet. The transient x-ray attenuation signal due to the fuel spray was measured by using a fast-response x-ray area detector, pixel array detector (PAD) with a temporal resolution of better than 1 ms. The transmission image was averaged for 20 cycles in order to improve the signal/noise ratio. A data processing program was developed to quantitatively determine X-ray transmission values, incorporating a noise-reduction technique. Then the program calculates the integrated mass distribution of fuel, which results in a time-resolved mass measurement. Videos of the gasoline spray have been produced from a group of transmission snapshots by modified commercial image processing software. The snapshots demonstrated the details of dynamic characteristics of the mass distribution of the hollow-cone gasoline spray at near-nozzle regions. These include time-dependent irregular density distribution and extremely high frequency pressure waves within the sprays, never-before discovered or reported by any conventional non-optical or optical spray diagnostic technique. Tomographic-type of x-radiographs have been collected to facilitate the model-dependent deconvoluting theme from four angles: 0°, 45°, 90°, and 135°.

Figure 1 shows a group of 2-D reconstructed transmission x-ray snapshots of the fuel spray at different time instances, which clearly displays the

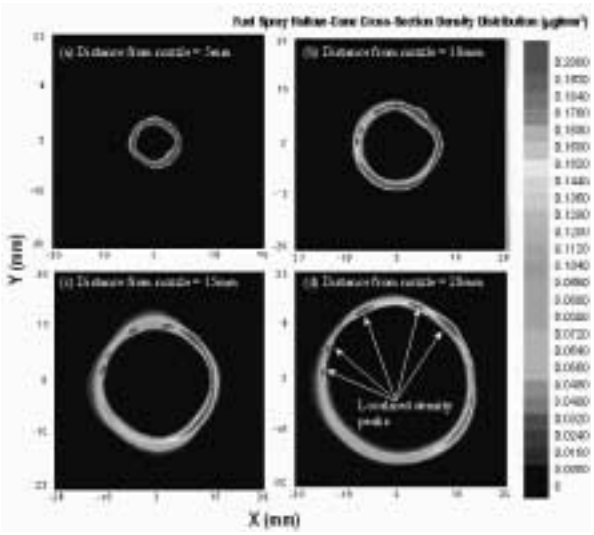

Figure 3. Experimental mass calculations and mass deconvolution model fitting at time 110.73 μs, 15 mm from the nozzle; (a) rotation angle 0°; (b) rotation angle 45°; (c) rotation angle 90°; (d) rotation angle 135°.

transience of gasoline sprays. Features such as asymmetry, local "streak," and pressure waves are readily evident in these snapshots. The circles on Figure 1(a) pinpoint the asymmetry of the spray that is present upon its exit from the nozzle. Although such asymmetry seems to moderate as the spray continues, quantitative analysis later revealed that the irregularity still existed throughout the duration of the spray. The streaks of local density peaks, labeled in Figure 1(c), demonstrate further asymmetry in the angular distribution of density. Another never-before-observed phenomenon is the pressure waves, shown in Figure 1(b), appearing as high-density columns. To illustrate more clearly the deconvolution method, Figure 2 depicts the 4-way tomographic-type of analysis which has been performed on the image data collected at the location 20 mm from the nozzle and at ca. 110.73 μs after the injection. Figure 3 displays the deconvolution regression fits at time 110.73 μs, 15 mm from the nozzle, on all four rotational angles. There are large differences in density in the angular direction. The radius of the annular cross-section also changes from one rotational angle to another, indicating the cross section of the spray cone is not perfectly circular. Figure 4 shows the cross-section rings of density distribution constructed from the calculated matrix, using a contour color fill graphing technique, at four

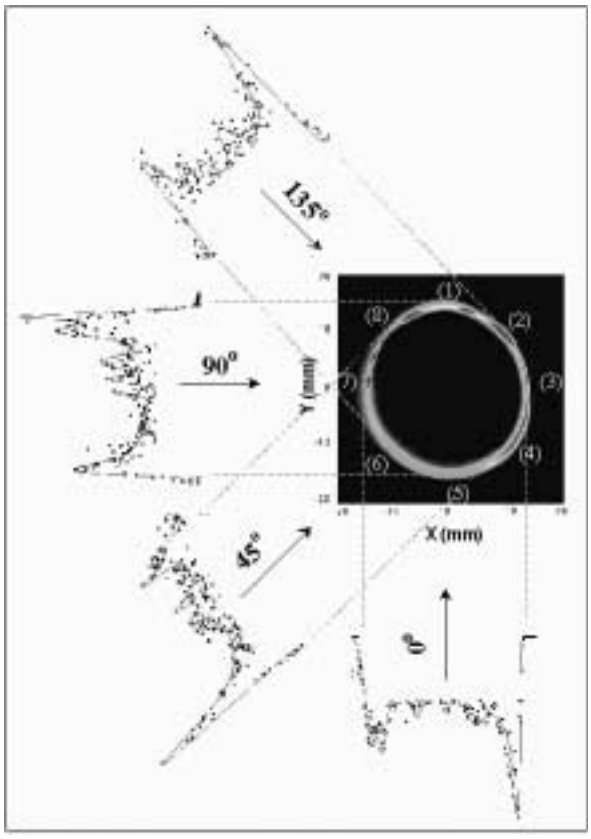

Figure 4. Reconstructed density distribution rings at 110.73 μs; cross-section slice (a) 5mm from nozzle, (b) 10mm from nozzle, (c) 15mm from nozzle, (d) 20mm from nozzle.

Distance from Nozzle (mm)	Average Radius (mm)	Max. Density (μg/mm^3)	Min. Density (μg/mm^3)
5	4.088	1.600	0.256
10	7.538	1.000	0.120
15	10.513	0.800	0.064
20	14.213	0.550	0.066

Table 2. Density Distribution Variation on the Fuel Spray's Cross-Sectional Rings

distances, 5, 10, 15, and 20 mm from the nozzle, all at time 110.73 μs after the start of the injection. They are denoted as a, b, c, d, respectively. Some important fitting parameters are listed in Table 2.

Conclusions

In light of the precise analysis that was performed on the experimental data obtained from measuring the fuel spray with X-radiography, we can conclude that observing the near-nozzle regions of the hollow-cone

gasoline spray with non-intrusive monochromatic x-rays is an effective method to study and document the characteristics of the never-before-seen area of the fuel injection process. The mathematical and numerical analysis presented in this study was able to efficiently and accurately construct a mass deconvolution model that fit the experimental data extremely well. From the parameters obtained from these models of various rotation angles of the spray, a cross-sectional density distribution model was reconstructed to fully represent the characteristics of the hollow-cone spray with its many irregularities. This successful cross-sectional construction can be readily compiled into a three-dimensional image model that will better show the continuity of the density distribution changes through time and space. The promising finding and novel methodology described in this work pave the way to a comprehensive understanding of the dynamic characteristics of high-pressure fuel spray in near-nozzle regions that can potentially benefit liquid-propellant rockets, gas turbines, internal-combustion engines, and even other industrial areas.

References

1. Quantitative Measurements of Direct-Injection Gasoline Fuel Sprays in Near-Nozzle Region Using Synchrotron X-Ray, Y. Yue, C. F. Powell, R. Poola, J. Wang, M.-C. Lai, S. E. Parrish, SAE paper SAE 2001-01-1293, 2001.
2. Synchrotron X-Ray Measurement of Direct Injection Gasoline Fuel Sprays, Y. Yue, C. Powell, R. Cuenca, R. Poola, J. Wang, ASME paper, accepted, 2001.
3. X-ray Propagation-Based Phase-Enhanced Imaging of Fuel Injectors, W.-K. Lee, K. Fezzaa and J. Wang, ASME paper, accepted, 2001.

Awards

1. Director's Award, Argonne National Laboratory, June 2001.
2. Finalist, Discover Magazine Award, June 2001.

B. University SIDI Combustion Projects

Jay Keller
Sandia National Laboratories
P.O. Box 969, MS 9053
Livermore, CA 94550-9053
(925) 294-3316, fax: (925) 294-1004, e-mail: jokelle@sandia.gov

DOE Program Manager: Rogelio Sullivan
(202) 586-8042, fax: (202) 586-1600, e-mail: Rogelio.Sullivan@ee.doe.gov

Introduction

A significant part of the overall OAAT engine combustion program is a well-coordinated University program. These projects were awarded from a carefully crafted competitive bid process; as a result, they form an integral part of the overall engine combustion program. Sandia National Laboratories provides technical management of these projects to ensure a well-focused overall program. Biannual meetings where recent research results are presented and future directions are discussed between the University projects, the National Laboratory projects, and the Industrial partners insure the program remains well focused and collaborative. University research includes both compression ignition direct-injection (CIDI) and spark ignition direct-injection (SIDI) work; following are the individual reports on SIDI work performed during phase II of these contracts (June 2000 to May 2001). For information on the CIDI projects, refer to the 2001 Annual Report on Combustion and Emission Control for Advanced Engines.

SIDI Mixture Formation, Emissions Sources, and Fuel Composition Effects

Ronald D. Matthews and Matthew J. Hall
The University of Texas at Austin
Grant Number DE-FG04-99AL66262

Objectives and Approach

The University of Texas is studying mixture formation, emissions sources, and fuel composition effects in spark-ignited, direct-injection (SIDI) engines. These experimental studies are being conducted in a 4-cylinder GM Twin Cam engine and an analog single-cylinder optical engine having an identical cylinder head. Both engines have one cylinder converted to SIDI operation. The emissions impact of the mixture formation phenomena observed in the optical engine is to be measured in the Twin Cam engine and extended to higher engine speeds and loads. The conversion to SIDI operation has been completed in both engines. A programmable engine controller has been built to allow independent control of the direct-injection cylinder and the other three port-injected cylinders in the Twin Cam engine. In the optical engine we have studied spray/flow interactions; wall wetting; and how the equivalence ratio near the spark gap is related to the injection timing, bulk flow, injector cone angle, and engine speed. In addition, we have studied particulate matter emissions under cold-start conditions and the origins of hydrocarbon emissions resulting from fuel wetting of the piston.

Results

We have found that the type of in-cylinder flow field has a tremendous effect on wall wetting and fuel/air mixing and that fuel composition affects hydrocarbon emissions. Using schlieren imaging, we found that fuel vapors can evaporate from the piston surface late during the power stroke, forming dense regions of fuel vapor that remain close to the

piston surface. This behavior may be a cause of high hydrocarbon emissions observed from SIDI engines. We have found that clouds of particulates can form as a result of pool fires on the piston. The particulates form during the power stroke at the point at which in-cylinder temperatures are too low to complete oxidation, leading to high particulate emissions. Work on the metal Twin Cam engine has been completed and the control system is being calibrated to operate the engine for the emissions and fiber optic spark plug measurements.

A new set of fiber optic spark plug measurements were completed in the optical engine to measure the effects of bulk flow and injection timing on fuel/air mixing under firing operation. Both parameters have a strong effect on engine indicated mean effective pressure (IMEP) and measured emissions. A tradeoff was found between wall wetting and mixing as a function of injection timing for early injection. Later injection timings resulted in less wall wetting, but also less time for sufficient mixing of the fuel and air to occur. The optimum timing for early injection was found to be 120 degrees after top dead center (ATDC) of intake. This resulted in minimal surface wetting yet sufficient time for mixing. It was found that at the earliest injection timing examined (60 degrees ATDC intake), between 10% and 15% of the injected fuel was lost to surface wetting for all of the bulk flows examined.

For late injection timings, a strong correlation was found between the measured equivalence ratio at the time of ignition and the measured IMEP. Higher equivalence ratios at the time of ignition resulted in higher IMEP. The equivalence ratio at the time of ignition was strongly dependent upon both the bulk flow and the injection timing. It was found that the cycle-to-cycle variation in the equivalence ratio at the time of ignition increased as the injection timing was retarded. These cycle-to-cycle variations were found to correlate well with cyclic variability in IMEP. In general, the strong bulk flows typified by tumble and swirl resulted in faster mixing, but also greater convection of inhomogeneities past the spark plug. This made engine performance for these flows more sensitive to both injection and ignition timing. The weaker bulk flows typified by reverse-tumble and low-tumble resulted in slower mixing, but a more stable charge near the spark plug.

The effect of piston wetting on particulate emissions was investigated in the metal Twin Cam engine. The engine was operated on 90% propane fuel while an injection probe was used to inject 10% liquid fuel onto the top of the piston. The liquid fuels were chosen to examine the effects of fuel volatility and molecular structure on the PM emissions.

A nephelometer was used to characterize the PM emissions. Mass measurements were compared with gravimetric filter measurements and particulate size measurements were compared with scanning electron microscope photos of particulates captured on filters. The engine was run at 1500 rpm at the Ford world-wide mapping point with an overall equivalence ratio of 0.9. The liquid fuels examined were California Phase II gasoline, n-pentane, iso-octane, toluene, and undecane.

With the injection of liquid fuel onto the piston, particulate matter mass emissions increased greatly over operation on propane alone and over operation where a similar fraction of the liquid fuel was port injected. Toluene and n-pentane had the highest mass emissions, reflecting the effects of fuel structure and volatility. They also had the largest mean particulate size. The particulates had mean scattering diameters in the range of 500 to 1000 nm. Time-resolved measurements taken at 2 second intervals showed the temporal variation of PM characteristics.

Particulate mass emissions correlated well with prior measurements of unburned hydrocarbon emissions taken under the same conditions.

Publications

1. Alger, T., Huang, Y., Hall, M.J., and Matthews, R.D., "Liquid Film Evaporation Off the Piston of a Direct Injection Gasoline Engine," Society of Automotive Engineers Paper 2001-01-1204, 2001.
2. Mehta, D., Alger, T., Hall, M. J., Matthews, R. D., and Ng, H. "Particulate Characterization of a DISI Research Engine using a Nephelometer and In-Cylinder Visualization," Society of Automotive Engineers Paper, to be presented at the SAE Fuels and Lubricants Meeting, Orlando, FL, May, 2001.

3. Warey, A., Huang, Y., Matthews, R. D., Hall, M. J., and Ng, H. "Effects of Piston Wetting on Size and Mass of Particulate Matter Emissions in a DISI Engine," submitted to Society of Automotive Engineers for 2002 World Congress, February, 2002.

4. Alger, Matthews, R. D., and Hall, M.J. "Effects of In-cylinder Flow on Fuel Concentration at the Spark Plug and Engine Performance and Emissions in a DISI Engine," submitted to Society of Automotive Engineers for 2002 World Congress, February, 2002.

Mixture Preparation and Nitric Oxide Formation in an SIDI Engine Studied by Combined Laser Diagnostics and Numerical Modeling

Profs. Volker Sick and Dennis N. Assanis
The University of Michigan
Grant No. DE-FG04-99AL66236

Objectives

Through the combination of advanced imaging laser diagnostics with multi-dimensional computer models, a new understanding of the performance of direct-injection gasoline engines (SIDI) is being pursued. The work focuses on the fuel injection process, the breakup of the liquid into a fine spray and the mixing of the fuel with the in-cylinder gases. Non-intrusive laser diagnostics will be used to measure the spatial distribution of droplets and vaporized fuel with very high temporal resolution. These data along with temperature measurements will be used to validate a new spray breakup model for gasoline direct-injection. Experimental data on near wall fuel distributions will be compared with modeled predictions of the spray-wall interaction and the dynamics of the liquid film on the surface. Quantitative measurements of local nitric oxide concentrations inside the combustion chamber will provide a critical test for a numerical simulation of the nitric oxide formation process. This model is based on a modified flamelet approach and will be used to study the effects of exhaust gas recirculation.

Experimental Approaches and Achievements

A single-cylinder optical SIDI engine was built that allows access to the entire combustion chamber for the observation of spray formation, fuel/air mixing, flame propagation and nitric oxide formation. The introduction and mixing of fuel (iso-octane) with air was studied via PLIF (planar laser-induced fluorescence) using toluene as a trace

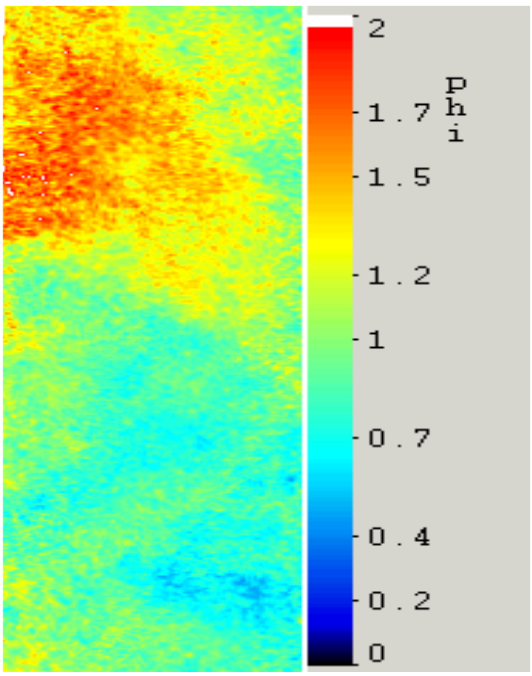

Figure 1. Equivalence Ratio Map, Measured Close to the Spark Plug at 600 rpm

because of its unique quenching properties that yield a fluorescence signal that is directly proportional to the fuel/air ratio. Figure 1 shows an example of an instantaneous ϕ distribution that was measured in the pentroof of the engine very close to the spark plug.

To assist the interpretation of the fuel/air mixing data, flow fields were investigated using Particle Image Velocimetry (PIV). It was found that the center of a strong swirl shifts as the engine speed is changed.

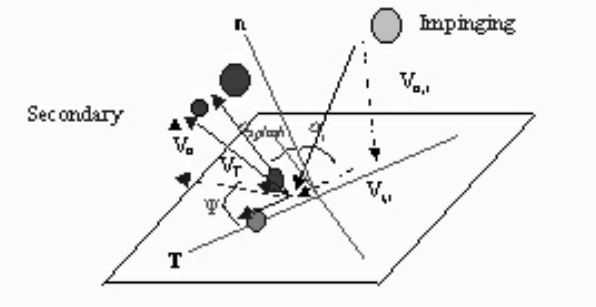

Figure 2. Splash of an Impinging Parcel

Modeling Approaches and Achievements

A spray/wall impingement submodel was developed and integrated into the KIVA-3V multidimensional computational fluid dynamics (CFD) environment to simulate the behavior of a spray impacting solid surfaces. The performance of the model was assessed by comparing numerical results to the data obtained from measurements conducted at the University of Michigan of a hollow cone spray impinging normally onto a flat plate under ambient conditions. The spray/wall impingement model conserved the mass, momentum, and energy of an impinging parcel before and after impact. Three splashing parcels and one wallfilm parcel were used to represent the shattering of an incoming droplet upon impact with the surface as shown in Figure 2.

The model showed improvements over the current KIVA-3V impingement model as shown in Figure 3 in predicting on-the-wall spray penetrations.

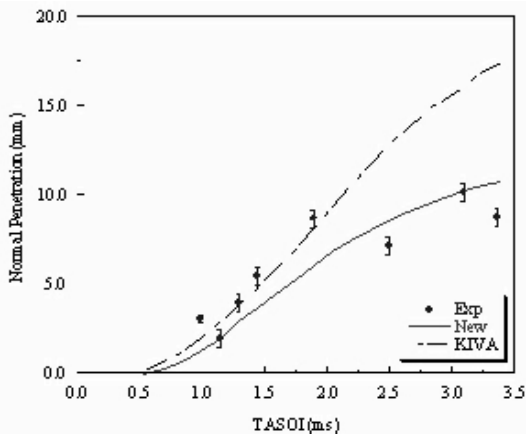

Figure 3. Comparison of the Normal Penetration Predictions of New Impingement Submodel and KIVA-3V Model with Experimental Data

Publications

1. Sick, V., Stojkovic, B., 2001, "Attenuation Effects on Imaging Diagnostics of Hollow-Cone Sprays," Applied Optics, 40, (15) pp. 2435 - 2442
2. Stojkovic, B., Sick, V. 2001, "Evolution and Impingement of an Automotive Fuel Spray Investigated with Simultaneous Mie/LIF Techniques," Applied Physics B 72, pp. 1-9
3. Grover, R., Assanis, D., 2001, "A Spray Wall Impingement Model Based Upon Conservation Principles," Proceedings of The 5th Int. Symposium on Diagnostics and Modeling of Combustion in Internal Combustion Engines, Nagoya, Japan, 2001.

Hydrocarbon Emission Formation Mechanisms in Direct-Injection Engines

Prof. Jaal B. Ghandhi
University of Wisconsin-Madison
Grant No. DE-FG04-99AL66264

Objective

The objective of this project is to investigate the major hydrocarbon emission formation mechanisms in a gasoline direct-injection (SIDI) engine. The two major sources of hydrocarbon emissions are the incomplete combustion of fuel in the lean regions of the stratified fuel-air mixture, and the evaporation of liquid fuel films from the combustion chamber surfaces following the flame propagation through the cylinder. An experimental approach has been taken to separately investigate both of these mechanisms.

Results

1) *The first direct observation of the lean flame quench phenomena in an engine* — Lean flame quenching has been postulated to occur in stratified-charge engines, contributing to hydrocarbon emissions, but it has never been directly observed. Using a combination of planar laser-based imaging techniques, lean flame quenching has been directly observed in an engine for the first time. Planar laser-induced fluorescence (PLIF) of 3-pentanone was used to mark the fuel, and PLIF of the hydroxyl radical was used to identify the product region. The engine was run at both 600 and 1200 rpm, an overall equivalence ratio of 0.3, and with naturally aspirated intake conditions. A clearly defined region of 3-pentanone fluorescence (fuel) was always observed late in the expansion stroke at the edge of the piston bowl. This region was also always found to be devoid of OH fluorescence. This combination provides evidence that the flame had not propagated into this region of the fuel cloud. Further, the late timings of these observations — up to 75 degrees after top dead center — indicate that further chemical conversion is not possible.

2) *Correlation of the lean flame quench phenomena with the engine operation* — Once lean flame quenching was observed, a series of experiments were performed to investigate the necessary in-cylinder conditions for avoiding the phenomena and the accompanying hydrocarbon emissions. Two types of tests were performed, both with the goal of increasing the end gas temperature. The first test involved advancing both the injection and ignition timings to phase the heat release earlier within the cycle. In spite of the slight increase in end gas temperature, flame quenching was still observed for the range of conditions that allowed acceptable combustion. The second test involved throttling the engine while maintaining a constant injected fuel mass. At an intake absolute pressure of 69 kPa the flame was observed to propagate across the entire combustion chamber, and quenching was not observed. There are two possible causes for this behavior: increased homogeneity due to the increase in the overall fuel-air ratio (although it is still well lean of stoichiometric) and the increase in the end gas temperature.

3) *Development of a robust fiber optic fuel film temperature measurement system* — A diagnostic has been developed to allow continuous single-point fuel film temperature measurement through the dual wavelength observation of the fluorescence of BTBP, which is doped into the fuel. The system uses a single optical fiber for both delivery of the laser light and collection of the fluorescence, and provides spatial resolution of 100 μm. The calibration has been made extremely robust so that fibers can be interchanged in the system without a change in the temperature calibration. Thus, multiple fibers from an engine can be used with no change in the system response, although the magnitude and time history of the fluorescence signals will be different.

4) *Preliminary fuel film temperature measurements in a firing direct-injection engine* — The fiber-based fuel film temperature system has been employed in a firing gasoline direct-injection, and preliminary data have been acquired. The fibers were mounted in the piston crown and were removed from the engine via a linkage within the Bowditch piston. No fiber durability issues were encountered. The results showed that the mean fuel film temperature was very close to the piston crown temperature, which was measured simultaneously with a thermocouple. No interference from combustion luminosity was observed. Further testing will be pursued in the near future.

C. Spark-Ignited Direct-Injected (SIDI) Homogeneous Combustion Research and Development

Richard Steeper and Greg Fiechtner
Sandia National Laboratories
PO Box 969, MS 9053
Livermore, CA 94551-0969
Steeper: (925) 294-2618, fax: (925) 294-1004, e-mail: steeper@sandia.gov
Fiechtner: (925) 294-3161, fax: (925) 294-1004, e-mail: gjfiech@sandia.gov

DOE Program Manager: Rogelio Sullivan
(202) 586-8042, fax: (202) 586-1600, e-mail: Rogelio.Sullivan@ee.doe.gov

Objectives

- Characterize the fuel injection process in SIDI engines.
- Determine the extent and location of wall-wetting, and identify its effects on combustion and emissions.
- Characterize the in-cylinder fuel-air mixing process, emphasizing fuel distribution in the vicinity of the spark plug at the time of ignition.
- Improve laser-induced fluorescence (LIF) diagnostic to achieve quantitative measurements of in-cylinder air-fuel ratio distribution.

Approach

- Apply LIF and laser elastic scattering methods to record bench-top and in-cylinder injector performance over a range of fuel temperatures and ambient pressures.
- Use flood LIF to measure fuel films that form on the piston window. Record simultaneous flame images and soot scattering images to identify pool fires that burn above the piston-top films and soot that is produced by the fires.
- Record in-cylinder fuel-vapor distributions using LIF of gasoline as well as custom fuel/tracer blends.
- Characterize the commonly used LIF fuel/tracer blend isooctane/3-pentanone, and test potentially improved octane/ketone blends.
- Present research results to industry, National Laboratories, and university partners, soliciting feedback and disseminating acquired information.

Accomplishments

- Collected comprehensive data documenting the formation of persistent piston-top fuel films, the ignition of pool fires, and the associated production of soot using current, high-pressure swirl injectors with 53° and 74° cone angles.
- Documented the non-ideal evaporative behavior of isooctane/3-pentanone mixtures used for LIF measurements. Identified an alternative ternary blend of isooctane/3-pentanone/3-hexanone that achieves improved fuel/tracer co-evaporation.

Future Directions

- Funding for SIDI engine research at Sandia National Laboratories was withdrawn at the end of FY01.

Introduction

The spark-ignition direct-injection (SIDI) engine is a promising alternative to compression-ignition direct-injection (CIDI) engines, approaching the fuel efficiency of the diesel engine while retaining the specific power of the gasoline engine. Several liabilities in current CIDI engine performance including higher particulate and NO_x emissions, lower specific power, lower public acceptability, higher noise, and lower fuel availability make the development of alternative strategies a wise investment.

Current SIDI engine designs incorporate both homogeneous charge and stratified charge operating modes. The SIDI engine program at Sandia comprises two laboratories configured to investigate the two different operating modes. One laboratory houses an engine configured with a vertical, centrally mounted injector and a flat piston, and the second contains an engine with an inclined injector mounted between the intake valves and targeted toward a sculpted piston. Both facilities are used to investigate fuel-air mixing, wall-wetting, combustion, and emission formation during homogeneous-mode operation.

Approach

Both research engines provide extensive optical access, enabling the application of advanced optical diagnostics. Planar LIF is used to characterize both liquid fuel distribution during injection and vapor fuel distribution at the time of spark. Flood LIF identifies liquid films that form in the cylinder. Laser-elastic scattering is applied for spray visualization as well as for soot detection. Direct flame imaging records premixed flame combustion as well as pool fires formed when fuel films on cylinder and piston surfaces ignite.

Results

A set of current-design swirl injectors were obtained for both engines, and the optical methods developed in FY00 were applied to the side-inject engine operating with the new injectors. In bench tests, the new injectors produced more symmetric sprays with reduced pre-and post-sprays than prior injectors tested. In the engine, however, the newer

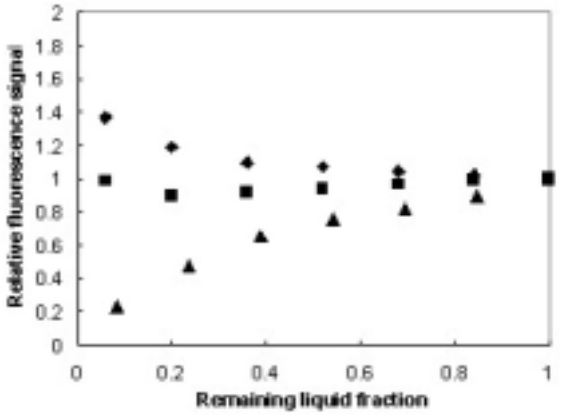

Figure 1. LIF tracer signal history of the vapor phase evaporating from three fuel/tracer mixtures at 90°C. Component volume percents for the three mixtures are: 10% 3-pentanone / 90% isooctane (triangles); 10% 3-hexanone / 90 isooctane (diamonds); 1% 3-pentanone / 9% 3-hexanone / 90% isooctane (squares).

injectors performed similarly to old injectors. Increased ambient (in-cylinder) pressure decreased the axial penetration of all sprays. Increased fuel temperature caused an increased droplet entrainment toward the spray centerline, forming a radially compact fuel cloud that penetrated to the piston crown in most cases. Both 54° and 74° injectors significantly wet the piston over a range of injection timings. Low radial penetration meant that the spray did not impinge directly on the cylinder walls. As with the old injectors, piston-top fuel films frequently ignited and burned as pool fires.

Evaporation experiments definitively demonstrated that 3-pentanone is preferentially evaporated from isooctane-3-pentanone mixtures commonly used for LIF measurements of in-cylinder fuel fraction. Figure 1 presents histories of the batch evaporation of several mixtures of isooctane and ketone tracers. LIF was used to measure the tracer concentration of saturated air leaving the evaporation chamber. In the figure, the LIF signal is normalized by the value recorded at the start of the experiment. The plots are read from right to left as remaining liquid fraction progresses from 1 to 0.

The triangle symbols in Figure 1 represent an initial mix of 10 vol% 3-pentanone in isooctane, and they indicate a dramatic drop in tracer concentration as the evaporation proceeds. The 3-pentanone

evaporates far faster than isooctane initially, depleting its concentration in the liquid phase and leading to a low vapor-phase concentration of the tracer late in the evaporation. These results imply that using this fuel/tracer blend in LIF engine experiments to track fuel (octane) concentrations will lead to incorrect results.

The diamond symbols in Figure 1 present the evaporation history of a 10 vol% mix of 3-hexanone in isooctane. This is a heavier ketone, and its vapor-phase concentration is seen to increase with time. But by blending the two tracers in a ternary mixture, a much more uniform LIF signal is obtained during the evaporation process, as shown by the square symbols. The fluorescent tracers in the 1:9:90 vol% mix of 3-hexanone/3-pentanone/isooctane co-evaporate with the isooctane and can be expected to faithfully track octane vapor concentration. These results and tests of the ternary fuel/tracer blend in a fired SIDI engine were submitted for publication.

Publications/Presentations

1. R. R. Steeper and E. J. Stevens, "Characterization of Combustion, Piston Temperature, Fuel Sprays, and Fuel-Air Mixing in a DISI Optical Engine," SAE Paper 2000-01-2900, presented at the Fall Fuels and Lubes Meeting, Baltimore, October, 2000.
2. E. Stevens and R. Steeper, "Piston Wetting in an Optical DISI Engine: Fuel Films, Pool Fires, and Soot Generation," SAE Paper 2001-01-1203, presented at the SAE Congress, March, 2001.
3. R. R. Steeper and E. J. Stevens, "Effects of Piston Wetting in an Optical DISI Engine," *Gasoline Direct Injection Engines Conference*, presented in Cologne, Germany, June, 2001.
4. D. Han and R. R. Steeper, "Examination of Isooctane/Ketone Mixtures for Quantitative LIF Measurements in a DISI Engine," submitted to SAE, SAE Paper 02P-294, 2001.
5. M. Davy, P. Williams, D. Han, and R. R. Steeper, "Evaporation Characteristics of the 3-Pentanone/Isooctane Binary System," submitted to *Experiments in Fluids*, 2001.
6. Presented research reports at two DOE Review Meetings convening DOE, National Lab, industry, and university partners.

D. Computer Modeling to Support GDI Engine Research

David J. Torres (Primary Contact), Peter J. O'Rourke
Fluid Dynamics Group T-3, MS B216
Los Alamos National Laboratory
Los Alamos, NM 87545
(505) 667-2638, fax (505) 665-5926, e-mail: dtorres@lanl.gov

DOE Program Manager: Rogelio Sullivan
(202) 586-8042, fax: (202) 586-1600, e-mail: Rogelio.Sullivan@ee.doe.gov

Objectives

- Provide 3-D Computational Fluid Dynamics (CFD) modeling support to research and production Gasoline Direct Injection (GDI) engines being experimentally tested at Sandia National Laboratories in Livermore, CA.
  - Interpret experimental data
  - Understand fuel/air mixture preparation
  - Improve computer submodels
- Implement a multicomponent model into KIVA-3V.
- Publish a description of the model and demonstrate its use in performing KIVA-3V calculations of multicomponent fuel sprays.

Approach

- Continue to perform engine simulations using the latest submodels in KIVA-3V and compare computations with experimental results.
- Research literature regarding multicomponent fuel evaporation.
- Develop equations for multicomponent fuel evaporation for spray and wall film.
- Implement multicomponent model into KIVA-3V.
- Present and publish multicomponent spray results at meetings and in journals.
- Use next-generation code CHAD (Computational Hydrodynamics for Advanced Design) when full-engine-cycle simulation capability is available in CHAD.

FY 2001 Accomplishments

- Compared measured and computed spray distributions in benchtop experiments using iso-octane and gasoline.
- Implemented a multicomponent fuel model into the fuel spray and wall film in KIVA-3V.
- Presented multicomponent description and multicomponent simulations
  - CRADA meeting in Livermore, CA, January 2001
  - ILASS meeting in Dearborn, MI, May 2001
  - University working group meeting, Madison, Wisconsin, June 2001

- Published "A Discrete Multicomponent Fuels Model for GDI Engine Simulations" in ILASS Americas Proceedings, 2001.
- Will submit "A Discrete Multicomponent Fuel Model" to *Atomization and Sprays* by mid-October 2001.

Future Directions

- Incorporate multicomponent fuel model into CHAD.
- Validate newly incorporated multicomponent fuel model by comparing KIVA-3V calculations with experimental measurements of liquid fuel spray and liquid film locations as well as vapor fuel distribution.
- Model the interior of a fuel injector to determine the sensitivity of the spray to fuel pressure, radius of curvature of surfaces, and azimuthal velocities.
- Continue to perform KIVA-3V calculations modeling Sandia research and production engines using latest submodels.

Introduction and Approach

Internal combustion engine performance relies on spatial and temporal fuel vapor distributions that produce efficient and reliable combustion. Predicting where and when liquid fuel will vaporize is invaluable information to designers of modern fuel-injected engines. KIVA-3V is a code developed at Los Alamos that is used extensively in industry as well as universities for engine studies. KIVA-3V has traditionally used a single component fuel in engine modeling. In order to model gasoline and diesel fuels, which are composed of many components, a representative fuel was traditionally used in KIVA-3V calculations. While this representative fuel can mimic many important features of a multicomponent fuel, it cannot account for certain effects arising from the differing volatilities of fuel components. These effects include preferential gas-phase vaporization of volatile fuel components that results in inhomogeneous fuel vapor distributions, or the accumulation of low-volatility liquid fuel components on a piston crown.

To improve KIVA-3V's modeling capabilities, we have developed a multicomponent fuel model and have implemented it into the spray and wall film submodels of KIVA-3V. Our model (unlike other models, Zeng and Lee 2000) tracks temperature and mass concentration variations within the interior of the droplet or wall film using an efficient computational scheme. We found that tracking internal variations inside the fuel is necessary in order to capture the complex spatial and temporal variations that occur during multicomponent fuel evaporation.

Fiscal Year 2001 Results

During the last year we have continued to compare experimental and KIVA computational results. Benchtop injection into a known quiescent room temperature and pressure was used to provide a controlled environment under which one could conduct comparisons. Iso-octane spray comparisons were made for injection fuel temperatures of 30°C and 90°C. Gasoline spray comparisons were made for injection fuel temperatures of 30°C. KIVA-3V computations of gasoline were performed with a preliminary multicomponent model.

Liquid fuel spray locations and penetration continue to differ between KIVA-3V and the experiment. Experimental laser-induced fluorescence images show significant spray cone filling, while KIVA-3V shows the spray structure to maintain a hollow cone shape. This difference in spray has led us to consider other liquid sheet breakup models. We also did not consider in our computations initial transients in the injector spray before the injector spray builds up enough angular momentum to achieve a steady shape. Modeling the interior and immediate external spray of a GDI injector with KIVA-3V may resolve how initial

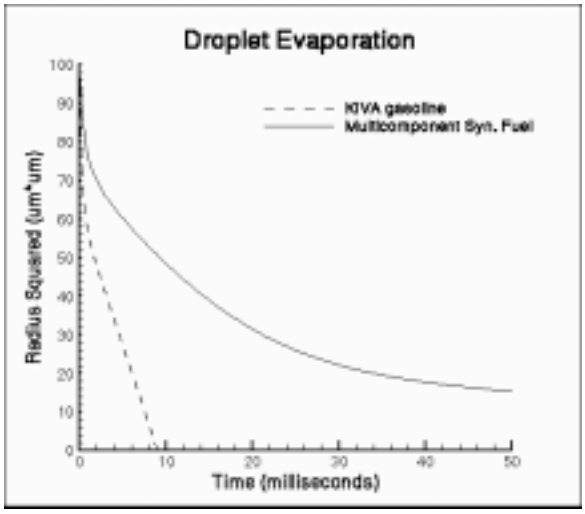

Figure 1. Droplet radius squared versus time for a 90°C single droplet evaporating in a 30°C, 1 atmosphere quiescent environment. Two fuels are shown—a 7 species multicomponent "gasoline" called syn. fuel and a single-component fuel, KIVA gasoline.

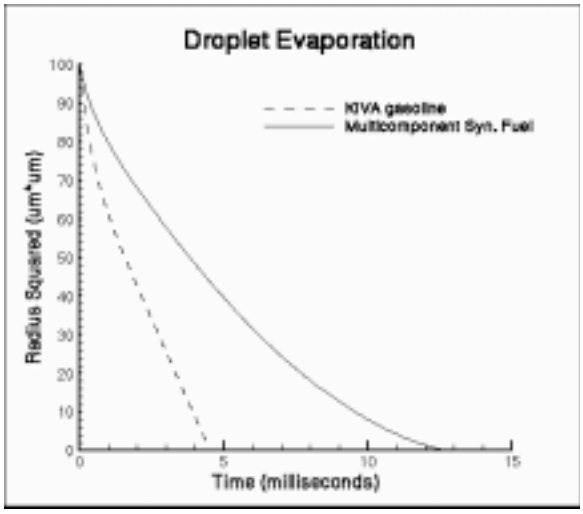

Figure 2. Droplet radius squared versus time for a 90°C single droplet evaporating in a 120°C, 2.6 atmosphere quiescent environment. Two fuels are shown—a 7-species multicomponent "gasoline" called syn. fuel and a single-component "gasoline", KIVA gasoline.

transients and liquid sheet breakup affect the overall spray behavior.

Much of our effort the past year has been devoted to developing the multicomponent model. We show that a multicomponent fuel behaves much differently than a single-component fuel by comparing single droplet evaporation and 2-D axisymmetric spray calculations.

Figure 1 shows how a multicomponent fuel blend (syn. fuel - composed of iso-pentane, cyclohexane, iso-octane, toluene, ethylbenzene, n-decane, and napthalene) designed to mimic gasoline (Greenfield et. al. 1998) compares with a single component "KIVA gasoline" used in the past to model gasoline. The 20 micron diameter droplet temperature was initially 90°C and evaporates in a 30°C, quiescent, 1 atmosphere environment. The multicomponent syn. fuel evaporates much more slowly than KIVA gasoline. While only the least volatile components (n-decane and napthalene) remain in the syn. fuel droplet after 40 milliseconds, these components allow the droplet to survive for 300 milliseconds (30 times longer than the single component KIVA gasoline). Figure 2 shows the same syn. fuel and KIVA gasoline droplet at 90°C which now evaporates in a 120°C, quiescent, 2.6 atmosphere environment. In this environment, the syn. fuel droplet evaporates faster, but still at a rate 2.5 times slower than the KIVA gasoline droplet. The dramatically different rates of evaporation between the single-component and multicomponent droplets have significant implications in predicting where and when the vapor fuel cloud will be available for combustion.

Figures 3 and 4 show a 2-D axisymmetric spray calculation of 90°C syn. fuel and KIVA gasoline respectively injected into a 1 atmosphere, 30°C chamber full of air. We see dramatic differences in how the spray behaves. The KIVA gasoline spray penetrates further and its spray angle has been reduced. The KIVA gasoline fuel vapor cloud is also more concentrated near the spray axis. The vapor cloud from the syn. fuel is more disperse and dilute.

Figures 5 and 6 show a 2-D axisymmetric spray calculation of 90°C syn. fuel and KIVA gasoline respectively injected into a 2.6 atmosphere, 120°C chamber full of air. Although the increased pressure reduces the spray penetration for both fuels (compared to Figures 3 and 4), we see that KIVA gasoline continues to penetrate further than syn. fuel. Significant differences in the fuel vapor cloud concentration and location are again evident.

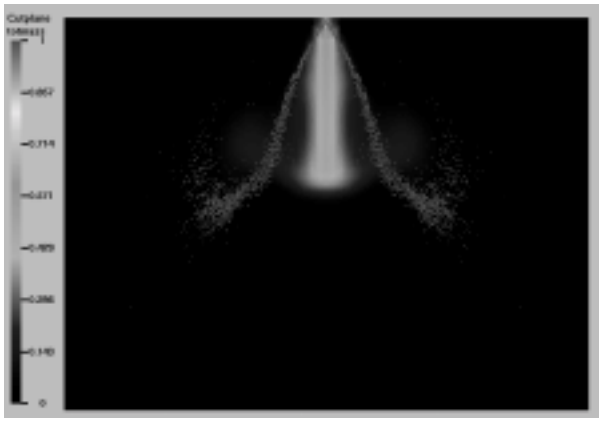

Figure 3. Spray droplets and total fuel vapor mass fraction for 90°C multicomponent syn. fuel injected into a 30°C, quiescent, 1 atmosphere axisymmetric chamber.

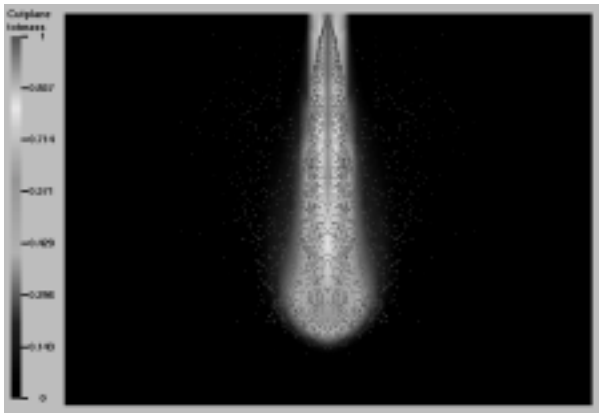

Figure 4. Spray droplets and total fuel vapor mass fraction for 90°C KIVA gasoline injected into a 30°C, quiescent, 1 atmosphere axisymmetric chamber.

Figure 5. Spray droplets and total fuel vapor mass fraction for 90°C multicomponent syn. fuel injected into a 120°C, quiescent, 2.6 atmosphere axisymmetric chamber.

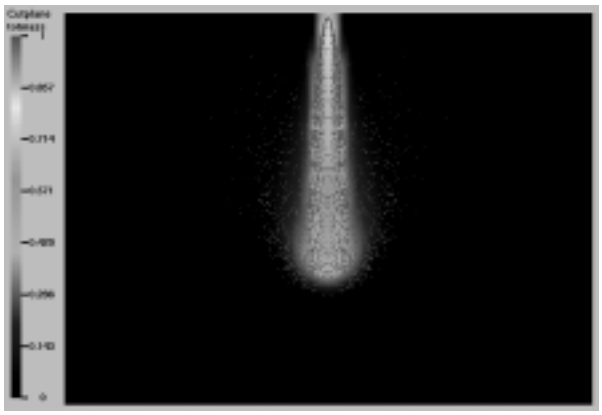

Figure 6. Spray droplets and total fuel vapor mass fraction for 90°C KIVA gasoline injected into a 120°C, quiescent, 2.6 atmosphere axisymmetric chamber.

Conclusions

We have continued to compare KIVA-3V computational and experimental results. Work needs to be done in matching experimental spray morphology and evolution. The main difficulty in matching the spray is that KIVA-3V's spray model (Han et al 1997) characterizes the injector based only on injector pressure, injector diameter, and cone angle. Such a reduced number of injector parameters may be insufficient to describe the spray emitted from the interior of a GDI injector.

We have developed a multicomponent fuel model and implemented the model into the spray and wall film submodels of KIVA-3V. We have published a paper describing the preliminary model and have presented our results at conferences. We are presently using the multicomponent model in 3-D engine simulations. Numerical simulations show dramatic differences in how multicomponent and single-component fuels behave. We believe that the automotive industry would benefit from adopting a multicomponent fuel model in their engine computations due to the large differences we encountered when comparing multicomponent and single-component fuels. It simply does not suffice to average the multicomponent fuel species properties to generate a single-component fuel.

References

1. Amsden, A.A., O'Rourke, P.J., and Butler T.D., "The KIVA-II Computer Program for Chemically Reactive Flows with Sprays," Los Alamos National Laboratory LA-11560-MS (1989).
2. Greenfield, M.L., Lavoie, G.A., Smith, C.S., Curtis, E.W., "Macroscopic Model of the D86 Fuel Volatility Procedure," SAE Paper 982724 (1998).
3. Han, Z., Parrish, S., Farrell, P.V., and Reitz, R.D., "Modeling Atomization Processes of Pressure-Swirl Hollow-Cone Fuel Sprays," *Atomization and Sprays* **7**, 663 (1997).
4. O'Rourke, P.J. and Amsden, A.A., "A Particle Numerical Model for Wall Film Dynamics in Port-Injected Engines," SAE Paper 961961 (1996).
5. O'Rourke, P.J. and Amsden, A.A., "A Spray/Wall Interaction Submodel for the KIVA-3 Wall Film Model," SAE Paper 2000-01-0271 (2000).
6. Zeng, Y., and Lee, C.F., "Modeling of Spray Vaporization and Air-Fuel Mixing in Gasoline Direct-Injection Engines," SAE Paper 2000-01-0537 (2000).

E. Active Flow Control for Maximizing the Performance of Internal Combustion Engines

Harold J. Schock (Primary Contact), Alvin Goh, Giles J. Brereton, Tom I-P Shih, Manoochehr M. Koochesfahani
Automotive Research Experiment Station
Michigan State University
East Lansing, Michigan 48824
(517) 353-9328, fax: (517) 432-334, e-mail: schock@egr.msu.edu

DOE Program Manager: Rogelio Sullivan
(202) 586-8042, fax: (202) 586-1600, e-mail: Rogelio.Sullivan@ee.doe.gov

Objectives

- Develop an understanding of the factors that influence the performance of a stratified charge (SC) internal combustion engine with emphasis on cycle-to-cycle variability.
- Determine how active flow control can be used to manage the air motion and fuel-air mixing in an internal combustion engine.
- Demonstrate the influence that active flow control has on the combustion process in a stratified charge engine using a 4-ohm speaker in the engine inlet system.

Approach

- Construct a motored optical engine assembly to be used to conduct evaluations of selective active flow technologies on the in-cylinder flowfield of a SC engine.
- Implement molecular tagging velocimetry to measure in-cylinder flows and develop the necessary diagnostic software to evaluate selected flow control technologies.
- Develop and implement the necessary simulation tools based on KIVA to allow for a numerical evaluation of the active flow control strategies.
- Demonstrate the influence that the most promising flow control strategy has on the variability in SC engine combustion.

Accomplishments

- The amplitude effect experiment showed that the largest amplitude (28 V) of the perturbation gave the maximum U rms and V rms reduction.
- Free-run perturbation at 270 CAD and 600 rpm showed that the effective perturbation frequency range is from 50 Hz to 400 Hz. For U rms, the best reduction case was 400 Hz. It showed about 25%-30% reduction at certain region of the flow field. As for V rms, the best reduction case was 200 Hz.
- Fixed-time perturbation from 0 CAD to 180 CAD, at 270 CAD and 600 rpm showed that the U rms was reduced about 20%-30%, when perturbed at 300 Hz and 400 Hz. As for V rms, the best reduction cases were at 400 Hz and 600 Hz.
- The sweeping perturbation experiment (sweeping frequency started at 100 Hz) showed that the U rms and V rms were reduced to about 20%. The best reduction case for U rms was sweeping from 100 Hz to 1200 Hz. The best reduction case for V rms was sweeping from 100 Hz to 800 Hz.
- The rest of the experiments for 270 CAD and 600 rpm did not show clear trends or huge U rms and V rms reductions.

Introduction

Cycle-to-cycle variation in turbulence and fuel-air-residual exhaust gas mixing is of primary importance to premix, stratified charge SIDI engines. In recent years, a significant amount of work has been done to improve the engine's performance and fuel efficiency. Recent research has shown a significant interaction between the mean flow and the fluctuating parts of the in-cylinder velocity [1]. Due to cycle-to-cycle variation, the engine fuel injector is operated to over-fuel the combustion chamber to avoid partial burns or misfires. In order to design better lean burn engines, one has to have a better understanding of the flow patterns during compression stroke and also needs to find a way to reduce cycle-to-cycle variation. If cycle-to-cycle variation is reduced, the in-cylinder flows are more predictable and thus one could employ leaner combustion without large torque variability or misfire. In return, this would improve fuel economy in engines. The ultimate goal of this study is to find a way of controlling the flow and reducing the cycle-to-cycle variation. As a result, one could provide control of the mixing and burning rates in an internal combustion engine.

The present study is intended to explore the extent to which in-cylinder fluid motion late in the compression stroke can be more regularized with less cycle-to-cycle variation using judicious acoustic excitation of shear layers adjacent to the intake valves during the intake stroke.

Approach

Optically Accessible Research Engine

A schematic of the optically accessible research engine is shown in Figure 1, and the engine specifications are listed in Table 1. This study was conducted with a 1999 model year Ford cylinder head with 4 valves and double overhead cams. The engine cylinder head was part of the left bank of a V8 prototype engine. A flat-head, optical access piston was used in the experiment. The bore and stroke were 90.2 mm and 90.0 mm, respectively. The length of the connecting rod was 150.7 mm. The cylinder used in the experiment was made from quartz so that it would be optically accessible.

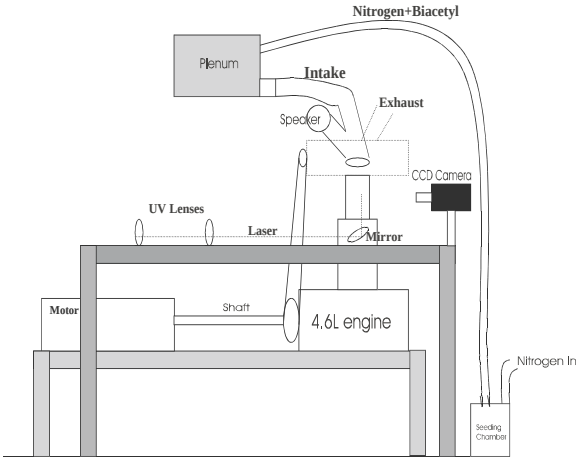

Figure 1. Schematic of the Research Engine Setup

Model and Make	Ford 4-Valve 4.6L
Bore and Stroke	90.2 mm / 90.0 mm
Connecting Rod Length	150.7 mm
Valve Activation	DOHC
Intake Valve Diameter	37.0 mm
Exhaust Valve Diam.	30.0 mm
Maximum Valve Lift	10.02 mm /120 CAD
Zero CAD	Intake TDC
Intake Valve Opening	6 CAD Before TDC
Intake Valve Closure	250 CAD After TDC
Exhaust Valve Opening	126 CAD After TDC
Exhaust Valve Closure	16 CAD After TDC
Compression Ratio	9.85 : 1
Piston Top	Flat

Table 1. Engine Specifications

The cylinder was mounted on a single-cylinder research engine that served as a reciprocating mechanism. The engine was first-order balanced in forces and moments and connected through a rubber-damped coupling to a 10 HP electrical motor. Two different belt drive setups were connected to the exhaust camshaft that would allow interchanging between the two engine stroke variants. The exhaust camshaft was linked by a roller-chain to the intake camshaft. The intake valve diameter was 37 mm and the exhaust valve diameter was 30 mm. The maximum valve lift was 10.02 mm at 120° crank angle. The valves of the investigated cylinder were the only valves activated. A 4-ohm, 4.5 inch mid-

woofer speaker was mounted at the intake manifold. The speaker power was 40 W, and it was driven by an input signal from a function generator. Before the input signal was fed into the speaker, it was amplified by a Hafler P1000 amplifier. The amplifier had a full power bandwidth of 0.1 Hz to 100 kHz.

Molecular Tagging Velocimetry (MTV) Setup

The velocity measurements were made using Molecular Tagging Velocimetry (MTV). MTV is a full-field optical diagnostic that allows for the non-intrusive measurement of a velocity field in a flowing medium. For gas-phase applications, MTV uses nitrogen as a working fluid and biacetyl as a long-lived luminescence tracer mixed with the nitrogen [6]. A pulsed UV laser is used to tag the flow in the regions of interest. The regions of interest are imaged at two successive times using a CCD camera. The measured Lagrangian displacement vector and the time over which the displacement occurred provide the velocity vector. For MTV, a Lambda Physik LPX 210i UV (308nm) laser operating at approximately 290 mJ (20 kV) provided the energy to generate phosphorescence from a working fluid mixture of nitrogen and biacetyl. Figure 2 shows the optical setup for the experiment. In order to measure the velocity field throughout a region, a series of vertical and horizontal laser lines were generated. These lines were orthogonal to each other. At this point, images were recorded by the intensified CCD camera. These images were considered as reference images. At certain delay later (normally it was about 200 microseconds for 270 CAD measurement) the tagged region was recorded again using the intensified CCD camera. These images were considered as delayed images. Post-processing by correlation-based techniques allowed the instantaneous planar velocity field to be deducted from the reference and delayed images. The MTV experiments were done with a field of view approximately 5 cm x 5 cm. The top of the grids was located about 1 cm below the intake and exhaust valves, and the edges of the grids were about 2 cm from the cylinder wall. The incoming laser beam was first split to form horizontal and vertical beams. Each laser beam was focused using a combination of two cylindrical lenses with focal lengths of 150 mm and 50 mm. By going through these two lenses, a very thin laser sheet was

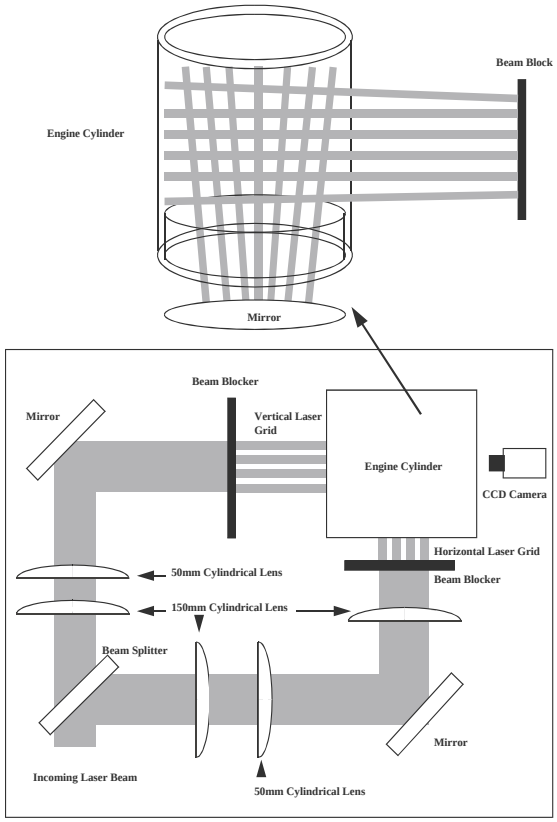

Figure 2. Optical Setup for the Experiment

generated for each beam. Beam blockers with series of thin slits cut through them were used in each beam path to generate a series of 12 lines for the horizontal and 15 lines for the vertical.

Data Acquisition and Processing

A Xybion CCD video camera, model ISG-350 with a Nikkor 50mm f1.2 lens was used to take images in the experiment. An engine encoder was coupled to the camshaft to produce a 5-V TTL signal at a desired crank angle. The signal was then used to trigger the laser. The delay time for the laser beam to reach the engine cylinder was 1.3 microseconds. The software used together with the acquisition board was the MV-1000 Grab Sequence Application version 1.3 for Windows NT. A total of 500 instantaneous velocity fields were measured for each measurement condition. A convergence experiment was conducted to determine the number of instantaneous realizations needed to produce a good average. The results showed that 500 instantaneous realizations were sufficient to produce a good average.

The data processing process was performed using an in-house code developed over the past few years. When processing the data, the main objective was to determine the displacement vector of the tagged regions with the highest possible sub-pixel accuracy in order to increase the dynamic range of the velocity measurements. The displacement of the tagged regions was determined using a direct digital spatial correlation technique. The details of this approach can be found in Gendrich and Koochesfahani 1996 [2]. The basic idea of this approach is that a small window called a source window is selected from a tagged region in the reference or zero-delay image. It is then spatially correlated with a larger roam window in the delayed image. A well-defined correlation peak occurs at the location corresponding to the displacement of the tagged region by the flow. The displacement peak is found by using a multi-dimensional polynomial fit.

Results and Discussion

The experiment was carried out at an on engine speed of 600 rpm, at 270 CAD. The reason 270 CAD was chosen is because in-cylinder preflame air motion has been known to have a dominant effect on the firing behavior of internal combustion engines [3,4,5]. The flow patterns during compression stroke influence the succeeding combustion of SIDI engines.

An experiment was performed to determine the amplitude effect of the acoustic perturbations. The experiment was done on three different amplitude cases with the engine running at 600 rpm and perturbation at 50 Hz. The three different amplitudes included a small amplitude of 675 mV, a medium amplitude of 10 V and a large amplitude of 28 V. The crank angle of investigation was at 270 CAD. The results of the experiment showed that as the amplitude of the perturbation increased, the U rms and V rms were reduced. In other words, the trend of the experiment was the higher the amplitude, the lower the cycle-to-cycle variation. As for the U mean and V mean, the results showed that there were some changes in their means as the amplitude increased, but the increments were small. Thus, from the experiment, the highest amplitude (28 V) was chosen as the best parameter for the rest of the research and experiments.

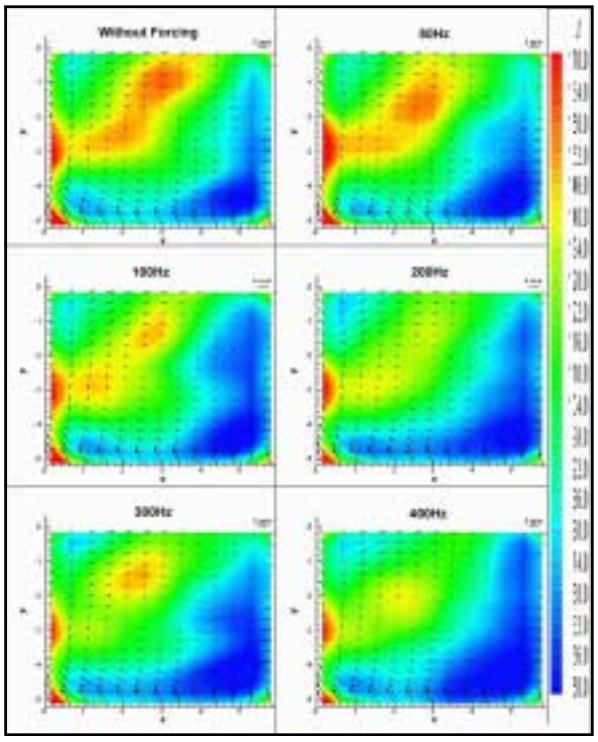

Figure 3. Free-Run Perturbation, U Mean and U rms at 600 rpm, 270 CAD

Free-run Perturbation Method

In this mode, the speaker was run freely with the engine without any timing. The perturbation was done throughout the crank angles with the desired frequency at the maximum amplitude (28 V). It was initially thought that the best cycle-to-cycle variation reduction would occur in a high frequency range, namely 1000 Hz onwards. However, from this experiment, it was found that the best reduction occurred at a lower frequency, below 400 Hz. In the experiment, the range of frequencies investigated was from 50 Hz to 4000 Hz. However, the best cases were only in the range of 50 Hz to 400 Hz. Beyond 400 Hz, there was no significant reduction in velocity rms or cycle-to-cycle variation.

Figure 3 shows the results for U mean and U rms taken from running the engine at 600 rpm, 270 CAD. The color contour shows the U rms that gives the information on the average deviation of the instantaneous flows from the U mean flow. In other words, the cycle-to-cycle variation and turbulence are reduced if the rms value is reduced. The trend of the results was as the frequency of the perturbation

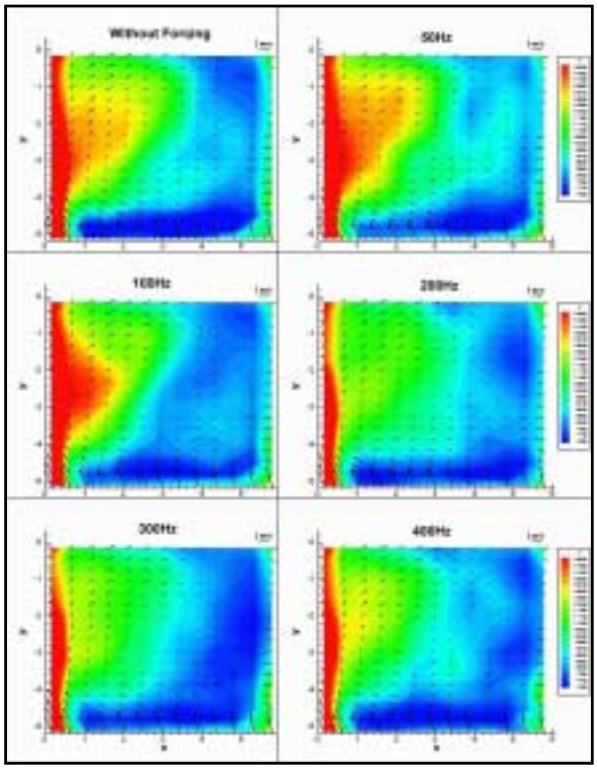

Figure 4. Free-Run Perturbation Method, V Mean and V rms at 600 rpm, 270 CAD

increased, the U rms decreased until 400 Hz. After 400 Hz, the U rms increased back again. Comparing the perturbed cases with the unperturbed case, one could notice that the contour color gets less red or yellow and becomes more green and blue. According to the color scale, the rms value is smaller when it is green or blue in color. Figure 4 shows the results for V mean and V rms. The trend of V rms was the same as with U rms. As the frequency increased, the V rms was reduced, but after 400 Hz, the V rms increased again.

Figures 5a and 5b, and 6a and 6b show graphs taken along a line at y=-1.2, about 1.2 cm below the intake and exhaust valves. It is obvious that the perturbation did not effect the U mean and V mean. The U mean and V mean stayed about the same values throughout all frequencies. However, the perturbation had huge effect on the U rms that represents the cycle-to-cycle variation and fluctuating velocity field. As the frequency increased, the U rms decreased. The largest reduction among all was the 400 Hz case. It showed about 25% to 30% reduction at certain region of the

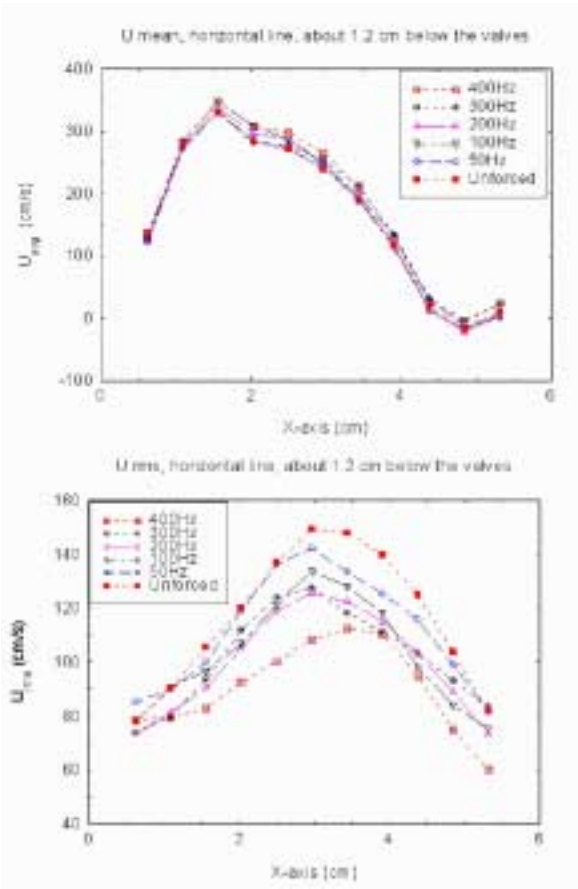

Figure 5. Effect of Perturbations on the U Mean and U rms at Horizontal Line about 1.2 cm below the Intake and Exhaust Valves

flow field. As for V rms, the reduction was only about 20%, and the best case was again 400 Hz.

Fixed-time Perturbation Method

In this experiment, the starting and ending points of the perturbation were timed. The timing of the perturbation was done by using the burst mode of a function generator. The speaker would only start perturbing when the piston reached Top Dead Center (TDC). It would continue to perturb from 0 CAD to 180 CAD and then stop when the piston reached 180 CAD. The engine condition was the same as in the previous experiment. The experiment was done at 600 rpm and 270 CAD. The range of frequencies investigated was from 50 Hz to 4000 Hz. Each frequency case had an average from 500 continuous, instantaneous flows. The reason of choosing the frequency range was based on the previous experiment (free-run experiment). From the

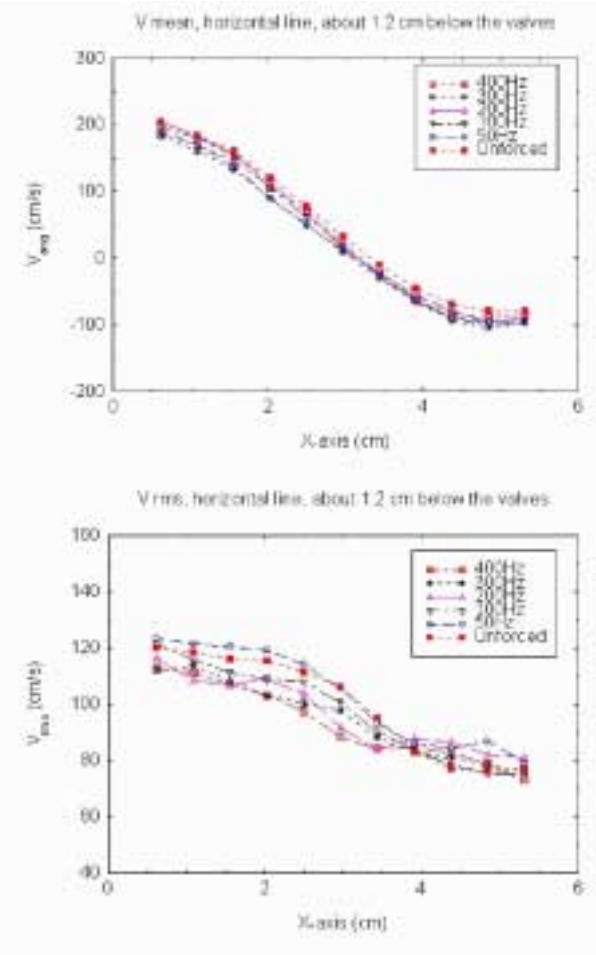

Figure 6. Effect of Perturbations on the V Mean and V rms at Horizontal Line about 1.2 cm below the Intake and Exhaust Valves

experiment, it was found that the perturbation had no effect beyond 4000 Hz or below 50 Hz. The results had the same trend as the free-run results. There was a noticeable reduction in U rms and V rms at 300 Hz and 400 Hz. The reduction was about 20%-30%. As the frequency increased, the U rms and V rms decreased until 400 Hz, and it increased at frequencies over 400 Hz. In the previous free-run perturbation experiment, the U mean and V mean of the flow did not change for cases with or without perturbation. However, for this fixed-time perturbation, the U mean and V mean of the flow decreased in velocity. They appeared to be slowing down with the perturbation. See Figure 7 for more information.

Figure 8 shows results for V mean and V rms taken at 600 rpm and 270 CAD. Each of the frequency cases had an average of 500 instantaneous flows. The

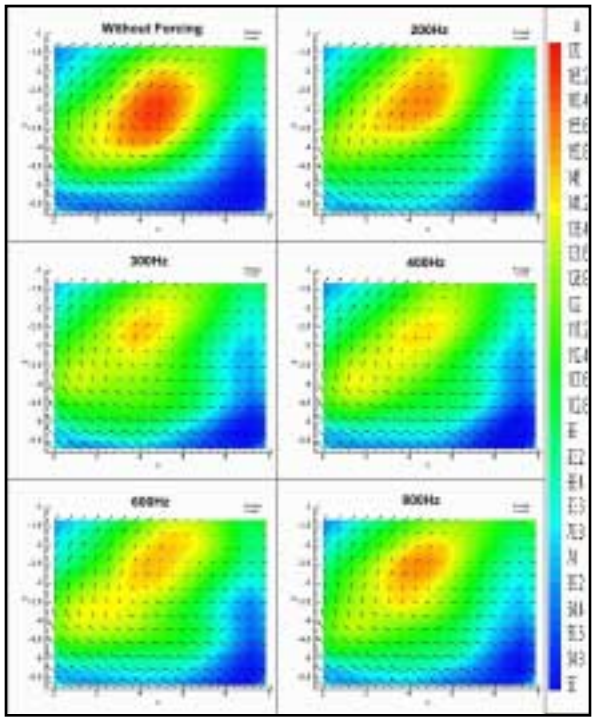

Figure 7. Fixed-Time Perturbation Method, U Mean and U rms at 600 rpm, 270 CAD

results did not show any clear trend as found in U mean and U rms previously. They appeared to have less rms reduction compared with U mean and U rms. The best V rms reduction cases were 400 Hz and 600 Hz. Figures 9a and 9b show graphs taken along a line at y=-3.1, about 3.1 cm below the intake and exhaust valves. From the graphs, it is obvious that the perturbation had some effects on the U mean flow. The U mean decreased as the frequency increased. In some places of the flow, the U mean decreased as much as 70% to 80% of the unperturbed flow. The flow direction had changed too in some places of the flow. As for the U rms, the perturbation had a huge effect on the U rms that represents the cycle-to-cycle variation and fluctuating velocity field. As the frequency increased, the U rms decreased until 400 Hz and then it increased beyond 400 Hz. The largest reductions were at 300 Hz and 400 Hz. In the 300 Hz case, it showed about 20% to 30% reduction at certain region of the flow field.

Figures 10a and 10b show that the perturbation had some effects on the V mean flow, the same effects that could be found on U mean flow. The V mean decreased as the frequency increased. In some places of the flow, the V mean decreased as much as 40% to 50% of the unperturbed flow. As for the V

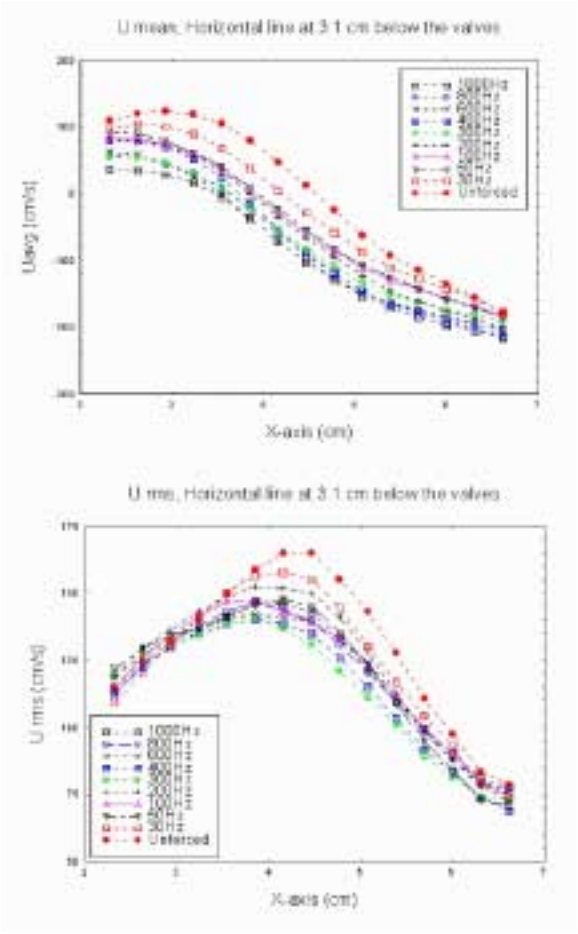

Figure 8. Effect of Perturbations on the U Mean and U rms at Horizontal Line about 3.1 cm below the Intake and Exhaust Valves

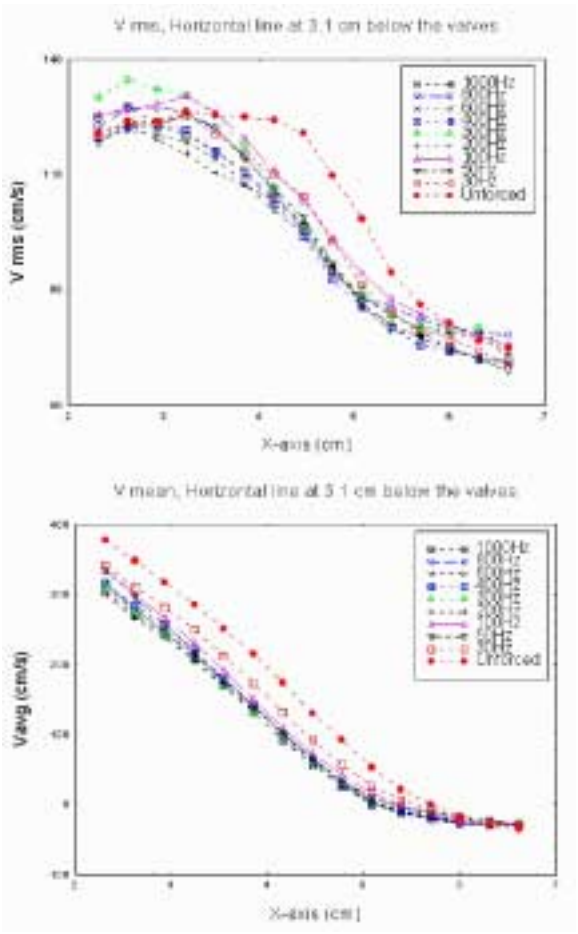

Figure 10. Effect of Perturbations on the V Mean and V rms at Horizontal Line about 3.1 cm below the Intake and Exhaust Valves

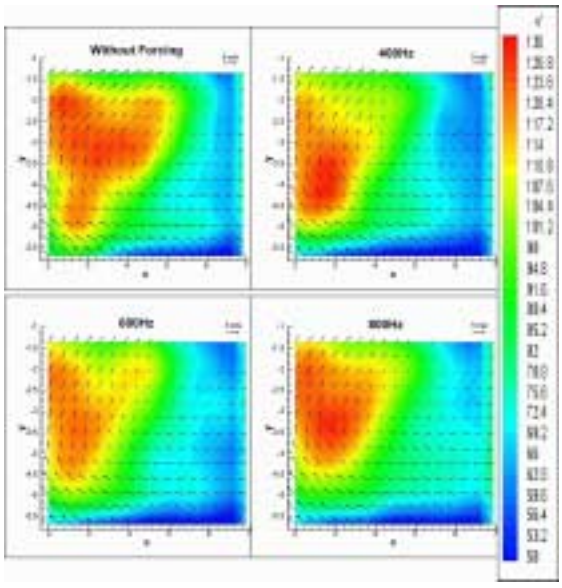

Figure 9. Fixed-Time Perturbation Method, V Mean and V rms at 600 rpm, 270 CAD

rms, the perturbation had some effects on the V rms too. As the frequency increased, the V rms decreased until the frequency reached between 400 Hz and 600 Hz. It increased beyond 600 Hz. The largest reductions were all at 400 Hz and 600 Hz. In the 400 Hz case, it showed about 20% to 30% reduction at certain region of the flow field.

Sweeping Perturbation Method (sweeping frequencies from 100 Hz to 2000 Hz)

This experiment was done with the sweeping mode of the function generator. As in the previous experiments, all the perturbation frequencies were fixed. For example, when the flow was said to be perturbed at 400 Hz, it was done by perturbing the flow constantly at 400 Hz throughout the experiment using free-run method or fixed-time method. However, in this experiment, the perturbed

frequencies increased linearly but at a fixed starting point of perturbation, which was at TDC. Each case of experiment was done by perturbing the flow starting at 100 Hz and then sweeping linearly to the respective end frequency. Nevertheless, the duration of the sweeping was still only from 0 CAD to 180 CAD. In the case of the engine running at 600 rpm, the duration of sweeping was 0.05 seconds.

This experiment was necessary because the intake valves opened in a linear manner during the intake stroke. If the perturbation were fixed at a certain frequency, the flow would not be perturbed at that frequency during the period of the valves opening. In order to improve the maximum effect of the perturbation to the flow, the perturbation was done by sweeping the frequencies linearly. The range of frequencies investigated in the experiment was from 200 Hz to 2000 Hz. The first case of sweeping frequencies was sweeping from 100 Hz to 200 Hz, and the last case was sweeping from 100 Hz to 2000 Hz.

The cases investigated were as follows:

sweeping from 100 Hz to 200 Hz
sweeping from 100 Hz to 300 Hz
sweeping from 100 Hz to 400 Hz
sweeping from 100 Hz to 600 Hz
sweeping from 100 Hz to 800 Hz
sweeping from 100 Hz to 1000 Hz
sweeping from 100 Hz to 1200 Hz
sweeping from 100 Hz to1400 Hz
sweeping from 100 Hz to 1600 Hz
sweeping from 100 Hz to 1800 Hz
sweeping from 100 Hz to 2000 Hz

The range of U rms and V rms reductions were from 20% to 25% in the experiment. The best reduction case for U rms was sweeping from 100 Hz to 1200 Hz, and the best reduction case for V rms was sweeping from 100 Hz to 800 Hz. Figures 11 and 12 show the results. The U mean and V mean did not change much.

Conclusions

- The amplitude effect experiment showed that the largest amplitude (28 V) of the perturbation gave the maximum U rms and V rms reduction.

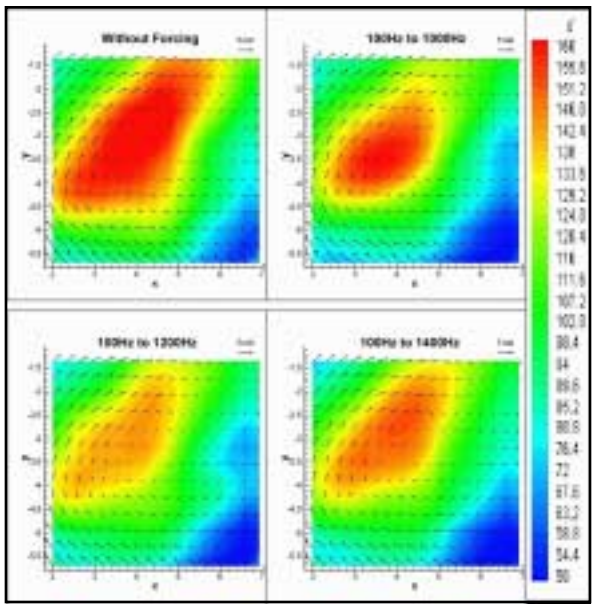

Figure 11. Sweeping Perturbation Method, U Mean and U rms at 600 rpm, 270 CAD

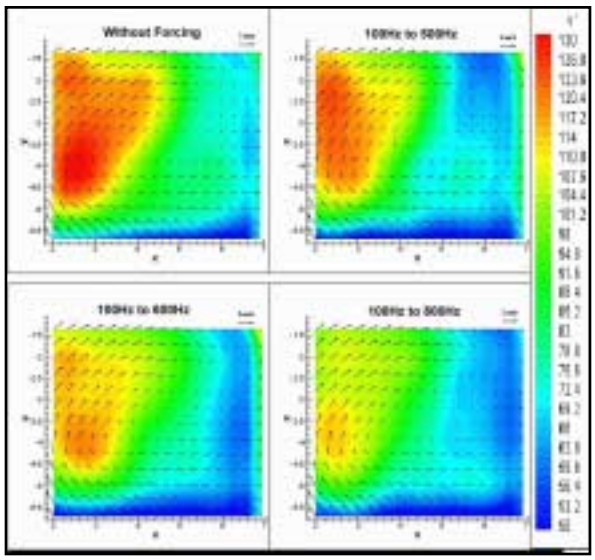

Figure 12. Sweeping Perturbation Method, V Mean and V rms at 600 rpm, 270 CAD

- Free-run perturbation at 270 CAD and 600 rpm showed that the effective perturbation frequency range is from 50 Hz to 400 Hz. For U rms, the best reduction case was 400 Hz. It showed about 25%-30% reduction at certain region of the flow field. As for V rms, the best reduction case was 200 Hz.
- Fixed-time perturbation from 0 CAD to 180 CAD, at 270 CAD and 600 rpm showed that the U rms was reduced about 20%-30%,

when perturbed at 300 Hz and 400 Hz. As for V rms, the best reduction cases were at 400 Hz and 600 Hz.

- The sweeping perturbation experiment (sweeping frequency started at 100 Hz) showed that the U rms and V rms were reduced to about 20%. The best reduction case for U rms was sweeping from 100 Hz to 1200 Hz. The best reduction case for V rms was sweeping from 100 Hz to 800 Hz.
- The rest of the experiments for 270 CAD and 600 rpm did not show clear trends or huge U rms and V rms reductions.

Acknowledgments

This research work was financially supported by the Ford Motor Company and Michigan State University in addition to the U.S. Department of Energy.

References

1. Hascher, H. G., Jaffri, K., Novak, M., Lee, K., Schock, H., Bonne, M., Keller P., "An Evaluation of Turbulent Kinetic Energy for the In-cylinder Flow of a Four-Valve 3.5L SI Engine Using 3-D LDV Measurements," SAE 970793, 1997.
2. Gendrich, C. P. and Koochesfahani, M. M., "A Spatial Correlation Technique for Estimating Velocity Fields Using Molecular Tagging Velocimetry," Experiments in Fluids, Vol. 22, pp. 67-77, 1996.
3. Lancaster, D. R., Krieger, R. B., Sorenson, S. C., and Hull, W. L., "Effects of Turbulence on Spark-Ignition Engine Combustion," SAE Paper 760160, 1976.
4. Davis, G. C., Tabaczynski, R. J., Beire, R. C., "The Effect of Intake Valve Lift on Turbulence Intensity and Burn Rate in SI Engines," SAE Paper 840030, 1984.
5. Hascher, H. G., Novak, M., Stuecken, T., Schock, H. J., and Novak, J., "The 3-D In-Cylinder Charge Motion of a Four-Valve SI Engine under Stroke, Speed and Load Variation," SAE 2000-01-2798, 2000.
6. Stier, B. and Koochesfahani, M. M., "Molecular Tagging Velocimetry (MTV) Measurements in Gas Phase Flows," Experiments in Fluids, Vol. 26, pp. 297-304, 1999.

III. ENGINE AND COMPONENT R&D

A. Development of Near-Frictionless Carbon Coatings for SIDI Fuel System Components

George R. Fenske (Primary Contact), Oyelayo Ajayi, John Woodford, Ali Erdemir, and Jeff Hershberger
Argonne National Laboratory
9700 S. Cass Ave.
Argonne, Illinois 60439
(630) 252-5190, fax: (630) 252-4798, e-mail: gfenske@anl.gov

DOE Program Manager: Rogelio Sullivan
(202) 586-8042, fax: (202) 586-1600, e-mail: Rogelio.Sullivan@ee.doe.gov

Objectives

- Develop low-friction, highly wear-resistant coatings for critical engine components needed to meet national emission goals, most notably fuel injection and valvetrain components for spark-ignited direct-injected (SIDI) gasoline engines.
- Evaluate the friction and wear resistance of Argonne's Near-Frictionless Carbon (NFC) coatings in tests simulating service conditions of SIDI engine components.
- Tune deposition parameters to optimize performance of NFC coatings on critical components in SIDI engines.

Approach

- Perform benchtop wear tests under conditions of load, speed, etc. which simulate service conditions of SIDI engine components.
- Apply coatings and perform wear tests on production fuel injector plungers.
- Use very-long-term (1 million cycle) wear tests to determine rates and mechanisms of wear which occur in extended service lifetimes.
- Introduce a variety of production gasolines into the wear contacts to include chemical interactions experienced in working engines.
- Investigate both conventional and reformulated gasolines.
- Characterize worn surfaces and determine failure mechanisms.
- Use advanced analytical techniques and post-testing characterization to guide optimization of NFC coating parameters and to recommend other surface treatments which may also improve component longevity.
- Upgrade custom-built benchtop Fretting Tester system to enable testing under the ISO12156 fuel lubricity standard.
- Perform Ball-On-Three-Disc (BOTD) industry standard wear tests on steel discs in gasolines and compare the data to the results of injector tests.

- Analyze gasoline wear debris using Scanning Electron Microscopy (SEM), Energy Dispersive Analysis of X-rays (EDAX), and Transmission Electron Microscopy (TEM).

Accomplishments

- Optimized NFC deposition plasma parameters for coating thickness on production fuel injectors.
- Modified Fretting Tester to hold a production fuel injector as a wear counterface instead of a steel ball.
- Completed a matrix of 1-million-cycle lifetime wear tests comparing the performance of fuel injector tips with two NFC coatings to uncoated fuel injector tips.
- Performance of NFCs were investigated in seven varieties of gasoline in addition to the baseline ethanol.
- Completed a matrix of BOTD comparisons to fuel injector tests in the same fuels.
- Upgraded Fretting Tester to ISO12156 compliance.

Introduction

Spark-ignited, direct-injected (SIDI) engines are being developed because of their ability to meet stringent emission standards, their potential for high fuel efficiency, and their relatively mature state of commercial development. Such engines will operate at higher injection pressures than today's port-injected engines and will utilize low-sulfur fuels that are being marketed to protect catalytic emission control devices. The tighter tolerances required on fuel delivery components to inject at higher pressures (e.g. approx. 100 bar vs. 4 to 5 bar for port injection) coupled with the low lubricity of gasoline (especially low-sulfur gasoline) will require advanced fuel delivery system designs and materials to meet reliability and durability goals.

Approach

The guiding principle of this project is to develop NFC coatings for SIDI engine applications via thorough wear testing and understanding of the wear mechanisms. The current year of effort builds upon the accomplishments of the previous year, where test materials and prototype engine components were successfully coated with NFC and the deposition parameters given initial adjustment. NFC coatings on steel balls and flats provided great improvements over uncoated metals in wear tests in gasoline, indicating compatibility of the coating with the conditions encountered in the engine environment. This year, development of the NFC coating for SIDI engines has focused on wear testing of production fuel injection parts, extension of tests to one-million-cycle lifetime duration, and exploration of what effects the next-generation fuels needed for working SIDI engines will have on the wear couples.

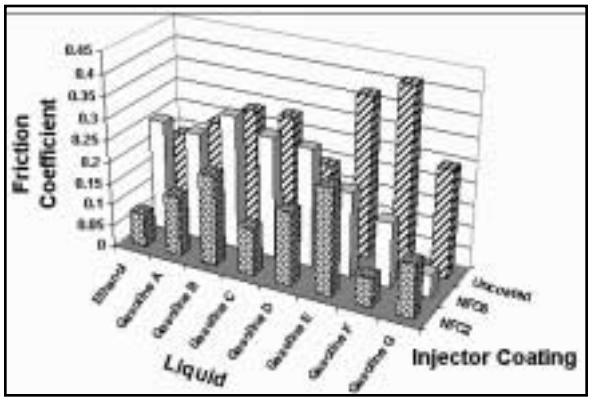

Figure 1. Friction of NFC-Coated and Uncoated Fuel Injectors in Several Gasolines

The central set of results discussed below are the friction and wear data from one-million-cycle wear tests of NFC2-coated, NFC6-coated, and uncoated fuel injectors in seven reformulated gasolines plus ethanol. The fuels used include summer and winter blends, premium and regular octane levels, and some contain additives under consideration for future blends. These friction and wear data are shown in Figures 1-4. Complementing this information are the industry standard BOTD fuel lubricity tests performed on uncoated discs in Figures 5-6. Further forensic examination of wear couples aids

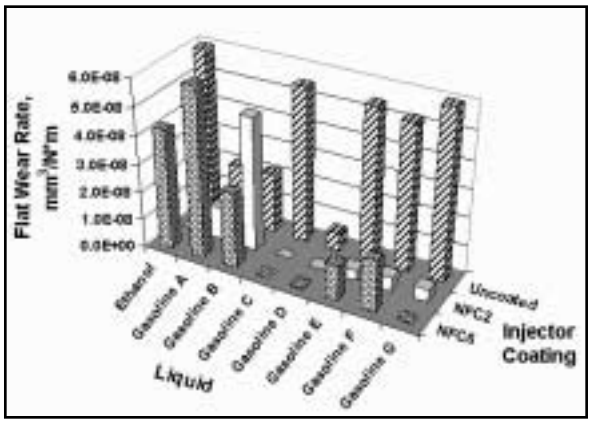

Figure 2. Wear Rate of Steel Flats Worn Against NFC-Coated and Uncoated Fuel Injectors in Several Gasolines

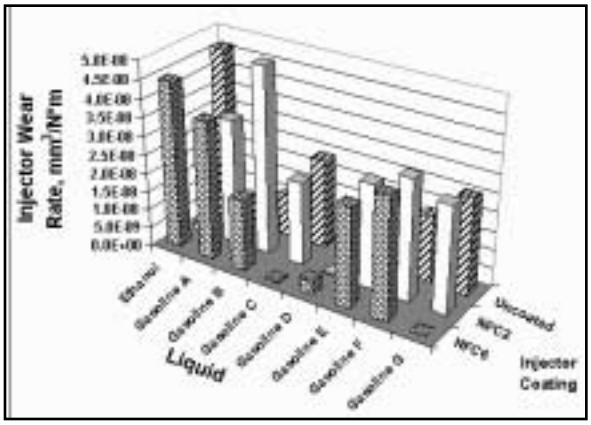

Figure 3. Wear Rate of NFC-Coated and Uncoated Fuel Injectors in Several Gasolines

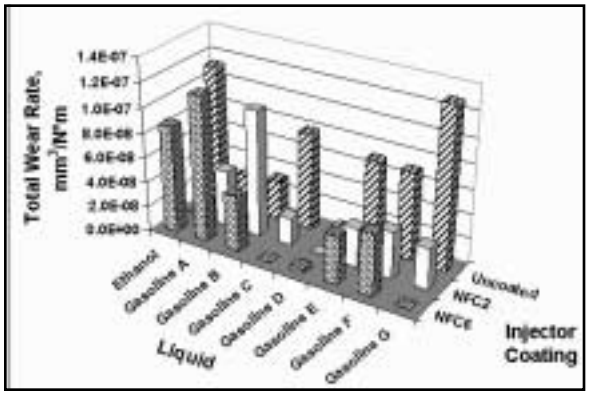

Figure 4. Combined Wear Rate of Steel Flats and Counterfaces of NFC-Coated and Uncoated Fuel Injectors Worn in Several Gasolines

Surface treatment	Friction coefficient average	Improvement
Uncoated	0.29	
NFC6	0.22	27% reduction over uncoated
NFC2	0.15	48% reduction over uncoated

Table 1. Friction for Three Surface Treatments Averaged over Seven Gasolines

interpretation of friction and wear data; microscopy and other characterization results are shown in Figures 7-10.

Trends in the friction data may be found by studying the averages of friction results for each coating over the seven gasolines used, and by averaging the friction results for each gasoline over the three coatings used. Table 1 shows the friction result for each of the three surface treatments averaged over the seven gasolines.

The NFC coatings provide clear improvements in friction over the uncoated fuel injectors. NFC6 gives 27% lower friction, while use of NFC2 results in a friction reduction of nearly a factor of two. This has important ramifications for part longevity, such as reducing local heat buildup at the contact point and the tendency to bind in close tolerances. Examining the other friction results, averaging the three coatings for each gasoline, gives tightly grouped numbers, each of which carries a large standard deviation. In other words, the major factor influencing friction is the coating, not the gasoline. Notable exceptions are ethanol and Gasoline G, which provide relatively low friction.

Similarly, trends in the wear data may be observed by averaging results for each coating over the seven gasolines, and by averaging the results for each gasoline over the three coatings. Attention to the differences between injector wear, flat wear, and the total wear reveal additional information. Table 2 shows the trends.

Applying NFC coatings on the injectors again provided clear improvements in total wear rate and wear rate of the flats compared to the uncoated injectors. These improvements ranged from an over one-third reduction of wear to over a factor of four

Surface treatment	Flat wear reduction	Injector wear reduction	Total wear reduction
Uncoated	Worst flat wear	-47% from NFC2	Worst total wear
NFC6	-56% from uncoated	-40% from NFC2	-39% from uncoated
NFC2	-77% from uncoated	Worst injector wear	-36% from uncoated

Table 2. Wear Rates for Three Surface Treatments Averaged over Seven Gasolines, Stated in Terms of Reduction from Worst Case

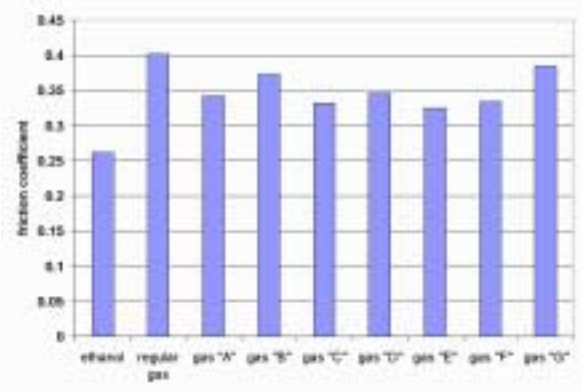

Figure 5. Friction in BOTD Lubricity Tests on Uncoated Steels in Several Gasolines

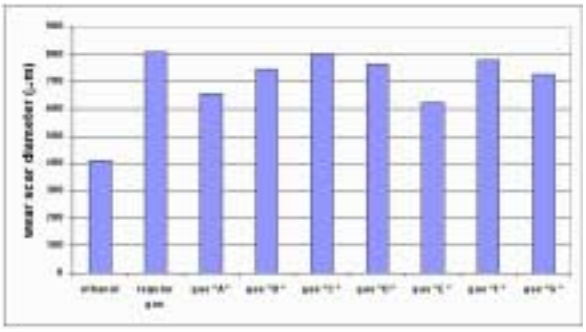

Figure 6. Wear Scar Diameter in BOTD Lubricity Tests in Several Gasolines

wear reduction. In the case of the coated injectors themselves, NFC6 provided a wear rate very similar to that of the uncoated surface while the NFC2 coating wore significantly faster than NFC6 and the uncoated part. Taking into account the extremely low friction provided by NFC2 in the tests, we may speculate that the NFC2 may be slowly sacrificing itself in order to reduce both friction and counterface wear. In contrast, NFC6 provides reductions of both friction and wear non-sacrificially. To consider the other wear results, averaging the three coatings for each gasoline, we see trends similar to that in the friction. Wear rate averages are tightly grouped but the averaged numbers (for different coatings) are highly variable. Gasolines A and B and ethanol produced somewhat higher wear on both flats and injectors, while Gasolines C and D lowered wear, but in general, the major factor influencing wear is the surface treatment, not the gasoline.

The BOTD test results shown in Figures 5 and 6 were produced on a Falex BOTD machine modified to provide output of friction data to a computer. The BOTD test is an industry standard which specifies a test duration, load, and an amount of fuel to be used. All tests were performed on uncoated steel discs, per the standard specification, to provide a measure of the lubricity of the gasoline. The friction and wear results are quite consistent, with fuels providing low friction also providing low wear. However, the differences in friction and wear among the fuels are relatively small. This is consistent with the observations above, that the gasoline is not the major factor influencing wear. At first glance, the friction and wear results appear inconsistent with the observations above regarding the effects of the gasolines on friction and wear rate for injector-on-flat contacts. However, closer examination of the data reveals that the differences are a result of inclusion of the coated materials in the previous results. Taking into account only the data from the uncoated injectors, to match the uncoated BOTD discs, results in a high degree of consistency between the two sets of results.

Figures 7 through 9 show the results of the advanced analytical techniques used to characterize the wear contact area. Figure 7 is a top-down view of a 3-D optical micrograph of a wear scar on an injector; the low areas are dark colors while the high areas are light. The curvature of the spherical injector tip has been mathematically removed, changing the image from a curved surface with a flat scar to a flat surface with a bowl-shaped scar. This aids visualization and quantification of the wear volume. In this image, the boundary between the coating and the substrate is clearly visible; the coating has worn smoothly, while the areas of exposed steel and the coating next to it are rough. Only a very small amount of substrate has been worn off in this experiment. Figure 8 is a standard optical

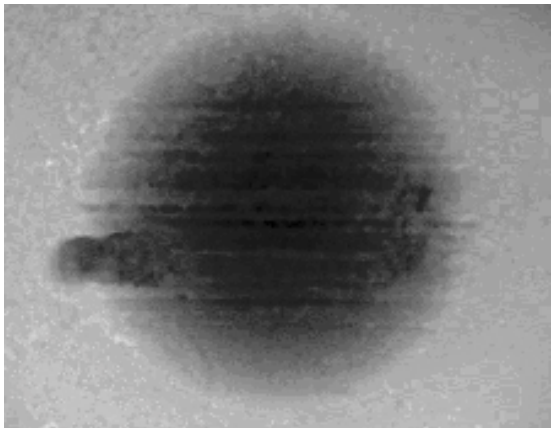

Figure 7. 3-D Optical Micrograph of a Wear Scar on an NFC-Coated Fuel Injector after a 1-million Cycle Lifetime Test

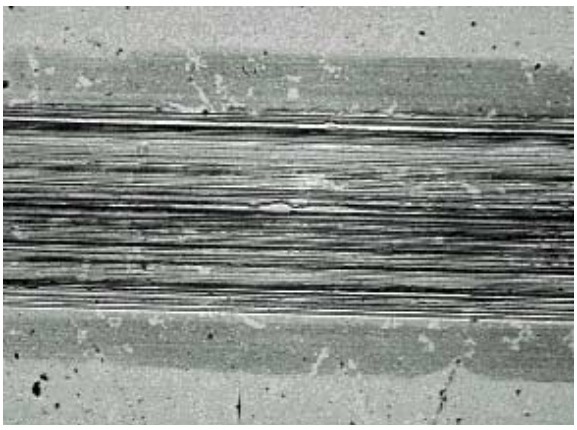

Figure 8. Optical Micrograph of Steel Flat Worn Against NFC-Coated Injector Shown in Figure 7 (above)

micrograph of the steel flat worn by that injector. Again the differences between the areas worn by NFC and the areas worn by the exposed substrate are clearly visible, despite the fact that the entire sample shown is steel. Figure 9 shows the friction trace of this test, indicating a sharp momentary rise in friction when the fresh steel substrate was exposed at approximately cycle 500,000. Figure 10 shows a set of Raman spectroscopy scans used to interpret the results of a different test. The response from the NFC coating on a worn injector is shown, which was substantially the same as the response from an unworn injector area. From this we know that the atomic structure of the NFC is not changed by the wear process. The response from the exposed substrate steel of the injector tip was also similar to that of the worn steel flat. A fragment of wear debris on the flat was also scanned, revealing it to be NFC.

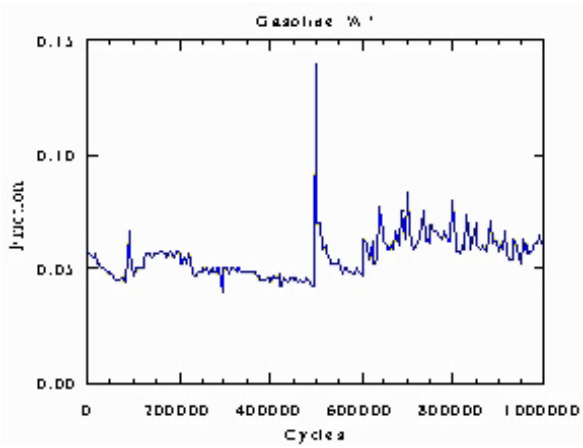

Figure 9. Friction Trace of 1-million Cycle Lifetime Test of Figures 7 and 8 (above)

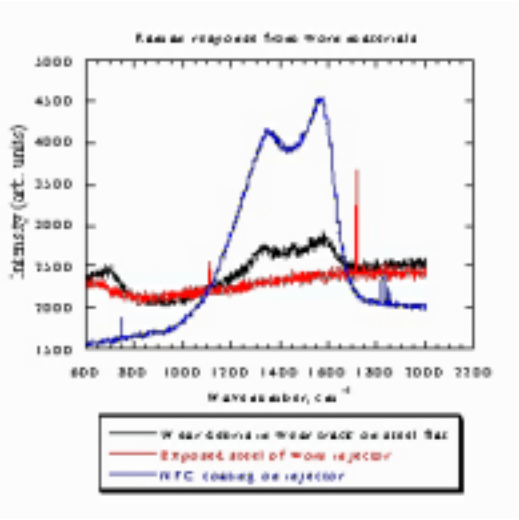

Figure 10. Raman Spectroscopy of NFC-Coated Injector, Steel Counterface, and Wear Debris after 1-million Cycle Lifetime Test

Conclusions

Argonne's NFC coatings have now been shown to provide outstanding benefits of friction and wear reduction for production fuel injectors in conditions simulating an operating engine environment. NFC6 reduces friction an average of 22% compared to uncoated parts while reducing the wear rate by approximately 40%. For applications where even more friction reduction and counterface wear protection is desired, NFC2 can be used, which provides a friction reduction of a factor of two and a mating-part wear reduction of over a factor of four by slowly sacrificing its own volume and still providing excellent lifetime performance.

B. Development of an Advanced Non-Impingement SIDI Combustion System and Associated Low Pressure Fuel System

Paul VanBrocklin (Principal Investigator and Program Manager)
Delphi Energy & Chassis Systems
P. O. Box 20366
Rochester, New York 14602-0366
(716) 359-6797, fax (716) 359-6061, e-mail: paul.g.vanbrocklin@delphiauto.com

DOE Program Manager: Rogelio Sullivan
(202) 586-8042, fax (202) 586-1600, e-mail: Rogelio.Sullivan@ee.doe.gov

Subcontractors: The Pennsylvania State University, State College, PA

Objectives

- To develop a non-impingement gasoline Spark Ignited Direct Injection (SIDI) combustion concept meeting modified Partnership for a New Generation of Vehicles (PNGV) objectives:

Engine characteristics, units	**Range or Goal**
Number cylinders	4
Total Displacement, cc	2000
Power output, kW	Approx. 55
Peak efficiency target, %	35-37
Cost	Within 10% of SI
Durability, hours	>5000
NO_x emissions, engine-out, g/kWh	<1.4
PM emissions, engine-out, g/kWh	<0.05
HC emissions, engine-out, g/kWh	<3.0
CO emissions, engine-out, g/kWh	<41.0

- To develop a low-pressure fuel injection system that allows an engine to meet the above requirements, which is consistent with the overall commercial considerations.
- To understand EGR and ignition requirements for a non-impingement SIDI system.

Approach

1. Determine the feasibility of a Jet-Stratified combustion system approach using Computational Fluid Dynamics (CFD) analysis, optical and single-cylinder engine testing.
2. Develop a Low Pressure Fuel System based on sub-system requirements generated earlier in the program, using analytical and experimental methods.
3. Implement developed sub-systems on a single cylinder research engine to demonstrate the performance of the combined systems.

Accomplishments

This program is approximately 80% complete. 2001 accomplishments to date include:

- Engine Hardware
  - Jet 4a and Jet 4b cylinder head designs were developed and built. The design of Jet 5 hardware has been recently completed and is being built. This Jet 5 concept will use a dedicated supplemental energy atomizer injection system on both the single-cylinder engine (SCE) and the optical engine (OE).
- Firing Single-Cylinder Engine
  - Jet 2, 4a, and 4b combustion systems have been run.
- Optical Engine at Delphi
  - Particle Image Velocimetry (PIV) to map engine flow fields has been run on Jet 3 and 4b hardware. The ability to fire the OE and capture combustion images has also been developed.
- Optical Engine at Penn State University
  - Additional testing using simultaneous Mie scattering and planar laser-induced fluorescence (PLIF) of two different Delphi injectors has been conducted to determine the liquid and vapor contents of the fuel spray.
- Computational Fluid Dynamics
  - Kiva 3v was used to model Jet 4a, determining that the optimal injector orientation for the Jet 4 design was approximately 7.5° from vertical. This resulted in the Jet 4b design. Correlation of simulated to experimental PIV results for Jet 2 was successful. Difficulties with the correlation for the Jet 3 and 4 design are being evaluated.
- Injector/Atomizer
  - The concept evaluation process reduced potential design approaches from five to three. First iteration hardware design, build and test loops on these three concepts have been completed. The second iteration of hardware build is in process.
- Fuel Pump
  - Two distinctly different designs using the same general gear pump concept have been designed, built, and undergone preliminary testing. The second design, although a radical departure from conventional gear pump designs, shows significant promise in the areas of reduced wear and friction.

Future Directions

- Aside from the formidable technical challenges of developing high efficiency combustion systems, atomizers, and pumps, a significant non-technical issue has arisen during the course of the program. The DOE has elected to not continue funding in the area of SIDI research in 2002. This has resulted in the OTT not having the funds to test a multi-cylinder engine at the National Lab of their choice. Since a multi-cylinder engine was intended to be the final deliverable of this program, a change in program direction was required. It was decided to not build a multi-cylinder SIDI engine, but to continue development and refinement in the areas of fuel pumps, injector/atomizers and combustion chamber design using a single-cylinder engine. This continued work is outlined in the respective Approach/ Results to Date sections. The program will conclude at the end of Q1 2002 as before, but with a report centering on engine performance data comparing a high efficiency pressure orifice atomizer and supplemental energy devices.

Introduction

Aside from significant vehicle level systems issues, the basic performance of today's production SIDI engines do not benefit from the years of refinement that port fuel injected (PFI) SI engines have had. Because of this, current systems have high costs and small efficiency improvements over current PFI systems, questioning the value of such SIDI systems in North America. By developing SIDI systems that meet the PNGV requirements, the goals and objectives of both the DOE and Delphi are met. This report builds upon last year's report published in the OTT 2000 Annual Progress Report.

The stratification mechanism currently employed in SIDI systems is to "bounce" injected fuel off a surface (typically the top of the piston) in combination with in-cylinder air motion to re-direct fuel to the spark plug. By impinging the piston, some portion of fuel is spread over a surface, leading to unburned hydrocarbons. An alternate, but unproven SIDI approach, is non-impingement or Jet stratification. Jet stratification is the principle of directing the fuel, as a well atomized jet, directly at the spark plug to avoid wetting combustion chamber surfaces. Because this type of system is in its infancy, Delphi Automotive Systems considers this approach to meet the DOE / PNGV requirements, while remaining commercially feasible, to be of higher risk than would normally be pursued. Participating in this cost-shared project with the DOE has allowed for participation in such a high-risk project, and it puts Delphi in the forefront of evolving technology.

Approach / Results to Date

An essential goal of the project is to obtain 35-37% overall engine efficiency. This efficiency target is significantly above the 22-28% efficiencies that current PFI or SIDI engines attain. To determine the individual goals of the project, the efficiency target was broken down into the areas of the base engine, injector and fuel supply system. This allows for power consumption to be used as an independent criteria for selection of engine, injector and fuel pump concepts. For example, an injector concept isn't viable if it uses significantly more than the allotted power. However, since the target is overall efficiency, there will be some power allocation trade-offs as the project progresses and individual concepts are grouped into complete systems. Figure 1 illustrates the efficiency breakdown of engine losses comparing empirical values for a production piston impingement SIDI engine to the predicted values for an Advanced Jet Stratified SIDI engine.

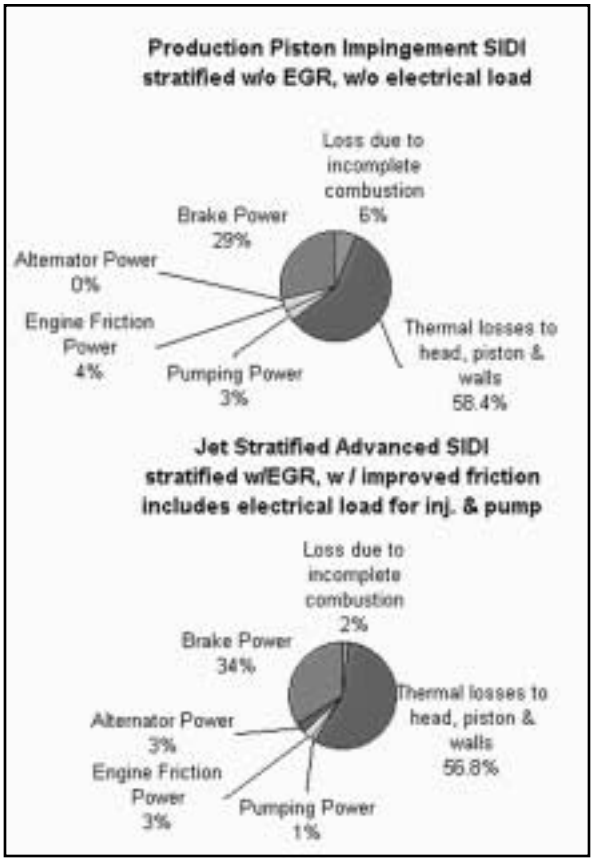

Figure 1. Comparison of Engine Power Usage Between a Production SIDI and Advanced SIDI

A governing direction of the project is to use lower fuel pressure (2.5 MPa) compared to current SIDI (5-10 MPa). This low pressure is beneficial in two areas of the project. 1) Less energy is expended to develop the required fuel pressure, thus helping to increase the overall energy efficiency. 2) By having a lower pressure, a single pump can be used, eliminating a significant amount of the cost associated with an engine-driven high-pressure pump that is required for current systems.

The project is broken into 3 functional areas: the combustion system, atomizer, and fuel supply.

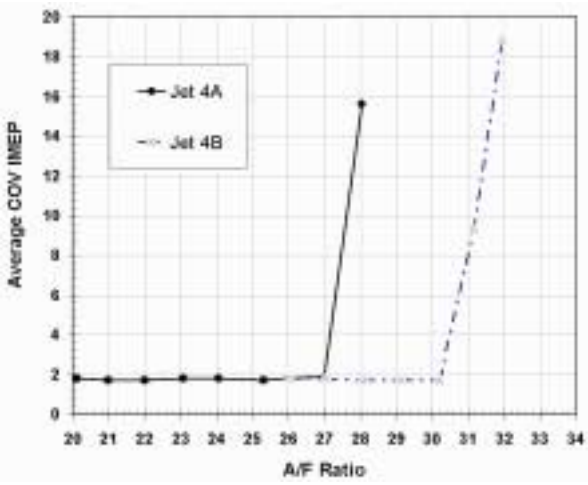

Figure 2. Combustion Stability Jet 4a (vertical injector) vs. Jet 4b (7.5° from vertical injector)

Engine / Combustion System

Existing Delphi gasoline DI injectors have been used to conduct engine experiments to date. Kiva 3v has been used along with particle image velocimetry in an optical engine to understand and predict engine performance, with the end result being the development of engine hardware. PIV has been used to validate the Kiva 3v model. Good results have been obtained with the Jet 2 design that uses a flat top piston. Correlation between the Jet 3 and 4 concepts that use a dome piston with a deep bowl has proven more difficult. Kiva 3v was used to predict that changing the angle of the centerline of the injector from vertical to 7.5° from vertical would increase the time over which an ignitable amount of vapor was in the location of the spark plug. Refer to Figure 2 for a plot of the coefficient of variation (COV) of indicated mean effective pressure (IMEP) (combustion stability) as a function of the air to fuel ratio for these two cases. The Pennsylvania State University has also conducted simultaneous Mie scattering and Laser Induced Florescence to determine vapor concentration of various Delphi injectors.

Atomizer

A main goal of the atomizer program is to develop injectors that provide lower spray penetration (velocity) by having lower inlet pressure, while maintaining a well atomized spray. Developing well atomized sprays with fuel having lower initial energy requires significant advancements in the area of injector atomizers. This can be done either by more efficient use of available energy stored in the fuel as pressure, or by adding external sources of energy to help atomize the fuel. To save development time, existing injector actuators were used and only improved atomizers were developed.

Of 42 initial concepts, five were brought forward into calendar year 2001. Initial hardware was built for the feasible concepts and bench testing was completed. Three concepts remain: a high efficiency pressure orifice atomizer and two supplemental energy pressure orifice devices.

A Taguchi designed experiment was completed on the high efficiency pressure orifice atomizer to gain an understanding of general design features and their relevance with respect to atomization. Figure 3 shows spray volume distribution results from this experiment. CFD modeling using Fluent was completed on the best design and correlated within 1% for flow. The calculated turbulent kinetic energy (TKE) output obtained from the CFD model was then used as a baseline indicator of atomization for comparative studies. Additional Taguchi Robust Engineering studies were completed to optimize the design for maximum TKE. Remaining work will include fabrication, assembly and testing of the second iteration of the high efficiency pressure orifice atomizer.

The second atomizer concept carried forward, a supplemental energy pressure orifice device, uses electrostatic repulsive forces to atomize and disperse fuel. Tasks completed on this concept include an evaluation of predictive software, charge flux modeling of initial concepts and design and fabrication of initial hardware. Remaining work will include completion of the Robust Engineering study for concept evaluation.

The third atomizer concept, also a supplemental energy device, was added to the program mid-year 2001. This concept, previously evaluated at Delphi, demonstrated spray/penetration performance meeting most of the atomizer requirements. As such, it is currently the leading atomizer concept. Detailed spray and flow testing as well as combustion testing will be the remaining focus for this concept.

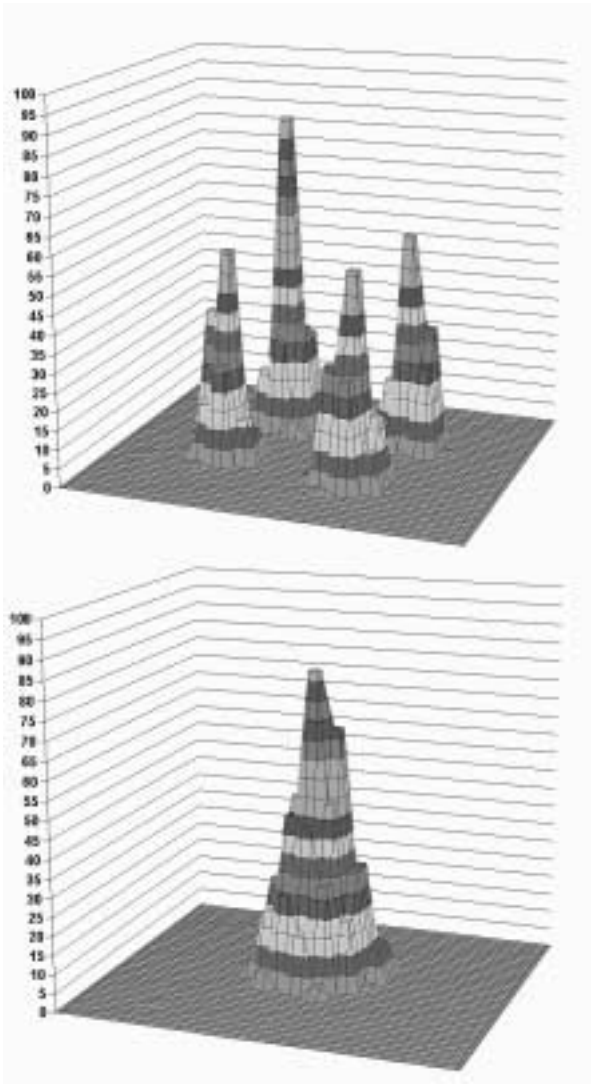

Figure 3. High Effective Pressure Orifice Atomizer Configuration 1 vs. Configuration 6 Spray Volume Distribution

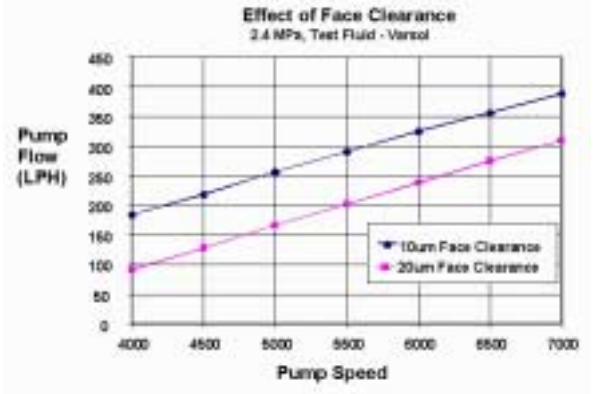

Figure 4. Effect of Face Clearance on Gear Pump Flow

Pump

Concept development originally identified an internal gear type pump as the most viable concept for the pressure range under consideration. The main development challenges for this technology have been flow performance and durability. Development for improved flow performance has involved reducing internal leakage by minimizing the clearance or bypass flow paths between moving parts. This has been done by optimizing valve ports and by improving the design of the interface between the pump and the drive mechanism. To improve durability, material selection, lubrication, and pressure balancing have been the main focus. The use of hydrodynamic lubrication, or the establishment of fluid films under dynamic conditions, is the primary focus for areas of relatively large surface area (flat plate type interfaces). In high-force/small-area interfaces, such as the interface between a gear rotating on a shaft, material selection is the primary direction. Finally, pressure balancing, or eliminating the pressure differentials between the two faces of the gear, is being used to minimize high wear forces. Dynamic modeling of a gear type pump has proven to be very difficult. For this reason, an empirical build and test loop has been the primary method of component development. Figure 4 shows an example of how face clearance affects flow performance.

Conclusions

Development, testing, and analysis to date has resulted in several key findings:

- Not all methods of entraining air into the fuel spray to provide an ignitable mixture are equally robust.
- An injector using supplemental energy for atomization may provide higher overall engine efficiencies due to the ability to operate with extreme residual levels.
- The division of allowable tolerance stack-ups within the gear section of the pump for high-pressure operation is not the same as that of gear pumps used in Port Fuel Injection applications today.

During the ensuing months, work will continue to resolve issues and further develop the individual components. Final single-cylinder engine testing will then be conducted.

C. Variable Compression Ratio Engine Technology

Charles Roehm
Argonne National Laboratory
9700 S. Cass Avenue
Argonne , IL 60439
(630) 252-9375, fax: (630) 252-3443, e-mail: croehm@anl.gov

Charles Mendler
Envera LLC
7 Millside Lane
Mill Valley, California 94941
(415) 380-5067, fax: (415) 380-5067, e-mail: mendler@earthlink.net

DOE Program Manager: Roland Gravel
(202) 586-9263, fax: (202) 586-6109, e-mail: Roland.Gravel@ee.doe.gov

Objectives

- Develop a variable compression ratio (VCR) engine having a comparable cost to today's production engines, capable of achieving U.S. Tier 2 and California LEV-II emissions certifications, and having an efficiency great enough to achieve a passenger car fuel economy of 80 mpg.

Approach

- Begin with a small displacement engine to achieve high energy conversion efficiency at low power levels.
- Supercharge and intercool the engine to achieve high specific power levels and to attain Partnership for a New Generation of Vehicles (PNGV) performance targets.
- Use variable compression ratio to prevent engine knock at high power levels and to substantially improve engine efficiency at low power levels.
- Use variable valve control to further improve efficiency and power.
- Use proven 3-way catalytic converter technology to achieve US Tier 2 and California LEV-II emissions certification.

Accomplishments

- Computer modeling at Ricardo, Inc. showed that the projected efficiency of the VCR engine should meet propulsion system requirements needed to reach the goal of 80 miles per gallon set by the PNGV.
- Dynamometer tests at AVL Powertrain validated the burn rates, compression ratio limits, and engine efficiencies predicted by the computer model. Engine-out emission levels were also shown to be similar to that of conventional engines.
- Envera LLC built a 2-cylinder VCR engine and demonstrated operability and durability of the VCR mechanism with dynamometer testing. Compression ratio was varied while the engine was running from 8.5:1 to 17.5:1.

Future Directions

- Build an optimized cylinder head for the 2-cylinder engine, and validate concurrently efficiency, emissions, and hardware.
- Optimize engine variables for efficiency, emissions, and minimization of parasitic losses. Project vehicle mileage with optimized test data.

Introduction

The Partnership for a New Generation of Vehicles (PNGV) targeted compression-ignition direct-injection (CIDI) engines, an advanced version of the diesel engine, as one of the promising technologies for achieving its fuel economy goal of 80 miles per gallon in a lightweight hybrid vehicle. However, due to increasingly stringent emission standards, development of a fall-back to the CIDI diesel engine was considered prudent. OAAT is sponsoring research to exploit the potential of using variable-compression-ratio (VCR) technology with supercharging to significantly improve spark-ignition engine efficiency while achieving low emissions using proven 3-way catalyst emission control technology.

A fuel economy of 81 mpg was projected for a PNGV-intent vehicle powered by a simulated spark-ignition gasoline VCR engine. The computer model was validated with single-cylinder dynamometer tests. A 2-cylinder VCR engine was built, validating operability, durability, and precision control of the VCR mechanism.

High Fuel Economy and Low Emissions

Conventional gasoline engines operate at a fixed compression ratio, which is set low enough to prevent premature ignition of the fuel, or "knock," at high power levels under fast acceleration, high speeds, or heavy loads. Most of the time, however, gasoline engines operate at relatively low power levels under slow acceleration, lower speed, or light loads. If the compression ratio were increased at low-power operation, gasoline engines could achieve higher fuel efficiency.

At the low power levels (0-20 kW), typical of most vehicle operating conditions, the VCR engine can achieve efficiency comparable to that of a diesel engine, a significant improvement over conventional port fuel-injected gasoline engines (see Figure 1). At the same time, because it is a gasoline engine, the VCR engine can achieve Federal Tier 2 and California LEV-II emission standards.

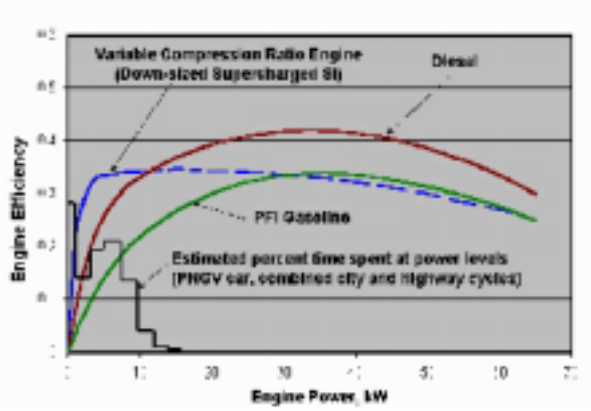

Figure 1. Variable compression ratio engine promises high efficiency at low engine power levels.

Approach

Step 1: Modeling

By using WAVE (the Ricardo one-dimensional gas dynamics and engine simulation model), in-house data on engine friction levels, and estimates of burn rate drawn from estimates of swirl and tumble within the combustion chamber and historical data for high compression ratio combustion, Ricardo was able to project the efficiency of the VCR engine. Ricardo then used their cycle simulation computer code to project vehicle mileage. Selected projections were validated by the National Renewable Energy Laboratory (NREL) using their ADVISOR cyle simulation computer code.

The simulated vehicle was assumed to have a 6-speed automated manual transmission and an

Figure 2. Efficiency testing at AVL in Graz, Austria

alternator that captures braking energy for powering accessory loads (electric forward drive not used). Vehicle weight and aerodynamic drag were comparable to an optimized PNGV-intent vehicle body.

Step 2: Engine Efficiency Validated

The projected engine efficiency depended on combustion burn rate assumptions for high compression ratio conditions that were based on relatively limited historical data. As a result, a development engine was built and tested at AVL powertrain to validate the efficiency values projected by the computer model and to quantify engine-out emission levels. Compression ratio was adjusted by shims in the test engine (Figure 2).

Step 3: VCR Mechanism Validated

A VCR 2-cylinder PNGV-intent prototype engine was built to evaluate its durability, reliability, precision control, response, and full variability within a range of 8.5:1 to 17.5:1. A donor cylinder head (cylinder head from an existing commercially available vehicle) was used to minimize program cost. All new components were designed and built from the head gasket down.

Results

Step 1: Modeling

A combined Environmental Protection Agency (EPA) city/highway fuel consumption of 81 mpg was projected for a PNGV-intent vehicle with a small displacement port-fuel-injected VCR engine equipped with on-demand supercharging, an automated manual 6-speed transmission, and accessory loads powered largely by regenerative braking.

The engine operated with a stoichiometric air/fuel ratio throughout the Federal Test Procedure (FTP) city and highway driving cycles, providing a high probability of meeting Federal Tier 2 and California LEV II emission standards using three-way catalyst-based emission control systems.

All vehicle gradeability, acceleration, and maximum speed targets were met.

Step 2: Engine Efficiency Validated

Development engine test results validated Ricardo's efficiency projections to within 98.5 percent accuracy. Light-load efficiency results are shown in Table 1. (Slightly higher efficiency values were projected at other engine speeds.)

Step 3: VCR Mechanism Validated

The VCR engine operated for about 20 hours with no abnormal bearing or engine wear detected. The engine ran full throttle for several hours with noise and vibration characteristics within acceptable limits. The compression ratio was varied from 8.5:1 to 17.5:1 during both part and full engine load, with high precision and responsiveness observed. Program expectations were surpassed.

Future Work

A compact combustion chamber is necessary for achieving high efficiency and low emissions from the VCR engine at high compression ratio settings. The compact combustion chamber shape is best facilitated by using a bore/stroke ratio of about 0.9 and a narrow valve included angle, preferably under 25 degrees. A VCR-intent cylinder head for the 2-cylinder prototype engine will be built and tested. Engine variables will be adjusted to provide optimum efficiency. Vehicle fuel economy projections will be made using the optimized engine efficiency test results. Projections will then be validated by conducting dynamometer tests of the

VCR engine. Vehicle fuel economy modeling and engine tests are intended to validate the potential for achieving the PNGV 80 mpg goal and to validate the practicality of attaining high efficiency and low emissions with the VCR engine as a complete system.

Conclusion

VCR technology exhibits potential for providing a step-change improvement in spark-ignition engine efficiency, while retaining proven 3-way emission control technology. Planned cylinder head and VCR engine testing is intended to validate commercial practicality of a PNGV-intent engine.

References

1. N. Miura, T. Raisen, G. Lu and N. Yamazoe, *Sensors and Actuators B 47* (1998) 84-91.

D. Performance of Plasmatron-Enhanced Lean-Burn SI Engine

Daniel R. Cohn (Primary Contact), PlasmaScience and Fusion Center, John B. Heywood, Andreas Lengwiler, Edward J. Tully, Sloan Automotive Laboratory
Massachusetts Institute of Technology
77 Massachusetts Avenue, NW16-106
Cambridge, MA 02139
(617) 253-5524, fax: (617) 253-0700, e-mail: cohn@psfc.mit.edu

DOE Program Manager: Rogelio Sullivan
(202) 586-8042, fax: (202) 586-1600, e-mail: Rogelio.Sullivan@ee.doe.gov

Objectives

- Map out a lean engine operating regime of a standard spark-ignition (SI) engine with different fractions of the gasoline fuel going to the engine via the plasmatron fuel to hydrogen converter.
- Determine the plasmatron-enhanced engine combustion characteristics, emissions levels, and efficiency at selected speed and load conditions.
- Develop a phenomenological model that predicts the lean plasmatron-enhanced SI engine behavior.
- Define the engine's operating requirements (fraction of fuel energy in plasmatron gas) required for high efficiency and low NO_x emissions operation with acceptable combustion stability.

Approach

- Develop phenomenological model that predicts engine torque, given the engine's operating conditions, for use in planning the experimental matrix and achieving desired test conditions.
- Use single-cylinder research engine and bottled gas mixture (H_2, CO, CO_2, N_2) to simulate plasmatron exit gas for initial mapping of the lean engine regime.
- Enhance engine combustion characteristics using swirl and/or tumble to assess minimum plasmatron gas requirements with a modern SI engine combustion system.
- At the appropriate stage in the development of this engine mapping program, confirm results in a multi-cylinder engine test.

Accomplishments

- A model for predicting plasmatron-enhanced lean engine performance has been developed and tested (Lengwiler, 2001).
- Preliminary data confirm that very lean engine operation with low emissions is feasible. More extensive tests have expanded the data set to leaner mixtures.

Future Work

- More complete mapping of the lean engine operating regime can expand the required database to leaner mixtures, with engine test conditions controlled more accurately.
- Engine modifications can be used to increase the burn rate of the single-cylinder test engine to enhance its lean limit capability.

Introduction

Hydrogen-enhanced lean gasoline operation using onboard conversion of gasoline to hydrogen could be a cost effective way to achieve significantly higher vehicle efficiency and lower emissions. The plasmatron, a discharge boosted fuel conversion device, can be used to provide a hydrogen-rich gas stream from gasoline when combined with a standard engine enable very lean engine operation. Such lean operation improves engine efficiency and lowers NO_x emissions substantially.

To develop this engine concept, the fraction of the gasoline that needs to be converted to a mixture of H_2, CO, and N_2 must be quantified. This project addresses this issue. The objective is to define the plasmatron exit gas flow required to achieve the efficiency and low emissions objectives while maintaining sufficiently fast and stable combustion.

Approach

The data which will define the required plasmatron gas flow as a function of engine operating conditions is being generated on a single-cylinder research spark-ignition engine. The efficiency, combustion and emissions characteristics of the engine will be mapped out over a range of plasmatron exhaust gas/gasoline mixtures, engine loads, engine speeds and relative air/fuel ratios. This is being done with bottled gas to simulate the plasmatron exit gas. A phenomenological model of this engine concept has also been developed to assist in selecting test conditions for the experiments and in interpreting the results (Lengwiler, 2001)

Results

The results obtained to date are preliminary; however, they show the expected trends. The addition of plasmatron gas to the gasoline vapor air mixture in the cylinder speeds up combustion and improves engine stability. The larger the relative amount of plasmatron gas, the greater the improvement. Figure 1 shows the coefficient of variation of indicated mean effective pressure, a common measure of combustion stability, versus the relative air/fuel ratio. Addition of plasmatron gas corresponding to 18% of the gasoline going directly to the plasmatron (where an 80% energy out/energy

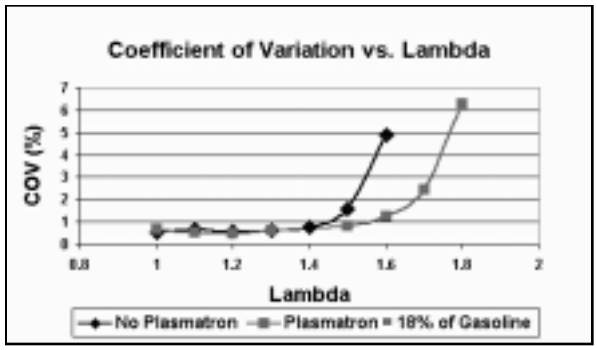

Figure 1. Combustion stability, defined by coefficient of variation in indicated mean effective pressure, as a function of relative air/fuel ratio (Lambda) for operation with gasoline and with 18 percent of the gasoline flow going to plasmatron. Net imep = 3.1 bar, 1500 rev/min.

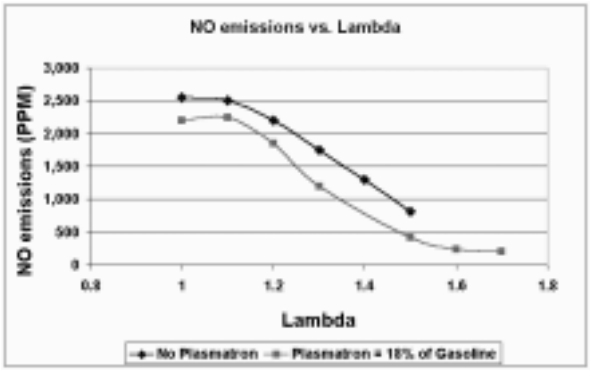

Figure 2. Engine-out NO_x emissions as a function of relative air/fuel ratio (Lambda) plotted up to stable lean operating limit; same conditions as Figure 1.

in ratio is assumed) extends the lean limit significantly.

The low emissions potential of the lean plasmatron enhanced engine is illustrated by the NO_x emissions data in Figure 2. At fixed engine load and speed, NO_x emissions decrease steadily from the high values of close to stoichiometric mixture operation. The plasmatron engine example shown has lower emissions at a given Lambda due to the additional N_2 in the plasmatron gas, and can operate leaner before combustion stability limits are reached. (Lambda is the actual air/fuel ratio divided by the stoichiometric air/fuel ratio.) This latter is the bigger effect and the primary objective. Hydrocarbon emissions are reduced by 10-20% with plasmatron enhanced lean operation due to better combustion.

The efficiency of the engine steadily improves as leaner operation is achieved. With the plasmatron-enhanced lean operating engine, net indicated efficiencies of about 37% have been achieved to date. Upon converting these to brake efficiencies (based on the power delivered by the engine driveshaft), using values of friction mean effective pressure typical of multi-cylinder engines, one obtains a brake efficiency of about 30%. This is substantially higher than typical current part-load SI engine efficiencies.

More extensive mapping of the engine's performance when enhanced by varying amounts of plasmatron H_2, CO, N_2 gas mixtures is in progress.

Conclusions

Preliminary results from single-cylinder engine tests, using appropriate synthesized gas mixtures to simulate plasmatron exhaust gases, show that faster and more stable combustion processes can be achieved. This extends the lean operating limit of the engine. Engine test results indicate the low NO_x emissions and high efficiency potential under these plasmatron-enabled lean operating conditions.

Publications

1. Lengwiler, A., "SI Engine Combustion and Enhancement Using Hydrogen from a Plasmatron Fuel Converter" Diploma Thesis ETH Zurich, winter semester 2000/2001; Sloan Automotive Laboratory, MIT, April 2001.

E. On-Board Distillation of Gasoline

Ron Matthews (Primary Contact) and Tom Kiehne
Engines Research Program
The University of Texas
Mail Code C2200
Austin, TX 78712
(512) 471-3108, fax: (512) 471-1045, e-mail: rdmatt@mail.utexas.edu

DOE Program Manager: Rogelio Sullivan
(202) 586-8042, fax: (202) 586-1600, e-mail: Rogelio.Sullivan@ee.doe.gov

Objectives

- Develop a model to explore the issues that might impact the implementation of the on-board distillation concept, and acquire the experimental data necessary for the model.
- Quantify the effects of the on-board distillation system on emissions; cold startability; cold driveability; and the Octane Ratings of the main fuel (the less volatile of the two fuels generated), including preliminary assessment of how this characteristic might be used to improve fuel economy.
- Demonstrate that on-board distillation is a practical and cost-effective technology for decreasing emissions of hydrocarbons.

Approach

- Modify a 2001 Lincoln Navigator to incorporate a gasoline on-board distillation system (OBDS). Perform tests to optimize the design and calibration of the OBDS.
- Develop a model to examine the issues of "too many hot starts" and "too many cold starts". Use the model to aid design and calibration of the OBDS.
- Perform tests to demonstrate that on-board gasoline distillation decreases emissions of hydrocarbons.
- Perform tests to demonstrate that the driveability is improved.
- Perform tests to demonstrate that the startability in cold weather is improved.
- Perform tests to quantify the Octane Rating of the main fuel. Analyze how this shift in Octane Rating can be used to improve fuel economy.

Accomplishments

- The OBDS has been fabricated and installed on the 2001 Lincoln Navigator. We are finalizing the OBDS control system and waiting for hardware and software from Ford that will allow us to re-program the Navigator's on-board computer.
- We have begun developing the model.

Future Directions

Once the OBDS control system is complete, and we receive the Ford RCON re-programming unit, we will:

- Optimize the design and calibration of the OBDS via a combination of experiments and modeling.
- Send the 2001 Navigator to Southwest Research Institute for tests of emissions, cold startability, and cold driveability.
- Send fuel samples to Ford for analysis of the Octane Rating.

Introduction

The first 1-2 minutes of vehicle operation contribute inordinately to tailpipe emissions of hydrocarbons (HCs), which are of concern because HCs contribute to ground level ozone formation. Typically, 60-80% of HCs are emitted during starting and warm-up for conventional gasoline engines, and ~40% for direct injection gasoline engines (References 1-4).

The primary goals of this project are to develop and demonstrate a new technique for decreasing hydrocarbon emissions from gasoline vehicles and to transfer this technology to the automotive industry. The new concept is on-board distillation. This allows the consumer to refill the fuel tank with a single fuel (gasoline), from which two fuels are generated on-board the vehicle. Specifically, the more volatile fractions of the gasoline are separated from the less volatile portion. The volatile fraction is used for starting the engine and during a portion of the warm-up transient. Because the "start-up fuel" is very volatile, the normal need for start-up over-fueling is minimized or eliminated. In turn, this significantly reduces emissions of hydrocarbons and "exhaust toxics". The high volatility of the start-up fuel also promises improved startability and driveability in cold weather. Furthermore, because on-board distillation changes the composition of the fuel that is used during the majority of driving, it is possible that an indirect fuel economy benefit will also be realized.

Approach

Ford has provided a 2001 Lincoln Navigator to use as a test platform. A gasoline on-board distillation system will be installed on this vehicle. The operation of the OBDS is illustrated in Figures 1 and 2. The OBDS hardware has been designed and fabricated and installed in the Navigator. We are near completion of the OBDS control system, which controls when and how long we generate start-up fuel, purging of the fuel rail with start-up fuel between starts, and how long the start-up fuel is used after each start. These are all functions that can be handled by the powertrain control module (PCM, the on-board computer) if this concept is incorporated into production vehicles. Additionally, we must

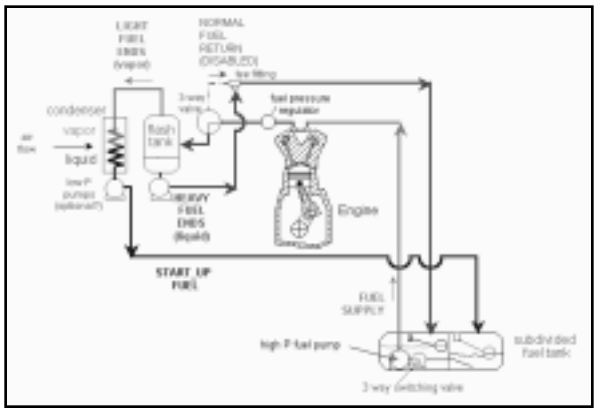

Figure 1. On-board Distillation System, Illustrating Generation of Start-up Fuel

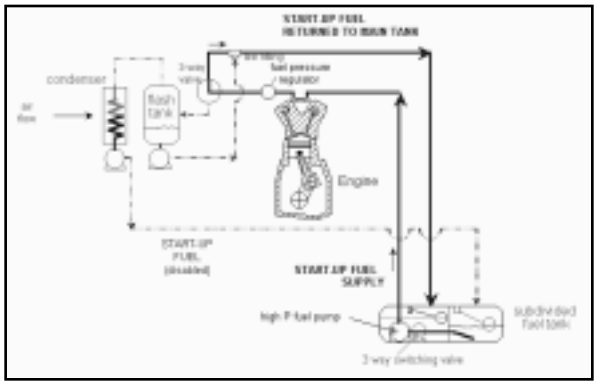

Figure 2. Fuel path during starting. Because the supply line and fuel rail are purged with start-up fuel following every engine shut down, start-up fuel is sitting on the injectors prior to starting.

minimize or eliminate the start-up over-fueling that the Navigator's PCM is programmed to command. We have been working with Ford to secure an RCON, which they use to re-program their PCMs. Once we have this unit, we will use a combination of experiments and modeling to optimize the calibration of both controllers.

Southwest Research Institute will perform standard emissions, cold-start, and driveability tests on the Navigator. Additionally, we will send fuel samples to Ford for Octane Ratings tests. We will use these results to explore the potential of a fuel economy benefit.

Results

Because this project is only in its fourth month, we do not yet have any results to report.

References

1. Crane, M.E., R.H. Thring, D.J. Podnar, and L.G. Dodge (1997), "Reduced cold-start emissions using rapid exhaust port oxidation in a spark-ignition engine", SAE Paper 970264.
2. Guillemot, P., B. Gatellier, and P. Rouveirolles (1994), "The influence of coolant temperature on unburned hydrocarbon emissions from SI engines", SAE Paper 941962.
3. Witze, P.O., and R.M. Green (1997), "LIF and flame-emission imaging of liquid fuel films and pool fires in an SI engine during a simulated cold start", SAE Paper 970866.
4. Stovell, C., R.D. Matthews, B.E. Johnson, , H. Ng, and B. Larsen (1999), "Emissions and fuel economy of 1998 Toyota with a direct injection spark ignition engine", SAE Paper 1999-01-1527; also in *Journal of Fuels and Lubricants* Vol. 108.

Awards/Patents

1. Matthews, R.D.,R. Stanglmaier, G.C. Davis, and W. Dai, "On-Board Gasoline Distillation for Reduced Hydrocarbon Emissions at Start-Up", U.S. Patent No. 6,119,637, issued Sept. 19, 2000.

IV. EMISSION SENSOR DEVELOPMENT

A. Exhaust Gas Sensors CRADA (HC)

Ai Quoc Pham (Primary Contact)
Lawrence Livermore National Laboratory
P.O. Box 808, L-644
Livermore, CA 94550
(925) 423-7140, fax: (925) 423-3394, e-mail: pham2@llnl.gov

DOE Program Manager: Rogelio Sullivan
(202) 586-8042, fax: (202) 586-1600, e-mail: Rogelio.Sullivan@ee.doe.gov

Objectives

- Identify factors influencing sensor response time.
- Develop new electrodes for faster sensor response time.
- Incorporate a hydrocarbon (HC) sensor to a self-heated device.

Approach

- Determine effect of electrode microstructure and electrode materials on sensor response.
- Investigate the response of composite electrodes having two or more different materials.
- Incorporate HC sensor on HEGO (Heated Exhaust Gas Oxygen) sensors provided by Ford.

Accomplishments

- Demonstrated a correlation between electrode thickness and sensor signal amplitude.
- Developed three new electrode formulations with response time faster than 1s.
- Developed self-heated sensors.

Future directions

- Improve sensor packaging.
- Evaluate long-term stability.

Introduction

Due to increasing environmental concerns, in 1994 the California Air Resources Board (CARB) and the U.S. Environmental Protection Agency (EPA) began implementing regulations that require automakers to incorporate comprehensive on-board diagnostics into new vehicles. The purpose is to monitor emissions, which will allow early detection of any malfunctioning of the engine and/or emission control system. Currently, monitoring of hydrocarbon (HCs) and NO_x emissions is regarded as being critical for evaluating car emissions. This report describes the progress we have made on the development of the HC sensors during FY01.

Approach

One of the major issues with HC sensing is the potential cross-sensitivity with CO, which has

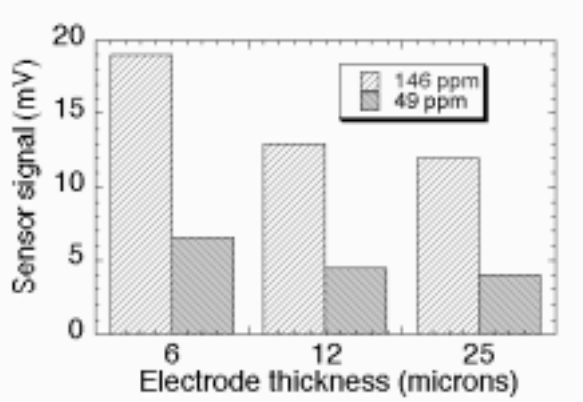

Figure 1: Effect of Electrode/Catalyst Thickness on Sensor Signal

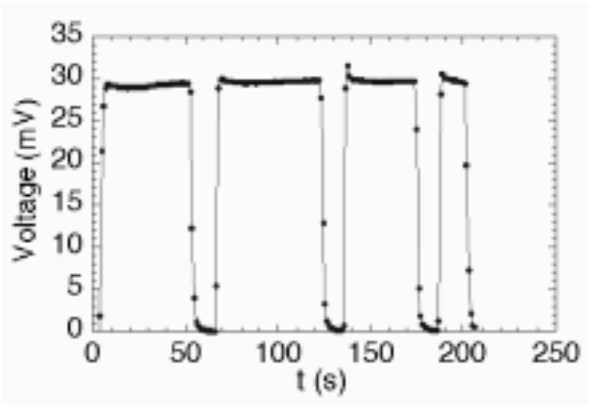

Figure 2: Sensor response to 194 ppm butane. The gas is switched on and off between each step. Time between two data points is 1 s.

similar chemical characteristics. Our approach has been to find chemical sensing reactions that will differentiate HCs from CO. One of the reactions considered was the dehydrogenation, which affects HCs only. The sensor itself can be either a hydrogen sensor or an oxygen sensor with a dehydrogenation catalyst covering one electrode only. The HCs will undergo the dehydrogenation reaction on the electrode having the catalyst layer, thus generating a hydrogen concentration difference across the sensor. This hydrogen concentration difference will generate a voltage across the hydrogen sensor, and the signal amplitude will be directly related to the gas phase concentration of HCs. If an oxygen ion conducting electrolyte is used instead of a proton conductor, and if oxygen is present, the hydrogen generated from the dehydrogenation will undergo a reaction with oxygen, causing an oxygen concentration difference across the sensor, thus providing similar sensing mechanism. Sensors based on the above approaches have been developed and characterized extensively. While a number of issues have been resolved, the sensor was still not suitable for real exhaust gas sensing because of the slow response time (from 10 seconds up to 1 minute). Thus, effort this year was focused on decreasing sensor response time to less than 1 s.

Results

Our effort was first to determine the various factors that could influence the sensor response, both in terms of signal amplitude and response time. For the same electrode/catalyst material, we found that the sensor signal decreased with increasing electrode thickness (Figure 1). On the other hand, the sintering temperature of the electrode, and thus the particle size, was found to have direct influence on the sensor response time: the lower the sintering temperature, the faster is the sensor response. However, the factor that had the strongest influence on sensor response time was the catalyst material itself. Iron oxide had a much faster response than zinc oxide, for instance.

Based on the above observations, we designed four different approaches to improve sensor response time. Three of the approaches involved the preparation of composite electrodes and/or multilayer structures. All sensors having composite or multilayer electrodes were found to exhibit extremely fast response to HCs. Figure 2 shows an example of the sensor response to butane. The measured response time of 2 s was limited by the gas phase exchange within the experimental chamber. Measurements performed at Ford Research Laboratory indicated an actual response time below 0.5 s. The sensors are thus fast enough for real exhaust gas monitoring.

The operating temperature of the present sensors is in the range of 600-750°C. The heating, currently provided by an external furnace, is not convenient for exhaust gas monitoring. The sensor has thus been miniaturized and mounted directly on a HEGO sensor provided by Ford (Figure 3). The HEGO sensor provided the necessary heating and could be used for monitoring the oxygen concentration in exhaust gas as well. Extensive characterization of the heated sensor is underway.

Figure 3: Photograph of LLNL HC Sensor Mounted on a HEGO Sensor

Conclusion

We have investigated the various factors that could influence sensor response time. The investigation has resulted in the development of three successful approaches to reduce sensor response time. The improved sensors exhibit a response time less than 0.5 s and are thus suitable for use in exhaust gas sensing. Efforts to package the sensor on a heater are underway.

B. Advanced Ion-Mobility NO_x Sensor

A. C. Raptis (Primary Contact) and S. H. Sheen
Argonne National Laboratory
9700 South Cass Avenue
Argonne, IL 60439
(630) 252-5930, fax: (630) 252-3250, e-mail:raptis@anl.gov

DOE Program Manager: Rogelio Sullivan
(202) 586-8042, fax: (202) 586-1600, e-mail: Rogelio.Sullivan@ee.doe.gov

Objectives

- The objective of this project is to develop a non-radioactive ion-mobility NO_x sensor that can be used in an engine exhaust emission environment to provide real-time measurements of NO_x emissions.

Approach

- Stage 1. Design and evaluation of a corona discharge ionization source.
- Stage 2. Design and evaluation of a laboratory prototype ion-mobility spectrometer (IMS).
- Stage 3. Parametric study of the non-radioactive IMS for detecting NO_x.
- Stage 4. Development of a field prototype that applies to a typical exhaust emission environment.
- Stage 5. Field testing of the IMS.

Accomplishments

- Developed a spark-discharge ionization source.
- Developed a method to reduce the water-vapor effects on IMS.
- Designed and evaluated a laboratory prototype IMS.
- Analyzed laboratory test data to determine the sensor performance.

Future Directions

- Design and fabricate a field prototype of IMS including control electronics.
- Conduct field tests.

Introduction

Future low-emission and high-fuel-efficiency vehicles need a sensor to monitor NO_x emissions for optimizing the performance of exhaust emission control systems. Such a NO_x sensor must have high sensitivity, fast response time (<1 sec), and be able to survive the hostile environment of an engine exhaust system. An ion-mobility spectrometer has been demonstrated as a low-cost gas sensor [1] that may meet the requirements of an exhaust gas application. Based on ion-molecule chemistry, the basic energy requirement for forming a negative molecular ion is determined by the electron affinity (EA) of the molecule. The EAs for the negative NO and NO_2 ions are about 0.02 eV and 2.3 eV, respectively [2]. Therefore, it is possible to measure the total NO_x emissions by simply measuring negative NO_x ions produced in IMS. The feasibility of using ^{63}Ni-IMS to detect negative NO_x ions has been successfully

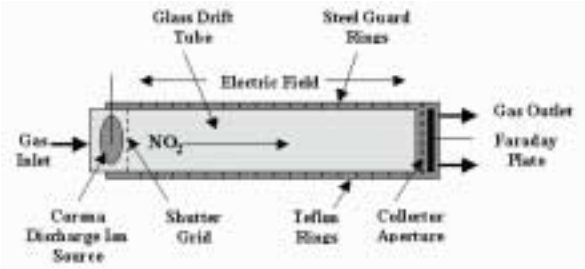

Figure 1. Basic Design of Ion-Mobility Spectrometer

demonstrated [3]. Because a radioactive source is unacceptable for an automotive application, alternative ionization sources such as corona discharge need to be developed. Tabrizchi,et.al. [4] described a design of such a pulsed corona-discharge ionization source which uses a point-to-point geometry. In FY 2001, we focused on development of a pulsed corona discharge ionization source with a needle-to-cylinder geometry. Preliminary results of such a non-radioactive IMS in detecting negative NO_x ions are presented.

Approach

The primary effort in FY 2001 was to develop a plasma-type ionization source to replace the ^{63}Ni β-emission source. Figure 1 shows the basic design of the laboratory prototype IMS sensor. It consists of a pulsed corona discharge ionization source, an ion drift tube, and a Faraday plate. The ion source assembly has a needle/metal-cylinder geometry. During operation the metal cylinder is biased with a negative voltage so that negative ions will be confined in the cell until the shutter grid opens. The drift tube of the IMS is a glass tube embraced by a series of steel-guard rings separated by Teflon rings, which establishes a uniform electrical field for detecting negative ions. Table 1 lists the specific design parameters and typical operating conditions of the IMS sensor.

Laboratory tests were conducted to evaluate the IMS sensor performance. The tests used a carrier gas typical of exhaust-gas composition mixed with NO_x/N_2. Both ion drift time and current output were measured and correlated with NO_x concentration. Water-vapor effect on the IMS spectrum was also examined, and a method to reduce the vapor concentration in the gas stream was developed.

Ion Source	Needle-surface gap	0.25 cm
	Applied voltage	-3.0/-4.0 kV
Shutter grid	Pulse width	2 ms
	Pulse voltage	140 V
	Frequency	12.5 Hz
Drift-tube electrical field		220 V/cm
Detection electronics	Filter (LP)	3 kHz
	Sensitivity	2 nA/V

Table 1. Design Parameters and Operating Conditions of the IMS Sensor

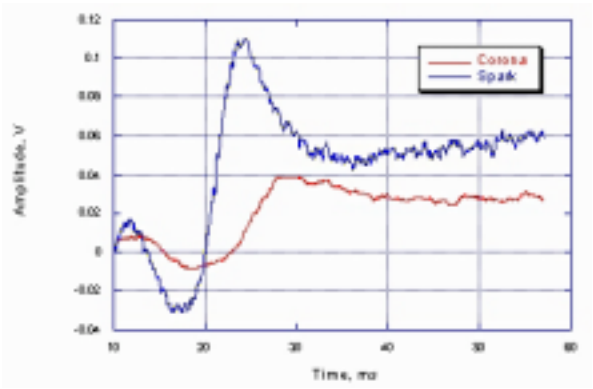

Figure 2. Negative NO_2 Ion Sprectra Produced by Corona and Spark Discharges

Results

Figure 2 shows the spectra of a gas mixture with 97 ppm of NO_2 in the carrier gas obtained under corona and spark discharge modes. The spark discharge (0.8 mA in-current) produces a better developed peak than does the corona discharge mode (0.1 mA in-current). The spark-discharge mode was chosen for IMS evaluation. Figure 3 shows dependence of peak amplitude on NO_2 concentration up to 500 ppm for NO_2/carrier-gas mixtures. Quantitatively, the NO_2/carrier-gas mixture produces more ions than NO_2/N_2 gas mixture, and the carrier gas mixture alone also produces an ion peak of significant magnitude with a delay time in the region where the NO_2 ions appear (14.5 — 16 ms). This suggests that NO_2 may be produced in the plasma during the spark-discharge process if the buffer gas has the carrier-gas composition. It is possible that the presence of oxygen (8.1%) in the carrier gas induces the reactions leading to NO_2 ion production.

The presence of water vapor in IMS tends to degrade the ion spectrum. In most cases, we found

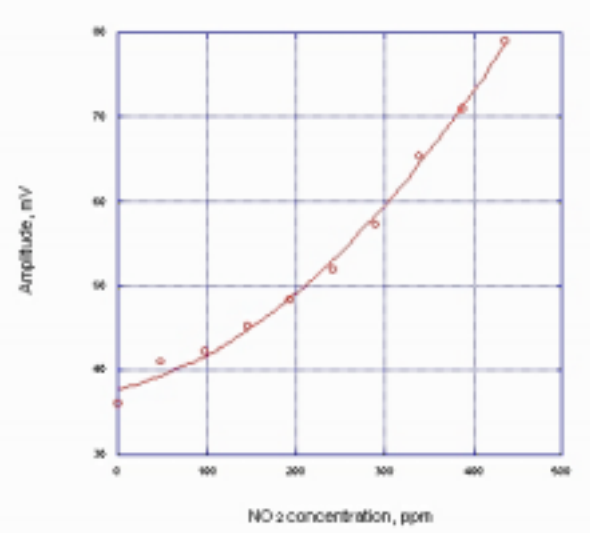

Figure 3. Peak Amplitude Versus NO_2 Concentration Measured with Carrier Gas and 5nA/V in Sensitivity

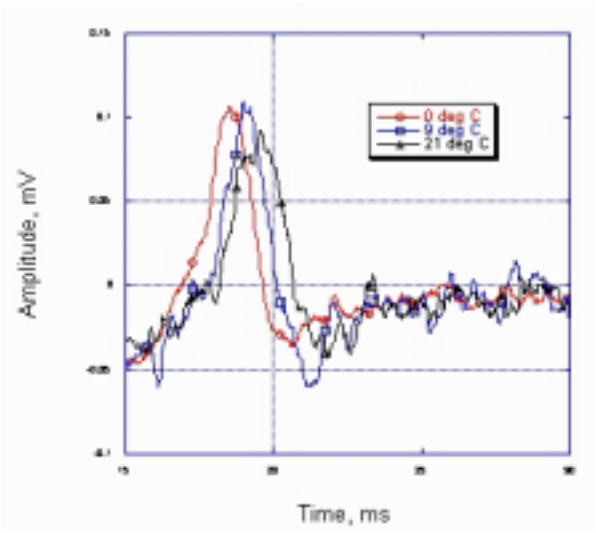

Figure 4. Negative NO_2 Ion Peaks Detected by Controlling the Carrier Gas Temperature

that the ion spectrum was completely masked by noise when the vapor content exceeded 1%. Therefore, a method to reduce the noise is necessary for practical applications. We investigated a cooling method using a thermoelectric cold plate that condenses water vapor before the gas enters the IMS. Figure 4 shows three ion spectra taken with vapor-saturated gas passing a cooling bath adjusted at the shown temperatures. The spectra show that as temperature decreases, the signal-to-noise ratio improves and the delay time of the peak decreases. The changes in delay time suggest that the size of water cluster may be reduced as the temperature decreases.

Conclusions

Preliminary results show that the spark-discharge mode of operation can be used to quantify the NO_2 concentration. The water-vapor effect has been examined. Without any pretreatment of the gas, the ion spectrum is completely masked by the noise when water content exceeds 1%. A thermoelectric cold plate was used to condense water from the gas stream before entering the IMS. Positive results to reduce the water effect were obtained. However, there are a few technical hurdles that need to be overcome before the IMS sensor can be used in an engine exhaust environment. These include (a) effects due to high-concentration water vapor, (b) drift time ambiguity, and (c) complexity of the ion-molecule chemistry due to variations of the exhaust-gas composition.

List of References

1. G. A. Eiceman and Z. Karpas, "Ion mobility spectrometry," CRC Press, 1994.
2. B. M. Smirnov, "Negative ions," McGraw-Hill Inc., pp. 27-31, 1982.
3. J. A. Jendrzejczyk, S. L. Dieckman, S. Slaughter, and A. C. Raptis, "Response of a prototype vehicle exhaust gas sensor to various hydrocarbons and other constituents," Argonne National Laboratory publication, ANL-99/5, 1999.
4. M. Tabrizchi, T. Khayamian, and N. Taj, "Design and operation of a corona discharge ionization source for ion mobility spectrometry," Rev. Sci. Inst. Vol. 71 (6), pp. 2321-2328, 2000.

C. Exhaust Gas Sensor Development

Fernando Garzon (Primary Contact)
MS D429, MST-11 Group
Los Alamos National Laboratory
Los Alamos, New Mexico, 87544
(505) 667-6643, fax (505) 665-4292, email: garzon@lanl.gov

DOE Program Manager, Rogelio Sullivan
(202) 586-8042, fax: (202) 586-1600, e-mail: Rogelio.Sullivan@lanl.gov

DOE Contractor: Los Alamos National Laboratory, Los Alamos, NM 87544

Objectives

- The goal is the development of low-cost solid-state electrochemical sensors that measure the non-methane hydrocarbon emissions of internal combustion engines.

Approach

- Develop solid-state electrocatalytic sensors based on zirconia ceramic electrolyte materials that produce a voltage output that is proportional to the non-methane hydrocarbon emissions concentrations in automotive exhausts.
- Novel thin-film metal oxide catalytic electrodes are used to sense the pollutants via electrode surface-electrochemical oxidation reactions.
- Modern electronic device fabrication methods are used to make the sensors.
- Electrochemical theory and modeling are used to optimize the device performance.

Accomplishments

- We have developed low-cost sensor prototypes that measure 10 - 2000 ppm concentrations of non-methane hydrocarbon gases (propylene and propane) under simulated high-temperature exhaust gas environments and engine dynamometer tests.
- We have reduced the cross interference of carbon monoxide to a ratio of better than 25 to 1.
- The devices exhibit almost no cross sensitivity for nitrogen oxides, water vapor or carbon dioxide gases.
- Our sensors exhibit excellent device-to-device response uniformity — less than 5% variability.
- We have improved the response times of our sensors from a minute to less than 3 seconds.
- Our hydrocarbon sensor technology has been combined with Ford Laboratory flat plate oxygen sensor technology to produce standalone sensors.

Future directions

- The program will not be funded in FY2002. Future directions include negotiations between sensor suppliers and the CRADA partners for technology commercialization.

Introduction

Internal combustion engines do not operate at a high enough efficiency to completely combust their fuel to carbon dioxide and water vapor. All internal combustion engines used in transportation require control and diagnostic sensor systems to reduce unwanted hydrocarbons, carbon monoxide and nitrogen oxide tailpipe emissions. Currently used automotive sensor systems are not performing adequately in this role and are responsible for a high maintanence workload for the manufacturers and the vehicle owners. Our goal is the development of low-cost solid-state electrochemical sensors that measure non-methane organic gas (NMOG) emissions (hydrocarbons) of internal combustion engines. The sensors need sufficient sensitivity to measure the performance of the automobile's emission control system to satisfy Federal On-Board Diagnostic requirements—typically, concentration levels of 10-500 parts per million of the regulated species. Ideally, the sensors should operate in-situ in hot exhaust gas streams. We have developed low-cost sensors to meet the needs of future on-board diagostic requirements.

Approach

Electrochemical sensors of the mixed potential class, operating at exhaust gas temperatures, offer a promising method of on-board emissions monitoring. The devices typically are comprised of two different catalytic electrodes deposited on an yttria-doped zirconium oxide solid electrolyte. Multiple charge transfer reactions occurring between the gas phase and the electrodes cause potentials of differing magnitude to develop at the dissimilar electrodes. The differences in heterogeneous kinetics, electrokinetics and the equilibrium potentials for these reactions all influence the device response to varying concentrations of analyte gas.

Miura and co-workers using electrochemical theory that invokes Butler-Volmer kinetics at high over-potentials have described the response behavior of mixed potential sensors. While this model does accurately describe the response behavior of many types of mixed potential sensors, the current model is inadequate for describing mixed potential sensors whose electro-kinetic reactions are mass transport limited or occurring at low over-potentials. For low concentrations of analyte gas, mass transport limitations must also be considered. Also, under some conditions, one of the electrodes may be operating at low over-potentials in the linear current voltage regime. We have developed models describing the behavior under non-Tafel response conditions. These models successfully predict the response behavior of the hydrocarbon sensors and provide insight on optimization of sensor design.

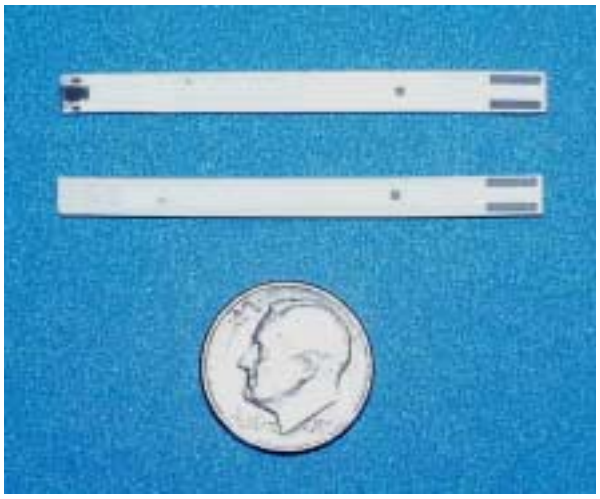

Figure 1. LANL hydrocarbon sensors fabricated on Ford self-heated ceramic substrates, top and bottom views. The small dark square on the left side of the top sensor is the electrochemical gas sensing element.

Our devices are based on thin-film transition metal oxides catalyst/noble metal composites deposited on oxygen ion conducting solid-state electrolytes. The metal oxide electrodes are central to the operation of the devices: they are electronically conducting and act as the electrodes for our sensors; they are catalytically active and can provide selective catalyzation under appropriate conditions; and finally, they conduct oxygen atoms and act as the source of oxygen for oxidizing reactions. Materials such as electron conducting perovskite oxides—lanthanum manganese oxide, lanthanum chromium oxide or fluorite structure oxides such as terbium zirconium oxide—have been successfully used to produce HC sensors. Sensors have been fabricated using bulk ceramic processing methods such as isostatic pressing and also by using physical vapor deposition technology. Figure 1 illustrates oxide electrode devices fabricated by

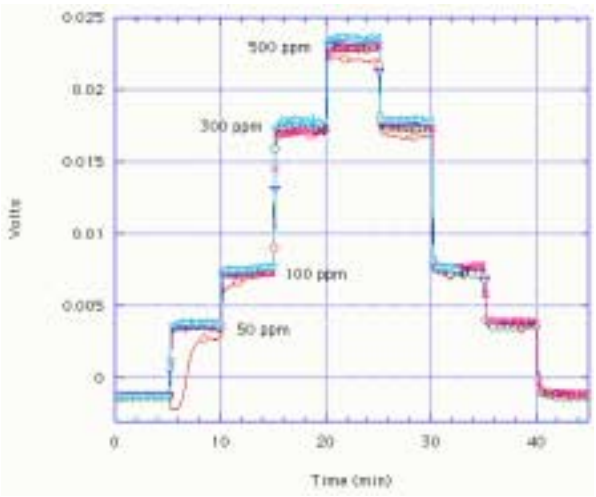

Figure 2. Hydrocarbon sensor response to part per million level changes of propylene gas concentration for six different runs.

LANL on sensor substrates developed by Ford Research Laboratory. The devices respond well to common hydrocarbon exhaust gases blended into nitrogen, carbon dioxide and water vapor mixtures-surrogate exhaust gas. Figure 2 displays the sensor's excellent response to propylene gas. Our sensors are proving to be robust devices that can reproducibly measure hydrocarbon emissions under laboratory conditions for long time periods. Our automotive CRADA partners have also extensively tested these devices under laboratory and engine exhaust conditions. A number of automotive sensor suppliers have expressed interest in the possible testing and subsequent commercialization of our devices.

References

1. N. Miura, T. Raisen, G. Lu and N. Yamazoe, *Sensors and Actuators B 47,* (1998) 84-91.

Publications

1. Fernando H. Garzon, R. Mukundan, and Eric L. Brosha, "Modeling the Response of Mixed Potential Electrochemical Sensors," *Solid State Ionic Devices II* , Vol. 2000-32 Electrochemical Society, 2000.
2. Fernando H. Garzon, Rangachary Mukundan, and Eric L. Brosha, "Solid State Mixed Potential Gas Sensors: Theory, Experiments and Challenges," *Solid State Ionics 136-137* (2000) 633-638.
3. R. Mukundan, E.L. Brosha, F.H. Garzon, "Solid-State Electrochemical Sensors for Automotive Applications," submitted to proceedings of the American Ceramics Society, Indianapolis, IN, 2001.
4. E. L. Brosha, R. Mukundan, D.R. Brown, and F.H. Garzon, "Zirconia-based Mixed Potential CO/HC Sensors with $LaMnO_3$ and Tb-doped YSZ Electrodes," *Solid State Ionic Devices II* Vol. 2000-32 Electrochemical Society, 2000.
5. E.L. Brosha, R Mukundan, D.R. Brown, F.H. Garzon, J.H. Visser, M. Zanini, Z. Zhou, and E.M. Logothetis, "CO/HC Sensors Based on Thin Films of $LaCoO_3$ and $La_{0.8}Sr_{0.2}CoO_3$."

Presentations

Invited Speaker

1. Rangachary Mukundan, Eric Brosha, Fernando Garzon, "Solid-State Electrochemical Sensors for Automotive Applications," presented at the Amercian Ceramics Society Conference, Indianapolis, Indiana, April 22-25, 2001.

Other Presentations

1. Fernando H. Garzon, R. Mukundan, Eric L. Brosha, "Modeling the Response of Mixed Potential Sensors," presented at the 198th meeting of the Electrochemical Society, Phoenix, Arizona, 2000.
2. Eric L. Brosha, Rangachary Mukundan, David R. Brown, Fernando H. Garzon, "Sensing System for Closed Loop Combustion Control," presented at the national conference of the American Society of Gas Engineers, Las Vegas, Nevada, June 11, 2001.
3. Eric L. Brosha, Rangachary Mukundan, David R. Brown, Fernando H. Garzon, J. H. Visser, David J. Thompson, D. H. Schonberg, and E.M. Logothetis, "Zirconia Based Mixed Potential CO/HC Sensors with $LaMnO_3$ and Tb-doped YSZ Electrodes," presented at the 198th meeting of the Electrochemical Society, Phoenix, Arizona, October 23-27, 2000.

Patents

1. "Mixed potential hydrocarbon sensor with low sensitivity to methane and carbon monoxide" R. Mukundan, E.L. Brosha, F.H. Garzon inventors. patent applied for- case #94675
2. "Enhanced Electrodes for Solid State Gas Sensors" F.H. Garzon and E.L. Brosha inventors. US Patent Granted

D. NO_x Sensor for Monitoring Vehicle Emissions

L. Peter Martin (Primary Contact), Ai-Quoc Pham
Lawrence Livermore National Laboratory
P.O. Box 808, MS L-333
Livermore, CA 94551-0808
(925) 423-9831, fax: (925) 424-3215, e-mail: martin89@llnl.gov

DOE Program Manager: Rogelio Sullivan
(202) 586-8042, fax: (202) 586-1600, e-mail: Rogelio.Sullivan@ee.doe.gov

Objectives

- Evaluate suitable electrolyte/electrode combinations for NO_x detection in vehicle exhaust.
- Investigate the effects of processing parameters on sensor response.
- Evaluate different sensor configurations.

Approach

- Utilize colloidal spray deposition to fabricate electrodes from ceramic powder precursors.
- Investigate mixed potential response of candidate electrode materials on an yttria-stabilized-zirconia (YSZ) electrolyte.
- Select most promising candidate electrode materials.
- Evaluate the effects of processing parameters on electrode response, including calcining temperature, particle size, and electrode thickness.

Accomplishments

- Identified two systems (Cr_2O_3, $NiCr_2O_4$) with mixed potential response of 40-60 mV.
- Evaluated the effects of calcining temperature and powder (precursor) particle size on response.
- Observed the effect of precious metal (catalyst) addition to metal oxide electrodes.

Future Directions

- Identify rate-limiting mechanisms in sensor response.
- Enhance sensor response time by engineering electrodes to minimize rate-limiting reactions.
- Investigate and minimize cross sensitivity with other potential exhaust gases.

Introduction

Recent regulations require automobile manufacturers to incorporate a comprehensive on-board diagnostic system for exhaust gas monitoring. The regulated pollutants include hydrocarbons, carbon monoxide, and oxides of nitrogen (NO_x). Increasingly more stringent emissions limits are being placed on each of these gases by both federal and state agencies. Because the need for a NO_x sensor is fairly recent, very few sensors of any kind are available, and most are still in the developmental phase. The most advanced NO_x sensing technology to date is based on solid state electrochemical devices. These devices typically consist of a solid (ceramic) electrolyte attached with two or more

metal or metal-oxide electrodes. Two electrodes having different sensitivity to the test gas can both be exposed to the exhaust stream, or one electrode may be isolated from the exhaust and exposed to a reference gas (air). These devices can be operated in either the amperometric mode, which measures the current-voltage response, or the potentiometric mode, which monitors the open circuit voltage. Potentiometric sensors are currently being investigated as a relatively simple, cost effective method for NO_x detection in vehicle exhaust.

In the potentiometric device, the open circuit potential difference between two electrodes is used to directly monitor the exhaust gas composition. This is the simplest mode of operation for these devices, with the measured (mixed) potential being directly related to the exhaust gas composition ($p(O_2)$, p(NO), etc.). During the FY 01 effort, the effects of electrode processing conditions upon the mixed potential NO sensitivity and response were evaluated for a number of material systems (Mn_2O_3, Cr_2O_3, $NiCr_2O_4$, CeO_2).

Approach

While there exist in the literature numerous reports of the mixed potential NO_x response of various metal oxides, these reports are often contradictory as to the measured response of the various oxides investigated [1,2,3]. The contradictory nature of the measured responses, sometimes reported by the same groups, are attributable to the potentially strong dependence of the mixed potential response upon the electrode morphology. That is, identical electrode materials deposited by, for example, sputtering and screen printing, may exhibit very different NO_x response characteristics. For these reasons, a logical starting point for this effort is to survey the NO_x response of potentially attractive metal oxide electrode materials as determined by the target environment and by the processing technique used in our laboratory (colloidal spray deposition). The spray deposition technique is a potentially ideal technique for application of the metal oxide electrodes because it allows close control of particle size and morphology, electrode thickness and porosity, and thermal history (i.e. calcining temperature). In this investigation, these processing parameters were evaluated for their effect on the NO_x sensitivity of selected metal oxide electrodes on yttria-stabilized-zirconia (YSZ) for the purpose of identifying the processing conditions providing optimal response characteristics.

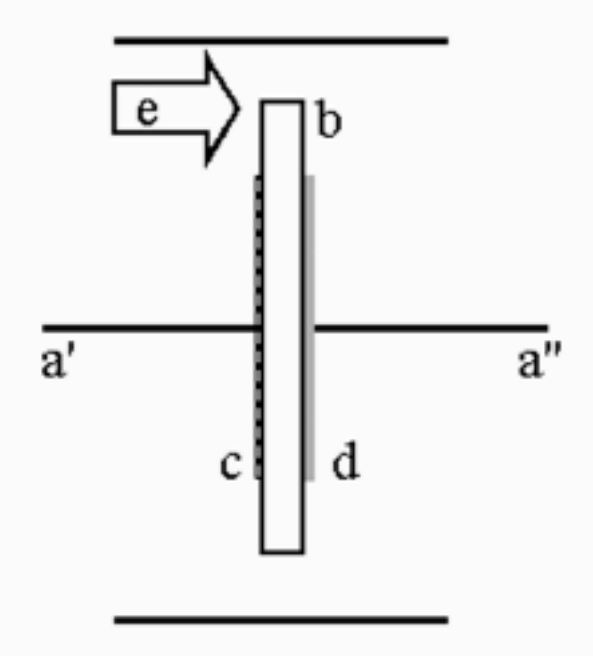

Figure 1: Schematic of the experimental test set-up showing: a', a") Pt wire leads, b) YSZ electrolyte, c) metal oxide electrode, d) Pt counter electrode, and e) test gas flow.

Results

Data obtained during FY 01 demonstrate mixed potential responses in excess of 40 - 60 mV for certain metal oxide (Cr_2O_3, $NiCr_2O_4$) electrodes exposed to 500 ppm NO at 500-600 ^oC and 10% O_2 (balance N_2). Figure 1 shows a schematic of the test configuration, where the sensor response is the open circuit voltage measured between the Pt leads a' and a". Other metal oxides were deemed too reactive (Mn_2O_3/Mn_3O_4) or refractory (CeO_2) to provide useful results by the processing techniques used here. The data also demonstrate clearly that the processing conditions of the sensor may significantly affect the sensor response. Figure 2 shows the open circuit potential of Cr_2O_3 on YSZ versus a Pt counter electrode at 500 ^oC. Data are shown for two different particle sizes and for a composite electrode including a precious metal catalyst. For the "coarse" powder data, the electrode was applied using the powder in its "as received" state, while for the "fine" data the powder was milled in ethanol for 48 hours prior to deposition. It is apparent that refinement of the

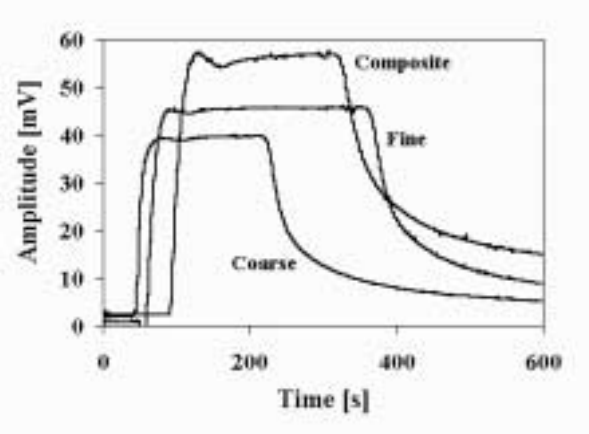

Figure 2: Open circuit potential of Cr_2O_3 on YSZ with Pt counter at 500°C in 10% O_2, balance N_2, with 500 ppm NO. Performance is shown for two different particle sizes and for a composite electrode including a precious metal catalyst.

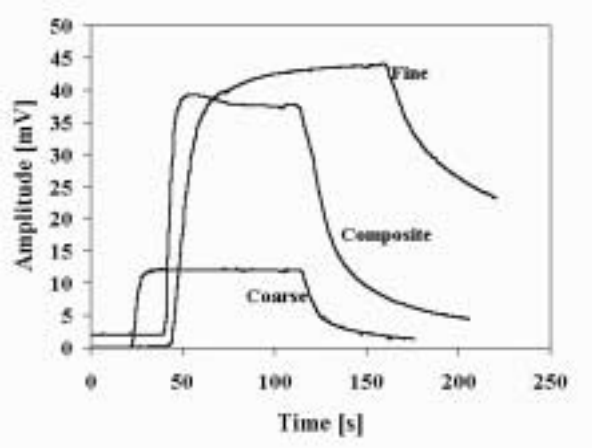

Figure 3: Open circuit potential of $NiCr_2O_4$ on YSZ with Pt counter at 550°C in 10% O_2, balance N_2, with 500 ppm NO. Performance is shown for two different particle sizes and for a composite electrode including a precious metal catalyst.

powder particle size leads to a slight increase in the response amplitude (46 vs. 40 mV) with approximately the same response time. Incorporation of the precious metal catalyst into the porous Cr_2O_3 electrode provides a further increase in signal amplitude (46 vs. 57 mV). Analysis of the electrochemical mechanisms responsible for the observed behavior is ongoing.

It is interesting to note that the specific effects of, for example, particle size refinement or metal catalyst addition may be very different for different material systems. For example, in Figure 3, the open circuit potential at 550 ºC of $NiCr_2O_4$ on YSZ with a Pt counter electrode is shown for two different particle sizes and for a composite electrode including a precious metal catalyst. Again, the "coarse" and "fine" designations indicate "as received" and after milling in ethanol for 48 hours. Note that in this case, the refinement of particle size leads to a very significant increase in both signal amplitude (12 vs. >43 mV) and response time. This is in contrast to the approximately constant response time observed in the Cr_2O_3 system, indicating that the surface-related mechanisms/kinetics dominating the responses in the two systems may be very different. Also, in contrast to the Cr_2O_3 results, both the amplitude and response time decrease with the incorporation of the precious metal catalyst. Quantitative data are not currently available for the relative reduction in particle sizes for the two sets of data shown. However, these data indicate that the contributions of the various electrochemical mechanisms involved in the NO response may be different for the Cr_2O_3 and the $NiCr_2O_4$ electrodes.

Determination of the effects of processing parameters such as particle size (surface area) or electrode thickness upon the mixed potential response can provide a means for evaluation, and comparison of, the dominant mechanisms involved in the NO_x sensor response. In addition, a strong understanding of processing effects is required to insure optimal sensor performance. The data presented here demonstrate that the effects of, for example, particle size can be isolated and quantified with respect to the NO_x sensor response. This will facilitate the further development of mixed potential sensors for vehicle exhaust monitoring.

Conclusions

To date, a number of metal oxide electrode materials have been evaluated for mixed potential electrochemical response. The most promising candidates, based upon response amplitude, have been Cr_2O_3 and $NiCr_2O_4$. These materials both show mixed potential responses in excess of 40 mV to 500 ppm NO under test conditions determined to be relevant to vehicle exhaust monitoring. A careful investigation of the effects of processing parameters

upon the response characteristics of these electrode materials indicate that electrode powder precursor characteristics and calcining temperature play a significant role in the measured mixed potential response.

References

1. V. Bruser, U. Lawrenz, S. Jakobs , H. -H. Mobius, and U. Schronauer, *Solid State Phenomena*, **39-40** (1994), 269-272.
2. G. Lu, N. Muira and N. Yamazoe, *Sensors and Actuators*, **B65** (2000), 125-127.
3. N. Muira H. Kurosawa, M. Hasei, G. Lu and N. Yamazoe, *Solid State Ionics*, **86-88** (1996), 1069-1073.

E. Improved Exhaust Emissions and Fuel Economy through the Use of an Advanced NO_x Sensor

G. Coffey, D. Rector, X. Li, L-Q. Wang, C. Habeger and Suresh Baskaran (Primary Contact)
Pacific Northwest National Laboratory
P.O. Box 999/MS K2-44
Richland, WA 99352
(509) 375-6483, fax: (509) 375-2186, e-mail: suresh.baskaran@pnl.gov

DOE Program Manager: Rogelio Sullivan
(202) 586-8042, fax: (292) 586-1600, e-mail: Rogelio.Sullivan@ee.doe.gov

CRADA Partner: Delphi Energy and Chassis Systems

Subcontractor: SRI International, Menlo Park, CA

Objectives

- Define the fundamental chemical reactions and the associated reaction rates on the current electrode systems of electrochemical NO_x sensors.
- Refine materials set and processing for the oxygen pump to improve sensor performance and durability.
- Optimize sensor structure for improved response time.
- Develop new materials for use as NO_x electrodes.

Approach

- Determine the optimum microstructure for sensor electrodes through analysis of electrode and other sensor subcomponents and electrochemical testing.
- Obtain fundamental electrochemical activity of electrode/electrolyte microstructures for O_2 and NO dissociation and transport.
- Develop models to correlate sensor performance to electrode and electrolyte performance and to physical parameters of sensor sub-components.
- Recommend sensor configuration based on the optimum structure derived from the models.
- Optimize the materials set and processing for improved durability and response.
- Determine potential for NO_x detection using alternative differential pulse voltametry method.

Accomplishments

- Sensor analysis has provided directions for design of optimal electrode microstructures and diffusion channels to and from the oxygen pump.
- Electrode performance was correlated to microstructural characteristics in current noble metal electrodes used in the oxygen pump, leading to identification of key parameters governing durability.
- Alternative oxide electrode compositions for the oxygen pump electrode were prepared and characterized.
- A computational model was constructed in order to relate the different geometrical parameters to an oxygen pump outlet PO_2 and, ultimately, response characteristics of devices.
- The differential pulse voltametry method showed potential for high NO sensitivity.

Future Directions

- Complete electrochemical characterization of oxygen pump and NO_x electrode materials, and provide recommendations for optimal materials, synthesis and microstructural design.
- Complete and test models relating sensor performance to physical parameters of the device and basic electrochemical performance of the electrode/electrolyte systems; provide recommendations on sensor design.

Introduction

Direct injection gasoline powertrains are being developed to effectively meet new emissions regulations while improving fuel economy. This technology allows for engine operation from rich conditions (9/1 Air/Fuel under loads) to very lean conditions (40/1 to 50/1 Air/Fuel) in economy mode. Because there are significantly higher NO_x emissions while operating in the lean mode, these systems require an emission control device to convert the NO_x. Typically a NO_x absorber is used; however, a NO_x sensor is necessary to control the regeneration cycle.

A NO_x sensor behind the NO_x absorber will enable closed-loop control over the regeneration cycle as well as provide the diagnostics that indicate that the absorber is functioning properly. The increase in fuel economy that is directly related to the use of a NO_x sensor device for closed-loop control (versus a model-based approach) is estimated to be between 0.5 to 1%. This is significant in that it is about 7-15% of the total estimated fuel economy benefit provided by a Direct Injection Gasoline System (conservatively, about a 7% increase in total fuel economy). Therefore, this sensor is an enabling technology for the emission control devices and system to effectively meet the legislated emissions.

Most of the current NO_x sensor technology is built on the technology base used for today's exhaust oxygen sensors, but are much more complex. The complexity requires both sophisticated construction techniques and electronics processing on the sensor. The design of a prototypical NO_x sensor is shown in Figure 1. The sensor device contains many layers of dissimilar materials, gas diffusion channels, internal heaters, and multiple electrodes using different electrode materials.

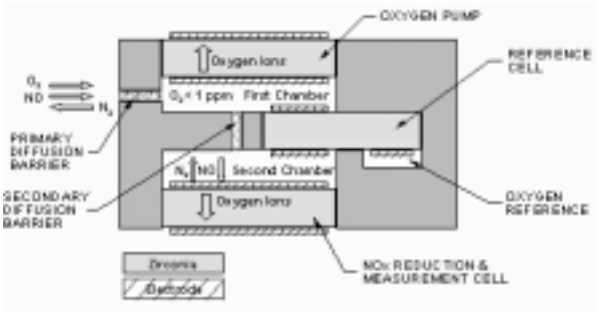

Figure 1. A Schematic Diagram Illustrating the Basic NO_x Sensor Function Model

While considerable progress has been made with zirconia electrolyte-based sensor technology, these products still suffer from poor durability, sensitivity to exhaust species, long response and recovery times after an extended rich operation, and measurement drift over time. In this project, the fundamental material and device parameters that govern these issues are addressed.

Approach

The project work focused on four areas:

1. Analysis of Sensor Devices

Microstructure and chemical analysis of several sensor designs was performed to understand the range of materials and microstructure in prototypical sensors. This effort provided guidance in design and development of optimal materials and microstructures for the various sensor sub-components.

2. Electrode Materials and Design

This task investigated the composition, processing and design parameters for existing noble metal electrodes and potential oxide electrodes in oxygen pumps within NO_x sensors. These

parameters control the physical and chemical mechanisms that determine sensor response. Both materials' design and fabrication are being optimized through improved fundamental understanding of the materials' surface chemistry, electrode reactions, morphological effects and electrode aging.

3. Device Modeling

Refined sensor models were constructed in order to predict the optimal design, geometry, size and configuration of the complete sensor structure.

4. Alternative Differential Pulse Voltametry Method of Detection

Current prototype sensors are based on amperometric measurements. This project also looked at using the differential pulse voltametry method applied to a zirconia-based sensor to detect a small quantity of NO_x in the mixture of O_2 and N_2. The potential for this approach was investigated by SRI.

Results and Conclusions

1. Analysis of Sensors

Several variations of two-stage zirconia-membrane based prototype NO_x sensors were compared. The diffusion channels to and from the oxygen pump cavity were compared for total length, area, grain size, and pore diameter/distribution. Sensor samples were flow tested, and compositions of the electrodes in each sensor were also compared. The electrode morphology showed some clear differences between various samples. These differences suggested some potential directions for optimal electrode design. The important parameters investigated were electrode thickness, triple phase boundary lengths, pore size/distribution, and primary grain size/distribution. The analysis of NO_x sensors provided insight in two designs areas for obtaining improved sensors. Optimal design and fabrication of diffusion channels to control gas flow to the oxygen pump cavity is critical for developing an accurate and sensitive sensor element. Second, carefully optimized grain morphology and pore structure in the electrode is required to obtain the desired electrocatalytic reduction behavior from electrode structures.

2. Electrode Materials and Design

2.1 Noble metal electrodes

The noble metal system is the baseline electrode material for oxygen pumps in NO_x sensors. The material shows promise for high selectivity of oxygen over NO adsorption using model surfaces, but key challenges with this material set are the lack of adequately high O_2 differentiation over NO in fabricated sensor devices, durability, and reliable performance.

The electrochemical dissociation/reduction behavior was correlated with microstructure for a set of prototypical noble metal Au/Pt electrodes. Microchemical analysis of the electrode materials indicated that this electrochemical behavior could be correlated to microchemical instabilities and variations in local composition between samples. Variations in Au/Pt concentration and distribution were observed after controlled high temperature processing. Gold migration is likely a key factor affecting reliability and aging response for some of the candidate Au/Pt O_2 pump electrodes studied, where high oxygen selectivity as well as high NO "de-selectivity" is needed. These investigations have directed material design and fabrication for imparting microstructural stability and providing improved, repeatable electrode characteristics.

2.2 Oxide electrodes

Oxide-based materials can also function as electrocatalysts for reduction of oxygen and are consequently used as state-of-the-art electrode materials in solid oxide fuel cells, electrochemical sensors and electrochemical oxygen pumps. To begin assessing the potential for oxide electrodes in oxygen pumps in the presence of NO, preliminary work was carried out in synthesis and microstructural development of porous perovskite materials. The baseline perovskite materials exhibited uniform porous microstructures with micron-scale grain sizes at the required processing temperatures. Preliminary electrochemical tests for the first baseline compositions showed electrocatalytic reduction activity for both O_2 and NO. These oxides and similar classes of oxides used in other similar high temperature electrolytic applications offer the potential for improving the relative dissociation/

adsorption/reduction behavior for oxygen over NO through careful doping and/or alloying.

3. Device Modeling

Using an experimentally measured diffusion channel resistance and pump parameters, a model was constructed to relate the different geometrical parameters to an oxygen pump outlet PO_2. This model was derived for a single geometry, a typical diffusion channel, and typical pump parameters. The model needs to be refined for multiple geometries with alternative dimensions and various modifications to diffusion channels, and the model's predictions will be correlated to experimental observations related to the effects of flow, geometry, and size on the sensitivity and response time of the sensor element.

4. Differential Pulse Voltametry Method of Detection

The DPV method can produce a useful detection limit for NO measurement. However, this approach requires development of stable sensor materials and sensor structure, in order to demonstrate sensing repeatability and fast response time in a practical sensor.

F. Fuel Vapor Sensor

S. H. Sheen (Primary Contact), H. T. Chien, and A. C. Raptis
Argonne National Laboratory
9700 South Cass Avenue
Argonne, IL 60439
(630) 252-7502, fax: (630) 252-3250, e-mail: sheen@anl.gov

DOE Program Manager: Rogelio Sullivan
(202) 586-8042, fax: (202) 586-1600, e-mail: Rogelio.Sullivan@ee.doe.gov

Objectives

- The objective of this project is to develop low-cost, fast-response, acoustic-based fuel-vapor sensors that can be used in an automotive environment to measure or monitor fuel-vapor mass flow rate and to detect variations in fuel-vapor composition.

Approach

- Stage 1. Design and test a laboratory prototype.
- Stage 2. Establish fuel-vapor acoustic relaxation spectra.
- Stage 3. Develop a fuel-vapor flow sensor.
- Stage 4. Develop field prototype sensors and conduct field tests.

Accomplishments

- Designed and fabricated a laboratory prototype for measuring acoustic properties of methane/nitrogen mixtures.
- Designed a signal processing and control system.

Future Directions

- Conduct tests to obtain acoustic properties of different fuel-vapor (ethane, propane and butane) compositions.
- Develop a prototype fuel-vapor sensor.
- Develop a prototype fuel-vapor mass-flow sensor.
- Conduct field tests.

Introduction

Vehicles sold in the U.S. have a carbon canister to trap fuel vapors from the fuel tank, greatly reducing hydrocarbon emissions. The fuel vapors are purged from the canister into the engine, where they are combusted during normal operation. The present engine control system strategy uses the oxygen sensor (in the exhaust gas manifold) to correct for rich shifts in the air-to-fuel ratio caused by the additional fuel vapors added to the engine during purge of the canister. A new requirement being phased in is to also trap all fuel vapors during refueling (on-board refueling vapor recovery). This increases the amount of fuel vapors to be purged into the engine during a drive cycle. The resulting large canister purge flow rates make it more difficult to reduce/eliminate driveability and stall problems and

to minimize disturbances in air-to-fuel ratio that may create an even bigger challenge to meet the increasingly stringent tailpipe emissions requirements. A feed forward system, in which a fuel vapor sensor located in the canister purge line would measure the mass of fuel vapors, is expected to result in a much more refined canister purge system. The system will also result in lower tailpipe emissions, less driveability problems, and a modest improvement in fuel economy by better controlling the air-to-fuel ratio. Unfortunately, such an automotive fuel vapor sensor currently is unavailable. Such a fuel-vapor sensor may have other related applications, including, for example, (1) a system that uses fuel vapor for vapor cold-start, and (2) a feedback system that improves combustion by monitoring hydrocarbon emissions.

This project is to conduct research and development leading to practical fuel-vapor sensors as specified in the objective, with the primary focus on development of a sensor that can speciate the fuel vapor and determine the vapor composition for engine combustion control. A fuel-vapor mass flowmeter will also be developed so that the fuel vapor can be quantified.

Approach

This program is a collaborative effort between Argonne National Laboratory (ANL), Ford Motor Company and Northwestern University (NU). ANL will primarily conduct the sensor development. The ANL speed-of-sound (SOS) sensor will be applied to measurements of acoustic properties of fuel vapors. The sensor will use SOS to predict the fuel-vapor concentration and determine the fuel-vapor composition by measuring the acoustic relaxation spectra. In FY 2001 we developed a laboratory prototype for measuring SOS and acoustic spectra of the fuel vapors. To study the acoustic relaxation phenomenon [1,2], the laboratory prototype uses a pair of transducers and measures the acoustic attenuation over a range of gas pressures. However, an array of transducers is proposed for the field-sensor design. A method to measure the vapor flow rate will also be developed and integrated with the composition and concentration measurements to form a fuel-vapor sensor. The sensor will then be tested at Ford.

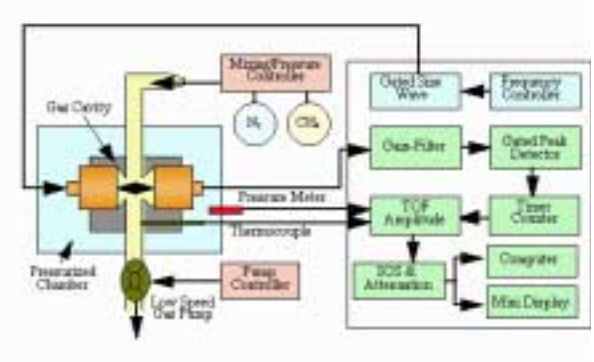

Figure 1. Schematic Diagram of the Laboratory Prototype Fuel-Vapor Sensor

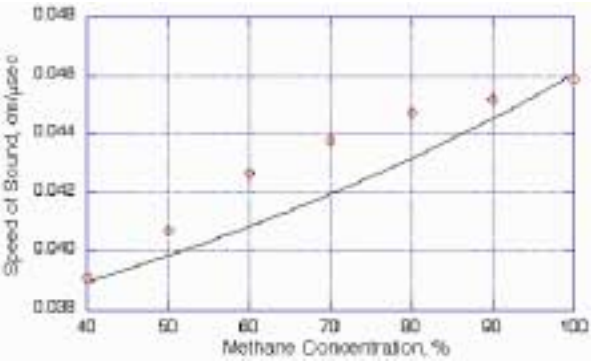

Figure 2. Speed of Sound in Methane/Nitrogen Mixtures (solid line is the calculated values using isentropic modeling)

Results and Conclusions

Figure 1 shows a schematic diagram of the laboratory prototype developed at ANL. It consists of two 0.5 MHz transducers operating in a pitch-catch mode. Gated sine waves of a fixed frequency (0.5 MHz or its harmonics) are propagated in a narrow flow channel, and their reflections are analyzed for variations in amplitude and time-of-flight, from which attenuation and speed-of-sound are measured. The prototype uses a high-pressure vessel to house the transducers and the flow cavity. To obtain the acoustic relaxation spectra, we vary the gas pressure because the attenuation in a gas depends on the ratio of acoustic frequency over the gas pressure.

Figure 2 shows the SOS in methane/nitrogen mixtures. The solid line represents the calculated values based on isentropic modeling. Although the measured SOS are higher than the calculated values, it is clearly shown that the SOS can be used to

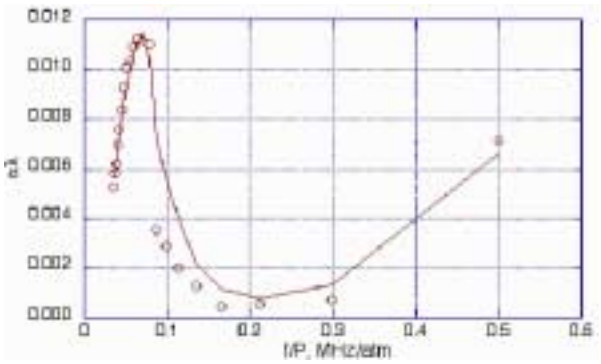

Figure 3. Dimensionless Attenuation Versus Frequency/ Pressure in 50% Methane in Nitrogen

predict the methane concentration in nitrogen gas. This is true as long as the carrier gas mixture has a fixed composition so that the mixture of methane and carrier gas can be considered as a binary gas mixture.

In Figure 3, the dimensionless attenuation (attenuation times wavelength, $\alpha\lambda$) is plotted against the frequency/pressure ratio (f/P) for 50% methane in nitrogen. The solid line represents the best-fit curve to the data. It is clearly shown that there exists a relaxation peak around f/P = 0.07; that is, under ambient conditions the relaxation peak appears at 70 kHz, which is much lower than model prediction [3].

In FY 2001, we have demonstrated that (1) SOS in a fuel-gas/air mixture can be used to measure the percent concentration of the fuel gas, and (2) it is feasible to use acoustic relaxation spectra to predict the fuel-gas composition.

References

1. H. J. Bauer, "Phenomenological theory of the relaxation phenomena in gases," Physical Acoustics vol. II part A, pp.48-132, 1965.
2. H. O. Kneser, "Phenomenological theory of the relaxation phenomena in gases," Physical Acoustics vol. II part A, pp.133-202, 1965.
3. Y. Dain and R. M. Lueptow, "Acoustic attenuation in a three-gas mixture: results," Submitted to J. of Acoustic Society of America.

ACRONYMS

2-D	Two-dimensional
3-D	Three-dimensional
ANL	Argonne National Laboratory
APS	Advanced Photon Source
ATDC	After top dead center
Au	Gold
BOTD	Ball-On-Three-Disc
CAD	Crank angle degrees
CARB	California Air Resources Board
cc	Cubic centimeter
CFD	Computational Fluid Dynamics
CHAD	Computational Hydrodynamics for Advanced Design
CHESS	Cornell High Energy Synchrotron Source
CIDI	Compression Ignition Direct Injection
cm	Centimeter
CO	Carbon monoxide
CO_2	Carbon dioxide
COV	Coefficient of variation
CRADA	Cooperative Research and Development Agreement
DI	Direct Injection
DOE	Department of Energy
DPV	Differential pulse voltametry
EA	Electron affinity
EDAX	Energy Dispersive Analysis of X-rays
EGR	Exhaust gas recirculation
EPA	Environmental Protection Agency
eV	Volts electric
FTP	Federal Test Procedure
FY	Fiscal year
g	Gram
GDI	Gasoline Direct Injection
GM	General Motors
H2	Diatomic hydrogen
HC	Hydrocarbon
HEGO	Heated exhaust gas oxygen
HP	Horsepower
Hz	Hertz
IMEP	Indicated mean effective pressure
IMS	Ion-mobility spectrometer
keV	Kilovolt electric
kHz	Kilohertz
kPa	Kilopascal
kV	Kilovolt
kW	Kilowatt
kWh	Kilowatt-hour
L	Liter
LANL	Los Alamos National Laboratory
LEP	Low Emission Partnership
LEV	Low Emission Vehicle
LIF	Laser-induced fluorescence
mA	Milliamps
mJ	Millijoule
mm	Millimeter
$mm^3/N*m$	Cubic millimeter per Newton-meter
MPa	Megapascal
mpg	Miles per gallon
MTV	Molecular tagging velocimetry
mV	Millivolt
N_2	Diatomic nitrogen
NFC	Near-Frictionless Carbon
nm	Nanometer
NMOG	Non-methane organic gas
NO	Nitric oxide
NO_2	Nitrogen dioxide
NO_x	Oxides of nitrogen
NREL	National Renewable Energy Laboratory
O_2	Diatomic oxygen
OAAT	Office of Advanced Automotive Technologies
OBDS	On-board distillation system
°C	Degrees Celsius
OE	Optical engine
OH	Hydroxyl radical
OTT	Office of Transportation Technologies
PAD	Pixel Array Detector
PCM	Powertrain control module
PFI	Port fuel injected
PIV	Particle Image Velocimetry
PLIF	Planar laser-induced fluorescence
PM	Particulate matter
PNGV	Partnership for a New Generation Vehicle
PNNL	Pacific Northwest National Laboratory
ppm	Parts per million
Pt	Platinum
Q1	First fiscal quarter
R&D	Research and Development
rms	Root mean square
TDC	Top dead center
rpm	Rotations per minute
s	Second
SC	Stratified charge
SCE	Single-cylinder engine

SEM	Scanning Electron Microscopy
SI	Spark Ignition
SIDI	Spark Ignition Direct Injection
SNL	Sandia National Laboratory
SOS	Speed-of-sound
TEM	Transmission Electron Microscopy
TKE	Turbulent kinetic energy
ULEV	Ultra low emission vehicles
UV	Ultraviolet
V	Volt
VCR	Variable compression ratio
vol%	Percent by volume
W	Watt
YSZ	Yttria-stabilized-zirconia
$\mu g/mm^3$	Micrograms per cubic millimeter
µm	Micrometer
µs	Microsecond

This document highlights work sponsored by agencies of the U.S. Government. Neither the U.S. Government nor any agency thereof, nor any of their employees, makes any warranty, express or implied, or assumes any legal liability or responsibility for the accuracy, completeness, or usefulness of any information, apparatus, product, or process disclosed, or represents that its use would not infringe privately owned rights. Reference herein to any specific commercial product, process, or service by trade name, trademark, manufacturer, or otherwise does not necessarily constitute or imply its endorsement, recommendation, or favoring by the U.S. Government or any agency thereof. The views and opinions of authors expressed herein do not necessarily state or reflect those of the U.S. Government or any agency thereof.


Printed on recycled paper

Office of Transportation Technologies Series of 2001 Annual Progress Reports

- Office of Advanced Automotive Technologies FY 2001 Program Highlights
- Vehicle Propulsion and Ancillary Subsystems
- Automotive Lightweighting Materials
- Automotive Propulsion Materials
- Fuels for Advanced CIDI Engines and Fuel Cells
- Spark Ignition, Direct Injection Engine R&D
- Combustion and Emission Control for Advanced CIDI Engines
- Fuel Cells for Transportation
- Advanced Technology Development (High-Power Battery)
- Batteries for Advanced Transportation Technologies (High-Energy Battery)
- Vehicle Power Electronics and Electric Machines
- Vehicle High-Power Energy Storage
- Electric Vehicle Batteries R&D

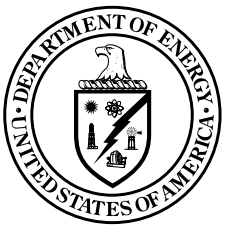

www.cartech.doe.gov

DOE/EERE/OTT/OAAT - 2001/006